"A THERMODYNAMIC STUDY OF LARGE TETRAAZA LIGANDS AND THEIR Cu (II) COMPLEXES "

Thesis submitted to the University of Stirling for completion of the degree of Doctor of Philosophy.

by

Malcolm J Macfie

Chemistry Department

University of Stirling

September 1988

This thesis is dedicated to the memory of
my late grandmother Mrs Frances Macfie.

Acknowledgements

I would like to thank Dr Robert Clay for his guidance, advice and supervision throughout this work and Dr Stuart Corr for his help and advice on many of the practical and synthetic aspects of this work. I am also grateful to many members of the chemistry department including Professor R W Hay, Dr F Riddell and Dr B G Cox for their advice and discussion, Dr I McEwan and Dr R Ferguson for their assistance in the use of the DSC II instrument and Dr P Millican, Mr Malcolm Baird and Mr Kenny Mathieson for their invaluable help and instruction on the use of the VAX 750 computer and to Marion for typing this thesis.

Abstract

Six macrocyclic (L_1-L_6) and ten non-cyclic (L_7-L_{16}) tetraaza ligands containing only secondary nitrogen atoms were synthesised and characterised. A further tetramine ligand (L_{17}) with two primary and two secondary nitrogen atoms was obtained commercially. The stepwise protonation constants of all of these ligands and the Cu(II) complex stability constants of all but three of the ligands (L_{10}-L_{12}) were determined by potentiometric titration. The Cu(II) complex formation enthalpies of L_1-L_9 and L_{13}-L_{17} were determined using a batch microcalorimetric technique. The enthalpies of solution of L_1-L_{17} were determined by isoperibolic calorimetry and the enthalpies of vaporisation of L_1-L_9, L_{16} and L_{17} determined using a custom built vapour pressure-weight loss apparatus.

The data for the ligands L_1-L_{17} and for a number of macrocyclic and non-cyclic tetraaza and tetramine ligands with smaller macrocyclic and/or chelate ring sizes ($L_{(I)}$-$L_{(XVIII)}$) has been examined to determine the effect of increasing macrocyclic and/or chelate ring size on the thermodynamic properties described above, and to determine the thermodynamic origins of the macrocyclic effect, the observed increase in stability of a macrocyclic ligand relative to that of an analogous non-cyclic ligand, and to determine the effect of increasing ligand size on the macrocyclic effect.

The enthalpy contribution to the macrocyclic effect has been shown to be equal to the difference between the hydration enthalpy of the free

macrocyclic and non-cyclic ligands. Differences in complex hydration appear to be small. The entropy contribution appears to be due to the greater loss of conformational entropy of the non-cyclic ligand on copper complex formation. The magnitude of the macrocyclic effect appears to be independent of ligand size but is dependent on the non-cyclic ligand chosen as a model for the macrocyclic ligand.

Contents

Chapter 1

INTRODUCTION

Co-ordination complexes of macrocyclic ligands have been known and studied since the early 20th century. The majority of these complexes were studied because of their importance in biological systems (i.e. porphyrin complexes in heme and chlorophyll) or because of their potential as pigments or dyes (i.e. phthalocyanine complexes). However, with few exceptions, it was not until the 1960's that the synthesis of saturated macrocyclic ligands[1] (particularly tetraaza macrocycles) and their metal complexes began to take place. It soon became apparent that these macrocycles were of considerable interest and potential importance since, when compared with similar non-cyclic ligands, they exhibited several unique properties including:

(i) The metal complexes of macrocyclic ligands were extremely inert and dissociated only slowly.

(ii) The macrocyclic ligands had the ability to induce unusually strong ligand fields. This was evident in the large ν (d-d) values obtained from the visible spectra of the metal complexes of these ligands.

(iii) The macrocyclic ligands had the ability to stabilise metal ions in high oxidation states.

(iv) The macrocyclic ligands formed thermodynamically more stable complexes than similar non-cyclic ligands. A similar enhancement of complex stability is seen in systems containing chelate rings when compared with the stability of a complex system which is as similar as possible but has fewer chelate rings. This effect, known

as the "chelate effect"[2] is well known and documented, and has been shown to be due entirely to entropy differences.

The enhanced stability of macrocyclic complexes, known as the "macrocyclic effect" has recently attracted much attention. Unlike the chelate effect, a great deal of controversy and speculation has arisen over the factors responsible for this observed enhancement of complex stability. A wide range of tetraaza macrocycles is now available and some thirty five macrocyclic and related non-cyclic ligands have beeen considered in this study. The structures and full systematic names of all these ligands are shown in figures 1:1 and 1:2. The ligands shown in figure 1:1 (with the exception of L_{17}) were synthesised in this study. Ligands shown in figure 1:2 have been studied previously.

The first published report of the existence of a macrocyclic effect was that of Cabbinessand Margerum in 1969,[3] who reported that the Cu^{2+} complex of the red(meso) isomer of the cyclic ligand "tet a" was more stable than the Cu^{2+} complex of the open chain ligand "2,3,2-tet"($L_{(IX)}$) by a factor of 10^4.

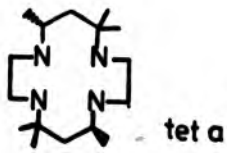

tet a

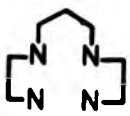

$L_{(IX)}$

L_1 1,4,8,11 - tetraazacyclopentadecane

L_2 1,4,8,11 - tetraazacyclohexadecane

L_3 1,4,8,11 - tetraazacycloheptadecane

L_4 1,5,8,12 - tetraazacyclohexadecane

L_5 1,5,8,12 - tetraazacycloheptadecane

L_6 1,5,8,12 - tetraazacyclooctadecane

L_7 2,5,10,13 - tetraazatetradecane

L_8 2,5,11,14 - tetraazapentadecane

L_9 2,5,12,15 - tetraazahexadecane

L_{10} 2,6,11,15 - tetraazahexadecane

L_{11} 2,6,12,16 - tetraazaheptadecane

L_{12} 2,6,13,17 - tetraazaoctadecane

L_{13} 3,6,9,12 - tetraazatetradecane

L_{14} 3,6,10,13 - tetraazapentadecane

L_{15} 3,7,10,14 - tetraazahexadecane

L_{16} 3,7,11,18 - tetraazaheptadecane

L_{17} 1,12 - diamino-4,9 - diazadodecane

Figure 1:1 Systematic names and structures of ligands used in this study

Amine protons have been omitted throughout this work for clarity.

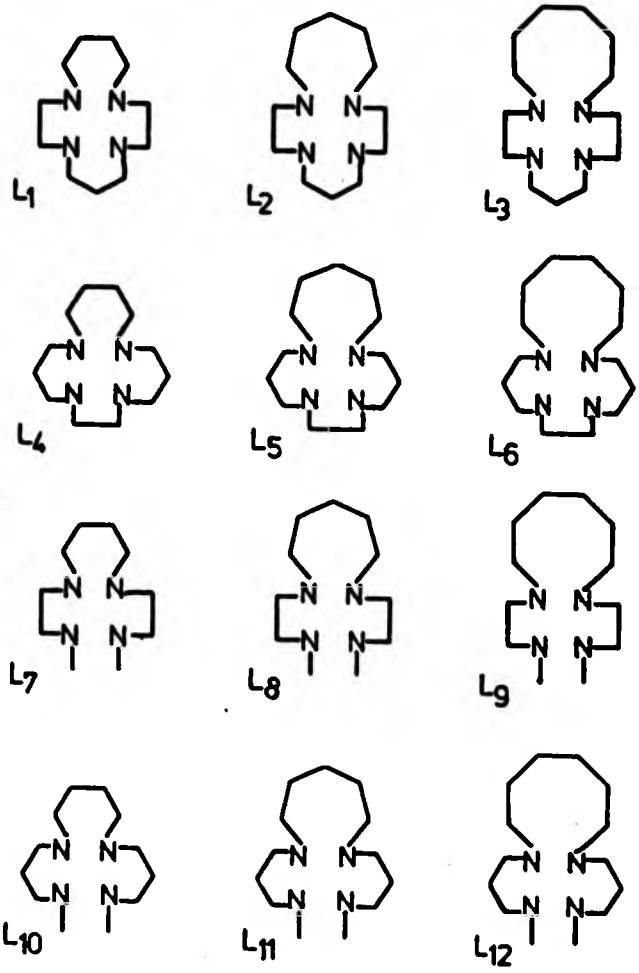

Figure 1:1 (continued)

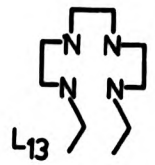

L_{13}

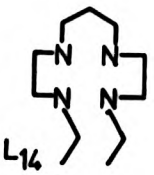

L_{14}

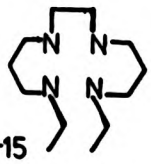

L_{15}

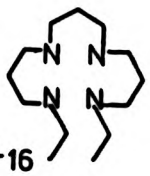

L_{16}

L_{17}

Figure 1:1 (continued)

$L_{(I)}$	1,4,7,10 - tetraazacyclododecane
$L_{(II)}$	1,4,7,10 - tetraazacyclotridecane
$L_{(III)}$	1,4,8,11 - tetraazacyclotetradecane
$L_{(IV)}$	1,4,8,12 - tetraazacyclopentadecane
$L_{(V)}$	1,5,9,13 - tetraazacyclohexadecane
$L_{(VI)}$	1,4,7,10 - tetraazacyclotetradecane
$L_{(VII)}$	1,5,9,13 - tetraazacycloheptadecane
$L_{(VIII)}$	1,8 -diamino -3,6-diazaoctane
$L_{(IX)}$	1,9 -diamino -3,7-diazanonane
$L_{(X)}$	1,10-diamino -4,7-diazadecane
$L_{(XI)}$	1,11-diamino -4,8-diazaundecane
$L_{(XII)}$	1,10-diamino -3,8-diazadecane
$L_{(XIII)}$	1,11-diamino -3,9-diazaundecane
$L_{(XIV)}$	1,12-diamino -3,10-diazadodecane
$L_{(XV)}$	2,5,8,11-tetraazadodecane
$L_{(XVI)}$	2,5,9,12 - tetraazatridecane
$L_{(XVII)}$	2,6,9,13 - tetraazatetradecane
$L_{(XVIII)}$	2,6,10,14 - tetraazapentadecane

Figure 1:2 Systematic names and structures of ligands used in previous studies

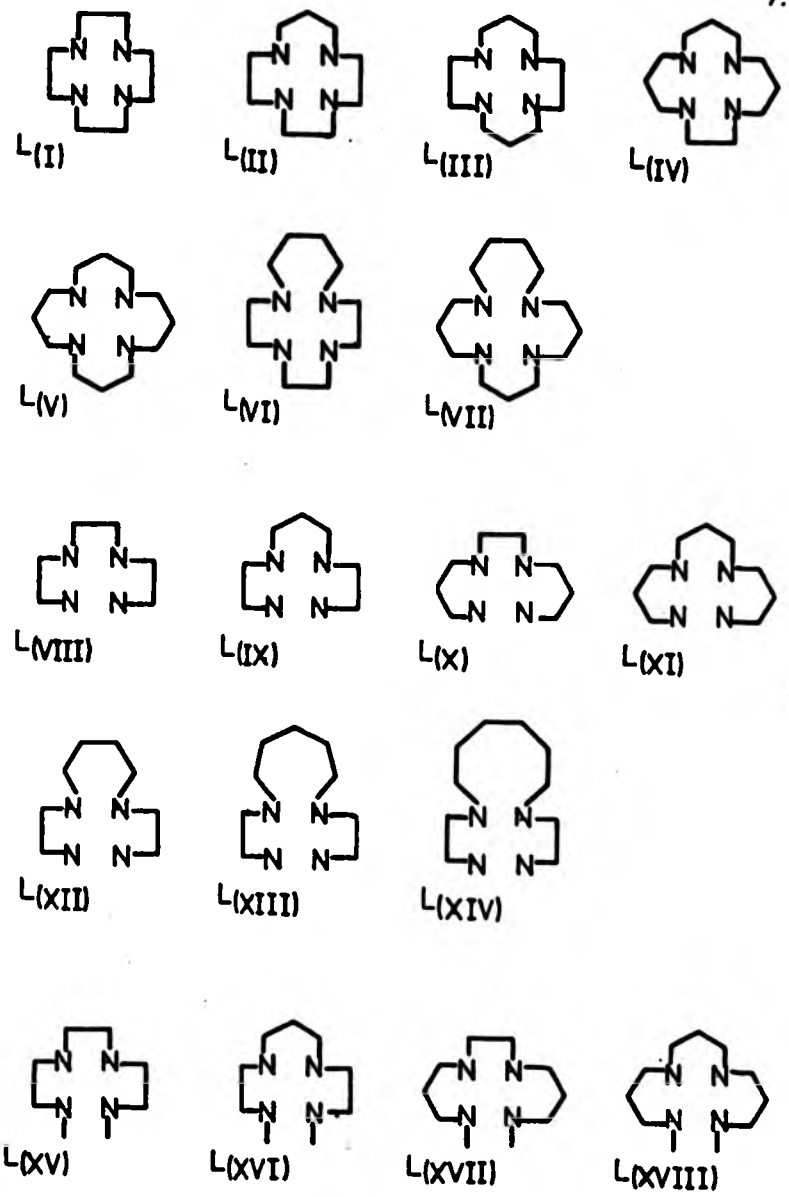

Figure 1:2 (continued)

Generally, the magnitude of the macrocyclic effect can be regarded as the free energy change ΔG_{mac} for the metathetic reaction:

$$[ML^n]^{2+}(aq) + L^c(aq) \longrightarrow [ML^c]^{2+}(aq) + L^n(aq) \quad \Delta G_{mac} < 0$$

where L^c = macrocyclic ligand; L^n = non-cyclic ligand

The macrocyclic free energy change ΔG_{mac} can be broken down into a macrocyclic enthalpy term, ΔH_{mac}, and a macrocyclic entropy term ΔS_{mac}. The values of these terms are derived from experimentally determined terms for each complex i.e.

$$M^{2+}(aq) + L^c(aq) \longrightarrow [ML^c]^{2+}(aq); \quad \Delta G_{ML}(L^c); \quad \Delta H_{ML}(L^c)$$

$$M^{2+}(aq) + L^n(aq) \longrightarrow [ML^n]^{2+}(aq); \quad \Delta G_{ML}(L^n); \quad \Delta H_{ML}(L^n)$$

$$\Delta G_{mac} = \Delta G_{ML}(L^c) - \Delta G_{ML}(L^n)$$

$$\Delta H_{mac} = \Delta H_{ML}(L^c) - \Delta H_{ML}(L^n)$$

$$T\Delta S_{mac} = \Delta H_{mac} - \Delta G_{mac}$$

Intrinsic properties of the macrocyclic systems such as limited solubility, slow rates of complex formation and high basicity led to difficulties in the measurement of ΔH_{ML} for these systems. Early values of ΔH_{ML} were obtained by indirect methods. These determinations

were extremely inaccurate and resulted in differing conclusions as to the magnitude and sign of ΔS_{mac} and ΔH_{mac}. For the Ni(II)-$L_{(III)}$ complex, the value of ΔH_{ML} obtained from the stability constant data[4] indicated that the macrocyclic effect was a combination of a large favourable enthalpy term and a small unfavourable entropy term. For the Cu(II)-$L_{(I)}$, $L_{(II)}$ and $L_{(IV)}$[5,6] complexes, ΔH_{ML} was obtained from polarographically obtained stability constant data. When these values were compared with directly obtained values of ΔH_{ML} for the Cu(II)-$L_{(VIII)}$ and $L_{(X)}$ complexes they indicated that the macrocyclic effect was due to a large favourable entropy term and a small favourable enthalpy term. Two possible explanations for these conflicting results were that the origins of the macrocyclic effect varied from system to system or (more probably) inaccuracies in the experimental data were too large to allow reliable or accurate conclusions to be reached.

The advent of a direct calorimetric method for the determination of ΔH_{ML}, using dilute solutions, a very sensitive microcalorimeter, and 1M NaOH as the solvent[7], allowed the accurate determination of ΔH_{ML}. Using this direct method it was discovered that many of the earlier determinations of ΔH_{ML} for tetraaza macrocycles had given values which differed by up to 20 kJ mol^{-1} from the directly determined value. Direct values of ΔH_{ML} have been determined for the Cu^{2+} complexes of the majority of ligands shown in figure 1:2. It has been shown for these ligands[8] that the macrocyclic effect has a favourable enthalpy term, varying with the match of the metal ion to the macrocyclic cavity, and an approximately constant favourable entropy term.

Further work has concentrated on the origins of the macrocyclic enthalpy term ΔH_{mac}. Consider the thermochemical cycle shown below.

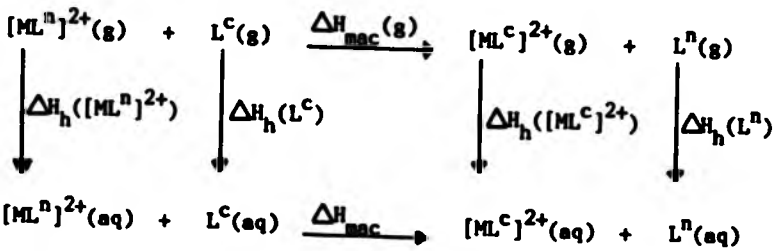

L^n = non-cyclic ligand, L^c = cyclic ligand

$$\Delta H_{mac} = \Delta H_{mac}(g) + (\Delta H_h(L^n) - \Delta H_h(L^c) + (\Delta H_h([ML^c]^{2+}) - \Delta H_h([ML^n]^{2+}))$$

The three component terms of ΔH_{mac} are:

(i) $\Delta H_{mac}(g)$

The gas phase macrocyclic enthalpy term. This is the term which will reflect any inherent enhanced stability of the macrocyclic complex relative to the non-cyclic complex. Any differences will arise from differences in M–N bond energies or from differences in ring strain.

(ii) $(\Delta H_h(L^n) - \Delta H_h(L^c)$

This term is the difference in solvation enthalpy of the free ligands and can, with some difficulty, be determined experimentally.

(iii) $(\Delta H_h[ML^c]^{2+}) - \Delta H_h([ML^n]^{2+})$

This term is the difference in the solvation enthalpies of the two complexes, which cannot be determined experimentally.

In earlier studies, ligands such as $L_{(VIII)}$-$L_{(XII)}$ were used as models for the macrocyclic ligands $L_{(I)}$-$L_{(V)}$, chosen because they had the same chelate ring sequence as the appropriate macrocyclic ligand. However, these non-cyclic ligands had two main disadvantages:

(i) They are chemically different from the macrocyclic ligands as they have two primary and two secondary nitrogen atoms whereas the macrocyclic ligands have four secondary nitrogen atoms.

(ii) They are smaller than the macrocyclic ligands and would therefore form complexes with smaller molecular volumes and consequently smaller effective molecular radii.

This meant that differences in ligand and complex solvation behaviour could arise because of the difference in the nature of the amine groups and differences in complex size. Also, if there were differences in the M-N bond energies of primary and secondary amines, this would be reflected in $\Delta H_{mac}(g)$. These factors would all affect the observed values of ΔH_{mac} and ΔS_{mac}.

The search for more appropriate model ligands for the tetraaza macrocyclic ligands led to the synthesis in 1981 of the non-cyclic ligand $L_{(XV)}$.[9] This ligand had several advantages as a model over its non

methylated analogue $L_{(VIII)}$ in that all of the amine groups in this ligand were secondary and the presence of the terminal methyl groups meant that the Cu^{2+}- $L_{(XV)}$ complex radius would match more closely that of the Cu(II)-$L_{(I)}$ and $L_{(II)}$ complex radii. Methylation of the terminal amine groups thus led to a more realistic model as differences in M-N bond energies and ligand complex solvation were minimised due to the chemical and structural similarity of the macrocyclic ligand and model. A comparison of the dimethylated non-cyclic ligands $L_{(XV)}$-$L_{(XVIII)}$ with the macrocyclic ligands $L_{(I)}$-$L_{(V)}$ has shown this to be the case,[8] as trends in both ΔG_{CuL} and ΔH_{CuL} parallel much more closely those of the macrocyclic ligands than was the case using the original model ligands $L_{(VIII)}$-$L_{(XII)}$.

Further work with the ligands $L_{(XV)}$-$L_{(XVIII)}$ involved the determination of the hydration enthalpies[10,11] of these ligands and of the ligands $L_{(I)}$-$L_{(V)}$. The differences in the hydration enthalpies of the macrocyclic and non-cyclic ligands were compared with the differences in the complex formation enthalpies ΔH_{CuL}. For a series of five pairs of tetraaza ligands with macrocyclic ligand ring sizes of 12-16, it was found that, within experimental error, the macrocyclic enthalpy term ΔH_{mac} could be accounted for by differences in the solvation enthalpies of the free ligands. Consequently, if it is assumed that the difference in the hydration enthalpies of the metal complexes is small, it follows that $\Delta H_{mac}(g)$ must be close to zero, suggesting that there is no inherent enhancement in stability of the macrocyclic complex over that of the analogous non-cyclic complex in the gas phase.

The principle aim of this work is to extend the above considerations by increasing the ring size of the macrocyclic ligands and the chain length of the non-cyclic model ligands by increasing the length of one methylene bridge, and thus to see if the earlier conclusions still hold for larger ligands. Work to be carried out to this end was planned as shown below.

(i) To synthesise and characterise the ligands L_1-L_{16} shown in figure 1:1.

(ii) To synthesise and characterise the Cu(II) complexes of the ligands L_1-L_{17}.

(iii) To determine the protonation ($\log K_{(1-4)}$, $\log \beta_4$) and Cu(II) stability constants ($\log K_{ML}$) of the ligands L_1-L_{17} by potentiometric titration.

(iv) To determine the Cu(II) complex formation enthalpies (ΔH_{ML}) of the ligands L_1-L_{17} by batch microcalorimetry.

(v) To determine the hydration enthalpies (ΔH_h) of the ligands L_1-L_{17} using a custom built weight loss apparatus to determine the enthalpy of vaporisation (ΔH_{vap}), and an isoperibolic calorimeter to determine the enthalpy of solution (ΔH_{sol}).

(vi) To investigate trends in the thermodynamic parameters determined in (iii)-(v) above, and to further investigate the thermodynamic origins of the macrocyclic effect and to determine the effect of increasing ligand size on the factors which are responsible for this effect.

The structures and full systematic names of all ligands which are relevant to this study are shown in figures 1:1 and 1:2. Unfortunately, the scope of this study was limited by two experimental problems.

(i) It was found that the ligands L_{10}-L_{12} behaved unusually in that they did not appear to form Cu^{2+} complexes. This limited the work carried out on these ligands to a determination of the protonation behaviour of the ligands.

(ii) Due to a combination of experimental difficulties and time limitations, it was not possible to determine the hydration enthalpies of the ligands L_{13}-L_{15}. This limited any investigation into the effect of increasing terminal alkyl group size and limited possible choices of model complex for the macrocyclic ligands to those used in chapter 6.

The study is based on the Cu(II) complexes of the tetraaza ligands for several reasons.

(i) The Cu^{2+} ion is less demanding in its complex structural requirements than many other metal ions. Small distortions from the ideal geometry are thus less likely to have a large effect on the thermodynamics of complex formation, allowing a relatively wide range of ligand systems to be studied.

(ii) The formation of the Cu^{2+} complexes of the tetraaza macrocyclic ligands is rapid.

(iii) Experimental procedures have been devised for the determination of ΔH_{ML}, log K_{ML} for the Cu^{2+}-tetraaza ligand systems and of ΔH_h for the free ligands.

(iv) A large database of thermodynamic information is available in the literature for the Cu^{2+}-tetraaza systems.

Chapter 2

SYNTHESIS OF THE LIGANDS AND THEIR Cu(II) COMPLEXES

An intriguing feature of tetra-aza ligand systems is the way that the size of the ligand can be changed relatively easily by synthetic means in such a way that the behaviour of a subsequently enclosed metal ion will be quite different. It is mainly for this reason that such a large body of work has been carried out on the synthesis and complexation of tetra-aza ligands since the "discovery" in 1969 of the so called "Macrocyclic Effect" by Cabbiness and Margerum.[3]

With few exceptions, the work carried out in this area to date has centred around 12-16 membered macrocycles and their acyclic analogues, and has been restricted to complexes which consisted only of 5 and 6 membered chelate rings.

The object of this work is to synthesize larger tetra-aza ligands in order to study the thermodynamics of formation of their copper(II) complexes. It is hoped that from this thermodynamic data, it will be possible to determine whether or not a macrocyclic effect exists for these larger ligands, and whether this effect can be ascribed to differences in the solvation terms of the free ligands as has been found with smaller, more symmetrical tetra-aza systems.[11]

It is also hoped to investigate the effect on complex stability which results when complexes with 7, 8 and 9 membered chelate rings are formed. In the case of the macrocycles L_1-L_6 it was hoped that by systematically

increasing the size of one chelate ring while maintaining the rest of the complex framework might lead to a macrocyclic complex which was more analogous to some corresponding acyclic complexes, i.e.-

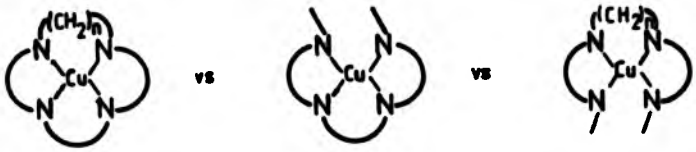

As n increases, it can be argued that the properties of the macrocyclic copper(II) complexes might become more like those of the analogous acyclic N,N'''-dimethylated and N,N'''-diethylated copper(II) complexes.

Synthesis of the ligands L_1-L_{16} was carried out using modifications of existing techniques based on Richman-Atkins type condensations,[12] involving the condensation of a bis-sulphonamide sodium salt and a sulphonate ester in a dipolar aprotic solvent (usually DMF) as shown below:-

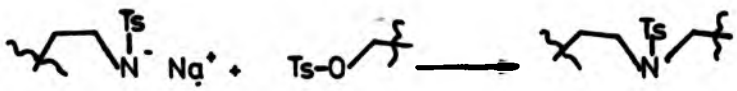

This method of synthesis is generally more convenient than other methods, as it does not utilize high dilution techniques or template effects in the cyclization step. In addition, the high equivalent weight of the p-toluene sulphonate groups makes the handling of small quantities of amine much more convenient.

In the past, the major drawback of this condensation was the difficulty encountered in attempts to cleave the sulphonamide to give the final product. Several methods have been used[13] and it has been found in this laboratory that the cleanest reaction and best yield was obtained using 80% H_2SO_4 at higher temperature (150-160 °C) for a short period of time (usually 30 mins to 1 hr). This method of hydrolysis gave yields of 50-80% of analytically pure amine.

The copper complexes were made by the addition of 2.0 mmol of copper(II) perchlorate hexahydrate or copper(II) nitrate in 25 ml ethanol to an equimolar amount of the appropriate free amine in ethanol or methanol, with subsequent recrystallisation from an appropriate solvent where possible.

1. Macrocycle Synthesis (L_1-L_6)

The macrocyclic ligands L_1-L_6 were synthesised using existing literature methods with some modifications. This method is outlined below for L_1.

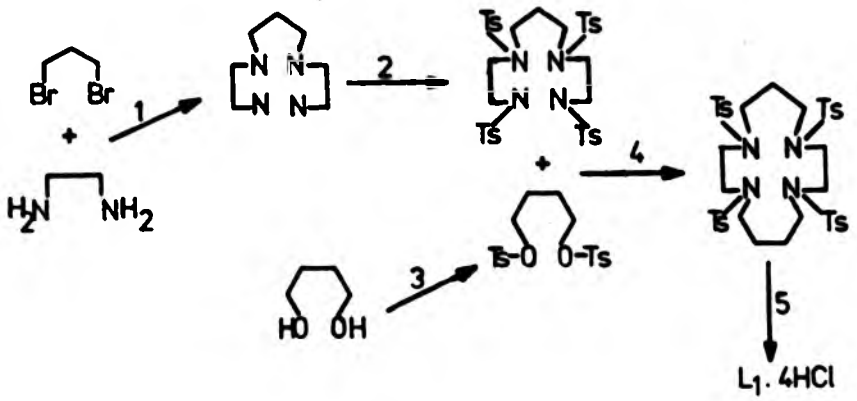

Step 1[14]

This step was unnecessary for the ligands L_4-L_6 as 1,12-diamino,-5,12-diazadecane ($L_{(X)}$) was obtained commercially, and used without further purification. The synthetic details for 1,11-diamino,-4,8-diazanonane ($L_{(IX)}$) were as follows. To an ice-cooled 1L beaker containing 300 ml (3 mol) of 1,2-diaminoethane was added 60.6 g (0.3 mol) of 1,2-dibromopropane over a period of 30 minutes with vigorous stirring. The resulting mixture was heated on a steambath for 90 minutes with constant stirring. After cooling, excess 1,3-diaminopropane was removed under reduced pressure using a rotary evaporator. The residual slurry was then treated with 33.7 g (0.6 mol) of crushed KOH pellets, and the mixture heated on a steam bath for a further 2 hours with frequent stirring.

The precipitate was removed by filtration at the pump, and repeatedly washed with diethyl ether. The filtrate and washings were combined, the ether removed using a rotary evaporator, and the resulting yellow oil fractionally distilled under reduced pressure, yielding a colourless oil. ^{1}H-nmr and infra-red spectra were consistent with the expected product.

Yield: 31.3 g (60%), b.p. 95 °C (0.2 mm Hg)

Step 2

The N,N',N'',N'''-tetratosylated (tosyl = p-toluenesulphonyl) amines were formed by adding a solution of tosyl chloride (4 equivalents) in the minimum volume of diethyl ether, dropwise with stirring, to a 30% (w/v) aqueus solution of the appropriate tetramine (1 equivalent) containing NaOH (4 equivalents).

The resulting two phase mixture was stirred for a further 4 hours during which time the product formed. In the case of $L_{(X)}$.4Ts, the product was a semi-crystalline solid which was suitable for use in step 4 after washing with H_2O followed by diethyl ether. $L_{(IX)}$.4Ts was a sticky, intractable brown/green gum which was purified by decantation of the liquid part of the reaction mixture, thorough washing with water and Et_2O, and refluxing with 3 portions of ethanol (250 ml). The resulting sticky gum was dried for 8 hours in a vacuum oven at 85 °C, giving a brittle, glassy solid which proved suitable for further reactions. ^{1}H-nmr spectrum and elemental analysis were consistent with the expected product.

$\underline{L_{(IX)}.4Ts:}$ 40.1 g (0.25 mol) $L_{(IX)}$, 209 g (1.1 mol) Tosyl chloride
40 g (1 mol) NaOH
Yield: 165.0 g (85%)

$\underline{L_{(X)}.4Ts:}$ 43.6 g (0.25 mol) $L_{(X)}$, 209 g (1.1 mol) Tosyl chloride
40 g (1 mol) NaOH
Yield: 184.2 g (93%)

Step 3

The O,O'-ditosylated diols were synthesised by adding dropwise a solution of tosyl chloride (2 equivalents) in the minimum volume of diethyl ether to a solution of the appropriate diol in a large (2-3 x) excess of triethylamine, with stirring. the resulting two phase mixture was stirred for six hours after addition was complete, by which time the white crystalline product had formed. The white precipitate was collected at the pump, washed liberally with water and diethyl ether, and dried in vaccuo over P_2O_5. Yields were typically 60-70%. ^{1}H-nmr and infra-red spectra were consistent with the expected products.

Step 4

An excess (2-3 x) of NaH (98% dry) was added in small portions to a stirred solution of the N,N',N'',N''' tetratosylamine in dry DMF(approximately 50 g in 500 ml). After 30 minutes of stirring in a flask protected from atmospheric moisture, excess NaH was removed at the pump by filtration directly into the reaction vessel (a 2 necked, 1L flask fitted with condenser and drying tube, and a dropping funnel). The solution was heated to 120 °C with stirring (magnetic follower) and a slight excess of the appropriate O,O'-ditosylated diol in dry DMF added (20g in 200 ml).

Once the addition was complete (approximately 45 minutes), the reaction mixture was stirred at 120 °C for a further 6 hours, cooled, and the volume reduced by 50% using a rotary evaporator. The resulting dark brown solution was then poured slowly onto three times its volume of ice/water, with vigorous mechanical stirring.

The resulting off white precipitate was washed thoroughly with water. Purification was by suspension in boiling methanol. The purified product was collected by filtration at the pump, washed with several portions of methanol, and dried in vaccuo over P_2O_5 for 48 hours. Infra-red, ^{1}H-nmr and ^{13}C-nmr spectra and elemental analysis were satisfactory.

$L_1$4Ts: 40.4 g (0.052 mol) $L_{(IX)}$.4Ts, 4.8 g NaH, 20.7 g (0.053 mol) O,O'-ditosyl-1,4-butanediol

Yield: 23.6 g (54.5%)

Elemental Analysis: C: 56.23%(56.36), H: 6.10%(6.06), N: 6.80%(6.14)
( ) calculated as $C_{39}H_{50}N_4S_4O_8$

$L_2$4Ts: 40.4 g (0.052 mol) $L_{(IX)}$.4Ts, 4.8 g NaH, 21.98 g (0.053 mol) O,O'-ditosyl-1,5-pentanediol

Yield: 23.3 g (53%)

Elemental Analysis: C: 56.78%(56.85), H: 6.10%(6.20), N: 6.64%(6.63)
( ) calculated as $C_{40}H_{52}N_4S_4O_8$

$L_3$4Ts: 40.4 g (0.053 mol) $L_{(IX)}$.4Ts, 4.8 g NaH, 22.60 g (0.053 mol) O,O'-ditosyl-1,6-hexanediol

Yield: 23.4 g (52.3%)

Elemental Analysis: C: 57.14%(57.32), H: 6.27%(6.33), N: 6.44%(6.52)
( ) calculated as $C_{41}H_{54}N_4S_4O_8$

$L_4$4TS: 43.5 g (0.055 mol) $L_{(X)}$.4Ts, 5.0 g NaH, 21.98 g (0.055 mol) 0,0'-ditosyl-1,4-butanediol

Yield: 24.6 g (55.8%)

Elemental Analysis: C: 57.02%(56.85), H: 6.20%(6.19), N: 6.70%(6.63) ( ) calculated as $C_{40}H_{52}N_4S_4O_8$

$L_5$4Ts: 47.85 g (0.06 mol) $L_{(X)}$.4Ts, 5.6 g NaH, 24.75 g (0.06 mol) 0,0'-ditosyl-1,5-pentanediol

Yield: 23.5 g (45.5%)

Elemental Analysis: C: 57.13%(57.32), H: 6.57%(6.33), N: 6.70%(6.63) ( ) calculated as $C_{41}H_{54}N_4S_4O_8$

$L_6$4Ts: 47.85 g (0.06 mol) $L_{(X)}$.4Ts, 5.6 g NaH, 25.6 g (0.06 mol) 0,0'-ditosyl-1,6-hexanediol

Yield: 23.4 g (44.6%)

Elemental Analysis: C: 57.80%(57.77), H: 6.30%(6.46), N: 6.42%(6.42) ( ) calculated as $C_{42}H_{56}N_4S_4O_8$

Step 5

The hydrolysis of the protecting sulphonamide groups was achieved using 3:1 H_2SO_4:H_2O (approximately 80% sulphuric acid by volume). The N,N',N'', N'''-tetratosylated macrocyclic tetramine was suspended in acid (3 ml per gram of substrate) in a large pyrex boiling tube. The suspension was then slowly heated to a temperature of 150-160 °C with frequent stirring, by immersion in an oil bath. The temperature was held at 150 °C for one hour after the solids had dissolved. The reaction mixture was cooled on ice and added very slowly and with vigorous stirring to 400 ml of 1:1 methanol:diethyl ether in a 1L beaker on an ice bath.

The resultant flocculant solid mass was filtered at the pump through a large sintered funnel, and was washed with diethyl ether. These hydrogen sulphate salts of the macrocycles were hygroscopic and difficult to purify or characterise and thus were converted to the corresponding tetrahydrochloride salts.

The impure hydrogensulphate salt was dissolved in 300 ml of distilled water and was heated on a water bath. To this solution was added an excess of $BaCO_3$ in small portions, controlling the resulting effervescence. Once the solution was alkaline to blue litmus paper, it was cooled and the precipitate of $BaCO_3/BaSO_4$ removed by filtration at the pump. The precipitate was washed thoroughly with hot water, and the washings and filtrate combined. This solution was boiled with decolourizing charcoal, filtered hot, cooled, and an excess of concentrated HCl added in small aliquots. This solution was then evaporated to dryness under reduced pressure on a rotary evaporator, and the crude solids recrystallized twice from aqueous ethanol. This procedure yielded analytically pure tetrahydrochloride salts in moderate yields.

$L_1.4HCL$: 30.0 g (3.6×10^{-2} mol) $L_1.4Ts$, 90 ml acid

Yield: 7.2 g (2.02×10^{-2} mol, 56%)

Elemental Analysis: C: 36.47%(36.68),H: 8.55%(8.39), N: 15.71%(15.55)

( ) calculated as $C_{11}H_{30}N_4Cl_4$

$L_2.4HCl$: 28.0 g (3.3×10^{-2} mol) $L_2.4Ts$, 85 ml acid

Yield: 4.45 g (1.2×10^{-2} mol, 36%)

Elemental Analysis: C: 38.53%(38.51), H: 8.73%(8.62), N: 15.17%(14.97)
( ) calculated as $C_{12}H_{32}N_4Cl_4$

L_3.4HCl: 30.4 g (3.5×10^{-2} mol) L_3.4Ts, 90 ml acid
Yield: 6.3 g (1.6×10^{-2} mol, 46%)
Elemental Analysis: C: 40.01%(40.22), H: 8.60%(8.83), N: 14.67%(14.43)
( ) calculated as $C_{13}H_{34}N_4Cl_4$

L_4.4HCl: 24.5 g (2.9×10^{-2} mol) L_4.4Ts, 75 ml acid
Yield: 4.74 g (1.3×10^{-2} mol, 44%)
Elemental Analysis: C: 38.22%(38.51), H: 14.85%(14.97), N: 8.84%(8.62)
( ) calculated as $C_{12}H_{32}N_4Cl_4$

L_5.4HCl: 18.7 g (2.2×10^{-2} mol) L_5.4Ts, 60 ml acid
Yield: 4.31 g (1.1×10^{-2} mol, 51%)
Elemental Analysis: C: 39.94%(40.22), H: 8.53%(8.83), N: 14.41%(14.43)
( ) calculated as $C_{13}H_{34}N_4Cl_4$

L_6.4HCl: 20.5 g (2.3×10^{-2} mol) L_6.4Ts, 60 ml acid
Yield: 4.60 g (1.2×10^{-2} mol, 51%)
Elemental Analysis: C: 41.67%(41.80), H: 9.01%(9.02), N: 13.93%(13.91)
( ) calculated as $C_{14}H_{36}N_4Cl_4$

Ligand Characterization

The ligands L_1-L_6 were characterized both gravimetrically (elemental analysis) and spectroscopically (infra-red, nmr spectroscopy). Elemental analyses have already been discussed. Relevant spectroscopic data is outlined below.

^{1}H N. M. R. Spectra (as tetrahydrochloride salts)

Chemical shift values are in ppm relative to NaTMS. Spectra were recorded on a Perkin-Elmer R32 NMR spectrometer, 90 MHz ^{1}H, D_2O solvent.

$L_1.4HCl$ 6.40(8H, s), 6.65(8H, m), 7.70(2H, qi), 8.10(4H, m)

$L_2.4HCl$ 6.35(8H, s), 6.60(8H, m), 7.70(2H, qi), 8.20(6H, m)

$L_3.4HCl$ 6.35(8H, s), 6.45(4H, t), 6.70(4H, t), 7.70(2H, q), 8.25(8H, m)

$L_4.4HCl$ 6.40(4H, s), 6.65(12H, m), 7.75(4H, qi), 8.10(4H, qi)

$L_5.4HCl$ 6.35(4H, s), 6.65(12H, m), 7.75(4H, qi), 8.20(6H, m)

$L_6.4HCl$ 6.40(4H, s), 6.70(12H, m), 7.75(4H, qi), 8.30(8H, m)

s= singlet, d=doublet, t=triplet, q=quartet, qi=quintet, m=multiplet

^{13}C N. M. R. Spectra (broad band) (as tetrahydrochloride salts)

Chemical shift values are in ppm relative to NaTMS. Spectra were recorded on a Bruker WP 80 spectrometer, 80 MHz ^{13}C, D_2O solvent.

$L_1.4HCl$ 23.36(1C), 24.37(2C), 43.72(2 x 2C), 45.77(2C), 47.79(2C)

$L_2.4HCl$ 23.29(1C), 24.44(1C), 25.78(2C), 43.55(2 x 2C), 46.04(2C) 48.33(2C)

$L_3.4HCl$ 24.57(1C), 26.25(2C), 26.99(2C0, 45.64(2C), 45.98(2C), 46.65(2C), 49.81(2C)

$L_4.4HCl$ 22.81(2C), 23.63(2C), 42.74(2C), 44.37(2C), 45.68(2C), 47.05(2C)

$L_5.4HCl$ 24.07(2C), 24.72(1C), 26.14(2C), 44.92(2C), 45.96(2C), 46.88(2C), 48.58(2C)

$L_6.4HCl$ 24.56(2C), 26.47(2 x 2C), 45.63(2C), 46.34(2C), 47.05(2C) 49.45(2C)

Infra-red Spectra (as N,N',N'',N''' -tetra tosyl amines)

$L_1.4Ts$ 3060–3020(wbmu), 2970–2915(mbmu), 1595(ssh), 1490(ssh), 1455(sb), 1400–1275(sbmu), 1225, 1210(wsh), 1155(sb), 1115, 1085(msh), 1040(wb), 1015(msh), 980(mb), 940, 920(wsh), 880(msh), 810(sb), 790(wsh), 770(wsh), 750–690(sbmu), 650(sb), 545(sb), 480(wb).

$L_2.4Ts$ 3070, 3050, 3020(wsh), 2910(sb), 2850(ssh), 1595(ssh), 1490(ssh), 1455(sb), 1395, 1375(wsh), 1350–1270(sbmu), 1240(wb), 1210(msh), 1180–1140(sbmu), 1110(wsh), 1080 (msh), 1045(wb), 1010(wsh), 985, 955, 940(wb), 890, 860 840(wsh), 810(sb), 775(wsh), 730(sb), 690(wsh), 650(sb), 580–515(sbmu), 480(wb).

$L_3.4Ts$ 3080, 3060, 3020(wssh), 2929(sb), 2860(ssh), (1675 occluded DMF), 1595(ssh), 1490(ssh), 1460(sb), 1400(wb), 1380(wsh), 1340(ssh), 1305, 1290, 1265(wsh), 1240, 1230 (wsh), 1210(wb), 1155(sb), 1110(wb), 1090(msh), 1040(mb), 1015(msh), 990(wb), 840(wsh), 810(ssh), 800(wsh), 770 (msh), 750–715(sbmu), 700(msh), 650(sb), 530–545(sbmu), 480(wb).

$L_4.4Ts$ 3040, 3020(wsh), 2980, 2960, 2930(sb), 2870(msh), 1600 (ssh), 1490(ssh), 1460(sb), 1395, 1380(wb), 1340(sb), 1310, 1300(wsh), 1290, 1270, 1250(msh), 1225(msh),

$L_4.4Ts$ 1180–1150(sshmu), 1120, 1110(wsh), 1090(ssh), 1055(wb), 1030, 1025(msh), 990(wsh), 960(msh), 940(wsh), 860, 845 (wsh), 820(ssh), 800(wsh), 730(ssh), 710, 700(wsh), 690 (msh), 650(ssh), 575, 545(ssh), 495–480(wshmu), 450(wb).

$L_5.4Ts$ 3060, 3030(wsh), 2970–2910(mshmu), 2850(msh), 1600(ssh), 1495(msh), 1465(mb), 1400, 1385(wb), 1340(sb), 1300, 1290, 1265, 1240, 1215(wsh), 1160(sb), 1120(wsh), 1090 (ssh), 1040(wb), 1020(msh), 1000, 985(wb), 965, 955, 945 (wsh), 820(ssh), 800(wsh), 785(wsh), 760–720(sshmu), 700 (msh), 655(ssh), 570–540(sshmu), 485(wb).

$L_6.4Ts$ 3080, 3060, 3020(wsh), 2920(sb), 2860(msh), (1675 occluded DMF), 1600(ssh), 1495(ssh), 1470–1450(mshmu), 1410, 1400, 1390, 1380(wsh), 1340(sb), 1305(wsh), 1290 (wb), 1265(msh), 1230, 1210(wsh), 1160(sb), 1115, 1090 (ssh), 1075(wsh), 1035(msh), 1020(msh), 1010, 1005(wsh), 975(ssh), 960(wsh), 930(ssh), 915(wsh), 860, 850(wsh), 815, 800(ssh), 790(wsh), 780(msh), 765(wsh), 750(msh), 720(ssh), 700, 690(wsh), 655(sb), 585–570(sshmu), 550 (sb), 510(wsh), 480(wb), 460, 440(wsh).

(KBr disc, Perkin-Elmer 577 Spectrometer)

s=strong, m=medium, w=weak, sh=sharp, b=broad, mu=multiplet

2. Open Chain Ligands

2a. Dimethylated tetramine Ligands

(i) Synthesis of L_7-L_9

The ligands L_7-L_9 were synthesised using the procedure outlined below for L_7.

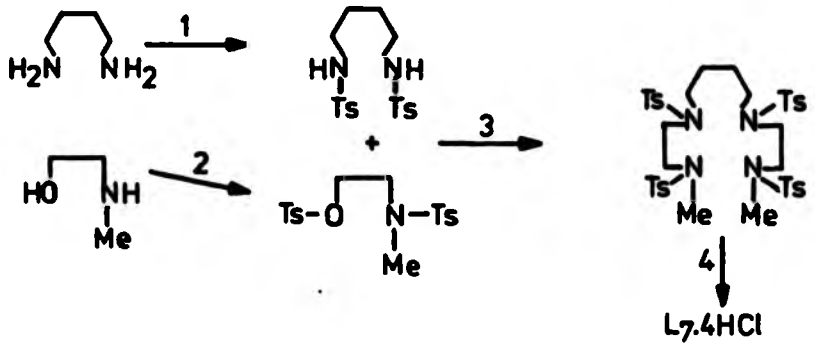

Step 1

This was accomplished by adding a solution of tosyl chloride (2 equivalents) in the minimum volume of diethyl ether dropwise to a stirred 5% (w/v) aqueous solution of the appropriate diamine containing 2 equivalents of NaOH, in a 500 ml 2 necked round bottomed flask fitted with condenser and dropping funnel. After addition was completed, the resulting 2 phase mixture was left stirring for twelve hours, and the resulting semi-crystalline off-white solid collected by filtration at the pump and thoroughly washed with several portions of water and diethyl ether. Typically yields of 65-70% of tosylated diamine were achieved. The products gave satisfactory ^1H nmr spectra and elemental analyses, and were used without further purification.

Step 2[15]

To an ice/methanol cooled 20% (w/v) solution of 0.25 mol N-methylamino-ethanol (1 equivalent) in dry pyridine in a 3 necked 1L round bottomed flask fitted with mechanical stirrer, condenser and drying tube and a powder feed tube, 2 equivalents of dry tosyl chloride was added slowly with stirring. During the addition, a bright orange coloration quickly developed. This colour persisted throughout the reaction. After the addition was complete (90 minutes) the bright orange solution was stirred for a further 2 hours on an ice/methanol bath, and 600 ml of ice/water added with vigorous stirring. The resulting yellow solid was filtered at the pump and washed thoroughly with several portions of water and several portions of cold ethanol. The precipitate was then dissolved in acetone and boiled with decolourizing charcoal. After filtration and removal of the acetone (rotary evaporator), the resulting semi-crystalline solid was recrystallised from ethanol as fine white needles with a faint yellow tinge and was dried in vacuo over P_2O_5. Satisfactory elemental analysis and ^1H nmr and infra-red spectra were obtained.

Elemental Analysis: C: 53.32%(52.25), H: 5.50%(5.52), N: 3.55%(3.65) ( ) calculated as $C_{17}H_{21}NS_2O_5$

Yield: 57.35 g (74%)

Step 3

To a stirred solution of the ditosylated 1,n-diamine (1 equivalent) in dry DMF (20% (w/v) solution) in a 2 necked round bottomed flask fitted with dropping funnel and condenser and drying tube, a slight excess of NaH (dry, 98%) was added in small portions. Once effervescence had

subsided, the resulting grey slurry was heated to 120 °C with stirring, and a 25% (w/v) solution of N,O-ditosyl-2-methylamino ethanol (2 equivalents) in dry DMF was added dropwise, over a period of 1 hr. During this addition, the reaction mixture underwent a change from a grey slurry to a brown solution. Once addition was complete, the reaction mixture was stirred for a further 4 hours, cooled, and left open to the atmosphere overnight. The volume of the solution was then reduced by 50% on a rotary evaporator, and the resulting concentrated solution poured slowly onto 3 times its volume of ice/water with vigorous mechanical stirring. In most cases, the resulting sticky precipitate could be purified by suspension in boiling methanol (10 ml per gram), giving a powdery white solid. All infra-red and ^{1}H and ^{13}C nmr spectra, and elemental analyses were consistent with the expected products.

$L_7.4Ts$ 19.8 g (0.05 mol) N,N-ditosyl-1,4-diaminobutane, 2.7 g NaH
38.3 g (0.10 mol) N,O-ditosyl-N-methyl-2-aminoethanol
Yield: 32.0 g (0.039 mol, 78%)

Elemental Analysis: C: 55.74%(55.72), H: 6.16%(6.15), N: 6.82%(6.84)
( ) calculated as $C_{38}H_{50}N_4S_4O_8$

$L_8.4Ts$ 20.5 g (0.05 mol) N,N'-ditosyl-1,5-diaminopentane, 2.7 g NaH
38.3 g (0.10 mol) N,O-ditosyl-N-methyl-2-aminoethanol
Yield: 31.0 g (0.037 mol, 74%)

This compound was only obtained as a gum.

L_9.4Ts: 21.2 g(0.050 mol)N,N'-ditosyl-1,6-diaminoethanol, 2.7 g NaH
38.5 g (0.10 mol)N,O-ditosyl-N-Methyl-2-aminoethanol
Yield: 30.5 g (0.036 mol, 72%)

Elemental Analysis: C: 56.72%(56.71), H: 6.50%(6.42), N: 6.56%(6.61)
( ) calculated as $C_{40}H_{54}N_4S_4O_8$

Step 4

The hydrolysis of the protecting sulphonamide groups was accomplished using the same method as for the macrocyclic ligands L_1-L_6, using 80% H_2SO_4(3:1 H_2SO_4)(page 23).

L_7.4HCl: 31.0 g (3.8×10^{-2} mol) L_7.4Ts, 90 ml acid
Yield: 8.9 g (2.6×10^{-2} mol, 67%)

Elemental Analysis: C: 34.57%(34.50), H: 8.68%(8.68), N: 15.97%(16.09)
( ) calculated as $C_{10}H_{30}N_4Cl_4$

L_8.4HCl: 30.0 g (0.036 mol) L_8.4Ts, 90 ml acid
Yield: 8.85 g (2.4×10^{-2} mol, 68%)

Elemental Analysis: C: 36.60%(36.48), H: 8.71%(8.90), N: 15.32%(15.47)
( ) calculated as $C_{11}H_{32}N_4Cl_4$

L_9.4HCl: 30.5 g (0.035 mol) L_9.4Ts, 90 ml acid
Yield: 8.2 g (2.2×10^{-2} mol, 62%)

Elemental Analysis: C: 38.20%(38.31), H: 9.16%(9.11), N: 15.00%(14.89)
( ) calculated as $C_{12}H_{34}N_4Cl_4$

Ligand Characterisation

Ligand characterisation was carried out as for the macrocyclic ligands. Elemental analyses were shown previously. Relevant spectroscopic data is outlined below.

Infra-red Spectra (as N,N',N'',N'''-tetratosylamines)

$L_7.4Ts$ 3060, 3040, 3020(wsh), 2980(wsh), 2930(mbmu), 2860(msh), 1600(ssh), 1495(msh), 1455(ssh), 1400(wb), 1370(msh), 1340(sb), 1308(msh), 1290(wsh), 1250(wsh), 1215(ssh), 1180(msh), 1155(sb), 1110, 1090(ssh), 1040(msh), 1025 (ssh), 1020(wsh), 970(ssh), 915(ssh), 880, 835(wsh), 810(ssh), 800(wsh), 760(msh), 720(ssh), 695(ssh), 660 (wsh), 640(wsh), 580, 570(msh), 550(ssh), 530(wsh), 510 (wsh), 480, 435(msh).

$L_8.4Ts$ 3060,3020(wsh), 2920, 2860(mb), 1600(ssh), 1495(msh), 1460(mb), 1400(wb), 1340(sb), 1305, 1290(wsh), 1215(wsh) 1185(wsh), 1155(sb), 1120, 1105(wsh), 1090(ssh), 1050 -1030(wshmu), 1015(wsh), 960(mb), 880(mb), 810(ssh), 715, 695(sb), 655, 645(ssh), 580(msh), 550(ssh), 530 (wsh), 475(wb).

$L_9.4Ts$ 3060-3020(wshmw), 2995, 2980(wsh), 2920(ssh), 2860 (msh), 2805(wsh), 1600(ssh), 1495(msh), 1465, 1455(ssh) 1400(wb), 1385, 1380(wsh), 1340(sb), 1320, 1310, 1290 (msh), 1240(wsh), 1215, 1190(msh), 1155(sb), 1120(msh), 1090(sb), 1050(wsh), 1040, 1025, 1015 (msh), 970(ssh),

L_9.4Ts 955(wsh), 910(msh), 850(msh), 835(wsh), 825(msh), 810(ssh), 800(wsh), 760(wsh), 780(msh), 770, 750(ssh), 650(ssh), 585,570(msh), 550(ssh), 535(ssh), 520(msh), 480(msh), 410(msh).

Spectra recorded as KBr discs (L_8.4Ts as a thin film) on a Perkin-Elmer 577 spectrometer.

^{1}H N. M. R. Spectra (as tetrahydrochloride salts)

Chemical shifts are in ppm relative to NaTMS. Spectra were recorded on a Perkin-Elmer R32 spectrometer, 90 Hz, D_2O solvent.

L_7.4HCl 6.50(8H, s), 6.80(4H, t), 7.20(6H, s), 8.15(4H, qi)

L_8.4HCl 6.50(8H, s), 6.85(4H, t), 7.20(6H, s), 8.25(6H, ms)

L_9.4HCl 6.50(8H, s), 6.85(4H, t), 7.20(6H, s), 8.25(4H, m), 8.50(4H, m)

^{13}C N. M. R. Spectra (as tetrahydrochloride salts)

L_7.4HCl 25.31(2C), 35.95(2C), 45.57(2C), 46.99(2C), 50.08(2C)

L_8.4HCl 25.45(1C), 27.80(2C), 35.95(2C), 45.57(2C), 47.05(2C), 50.62(2C)

L_9.4HCl 27.81(2C), 27.93(2C), 35.99(2C), 45.50(2C), 47.01(2C), 50.83(2C)

(ii) Synthesis of L_{10}-L_{12}

The ligands L_{10}-L_{12} were synthesised using two alternative routes as outlined below for L_{10}(route 1) and L_{11}(route 2).

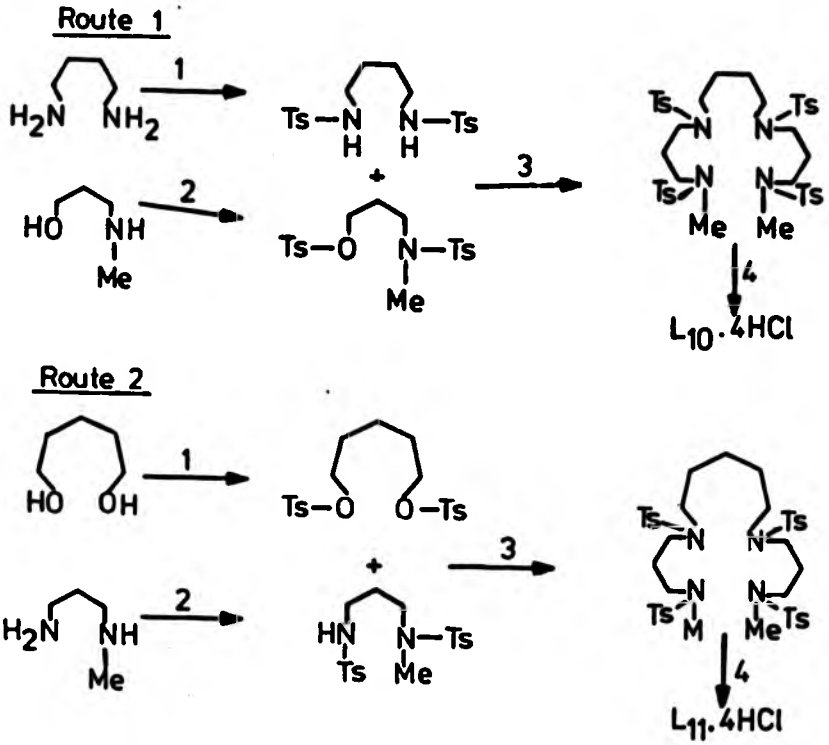

Both of the above routes were found to give products of similar purity, in similar yields. However, using route 2, L_{11}.4Ts was isolated as a solid, where route 1 only gave a sticky, intractable gum.

Route 1: L_{10}, L_{12}

Step 1

Details of this step are outlined in the synthetic procedure for L_7-L_9 (page 29).

Step 2[15]

N,O-ditosyl-N-Methyl-3-aminopropanol was synthesised under conditions similar to those used for the synthesis of N,O-ditosyl-N-Methyl-2-amino-ethanol, by the addition of dry tosyl chloride to an ice/methanol cooled solution of N-Methyl-3-aminopropanol in dry pyridine. The product was isolated by adding to 600 ml ice/water with vigorous mechanical stirring, and was purified by recrystallisation from methanol giving fine needles of a pale yellow solid. ^1H nmr, infra-red spectra, and elemental analysis were consistent with the expected product.

N,O-ditosyl-N-Methyl-3-aminopropanol: 133.7 g (1.5 mol) N-methylamino propan-3-ol, 350 ml dry pyridine, 581.5 g (3.05 mol) Tosyl chloride.
Yield: 312.6 g (0.79 mol, 52.5%)
Elemental Analysis: C: 54.52%(54.39), H: 5.94%(5.83), N: 3.71%(3.52)
( ) calculated as $C_{18}H_{23}NS_2O_5$

Step 3

Conditions for this step were identical to those used for L_7-L_9 (see page 30). Both $L_{10}{}^4Ts$ and $L_{12}{}^4Ts$ were isolated as white semi-crystalline solids after suspension in boiling methanol. Infra-red and ^1H and ^{13}C nmr spectra and elemental analyses were consistent with the expected product.

$L_{10}.4Ts$: 19.8 g (0.05 mol) N,N'-ditosyl-1,4-diaminobutane, 2.7 g NaH
39.7 g (0.10 mol) N,O'-ditosyl-N-methyl-3-aminopropanol
Yield: 40.0 g (0.047 mol, 96%)

Elemental Analysis: C: 56.52%(56.71), H: 6.50%(6.42), N: 6.57%(6.61)
( ) calculated as $C_{40}H_{54}N_4S_4O_8$

$L_{12}.4Ts$ 21.2 g (0.05 mol) N,N'-ditosyl-1,6-diaminohexane, 2.7 g NaH
39.7 g (0.10 mol) N,O-ditosyl-N-methyl-3-aminopropanol
Yield: 38.85 g (0.044 mol, 89%)

Elemental Analysis: C: 57.88%(57.64), H: 6.60%(6.68), N: 6.44%(6.40)
( ) calculated as $C_{42}H_{58}N_4S_4O_8$

Step 4

See step 4, route 2 (page 39)

Route 2

This route was used for the synthesis of L_{11}, as by this method, $L_{11}.4Ts$ was obtained as a solid rather than the intractable gum formed using route 1.

Step 1

O,O'-ditosyl-1,5-pentanediol was synthesized using the method outlined for the macrocyclic ligands on page 21

Step 2

A solution of tosyl chloride (58.0 g, 0.30 mol) in the minimum volume of diethyl ether was added dropwise with stirring to a solution of N-methyl

-1,3-propanediamine (13.2 g, 0.15 mol) in 200 ml water in a two necked round bottomed flask fitted with a condenser and dropping funnel. When the addition was complete (30 minutes), the two phase reaction mixture was stirred for a further three hours. The resulting white precipitate was filtered at the pump, washed with water and diethyl ether, and dried in vacuo over P_2O_5. Elemental anaylses and ^1H nmr and infra-red spectra were consistent with the expected product.

Yield: 47.0 g (0.12 mol, 79%)

Elemental Analysis: C: 54.49%(54.52), H: 5.98%(6.10), N: 7.18%(7.07) ( ) calculated as $C_{18}H_{24}N_2S_2O_4$

Step 3

An excess (2-3x) of NaH(98%, dry) was added in small portions to a stirred solution of N,N'-ditosyl-N-methyl-1,3-propanediamine in dry DMF (30.9 g, 0.078 mol in 200 ml). After stirring for 30 minutes while protected from atmospheric moisture, excess NaH was removed at the pump by filtration directly into the reaction vessel (a 2 necked, 500 ml round bottomed flask fitted with condenser, drying tube and dropping funnel). The resulting solution was heated to 120 °C, with stirring, on an oil bath, and a solution of O,O'-ditosyl-1,5-pentanediol (16.2 g, 0.039 mol) in 100 ml dry DMF was added.

Once addition was completed (30 minutes), the reaction mixture was left stirring for a further four hours at 120 °C. On cooling, the solution was concentrated to 50% of its original volume on a rotary evaporator, and added to three times its volume of ice/water with vigorous mechanical stirring. The pale brown solid precipitate was filtered at the pump, washed with water and ethanol, and dried in vacuo over P_2O_5.

^{1}H nmr and infra-red spectra and elemental analysis were consistent with the expected product.

Yield: 30 g (0.035 mol, 89%)

Elemental Analysis: C: 57.10%(57.18), H: 6.39%(6.55), N: 6.34%(6.51)
( ) calculated as $C_{41}H_{56}N_4S_4O_8$

Step 4 (also step 4, route 1)

As with the macrocyclic ligands and L_7-L_9 , cleavage of the protecting sulphonamide salts was carried out using 80% H_2SO_4 (3:1 H_2SO_4) at 150-160 °C (see page 23).

$L_{10}.4HCl$: 39.0 g (4.6×10^{-2} mol) $L_{10}.4Ts$, 115 ml acid

Yield: 10.5 g (0.028 mol, 61%)

Elemental Analysis: C: 38.09%(38.31), H: 9.02%(9.11), N: 15.08%(14.89)
( ) calculated as $C_{12}H_{34}N_4Cl_4$

$L_{11}.4HCl$: 30.0 g (3.5×10^{-2} mol) $L_{11}.4Ts$, 90 ml acid

yield: 8.7 g (2.2×10^{-2} mol, 64%)

Elemental Analysis: C: 39.91%(40.01), H: 9.40%(9.30), N: 14.31%(14.36)
( ) calculated as $C_{13}H_{36}N_4Cl_4$

$L_{12}.4HCl$: 38.0 g (4.3×10^{-2} mol) $L_{12}.4Ts$, 110 ml acid

Yield: 13.0 g (3.20×10^{-2} mol, 75%)

Elemental Analysis: C: 41.53%(41.60), H: 9.68%(9.47), N: 14.90%(14.89)
( ) calculated as $C_{14}H_{38}N_4Cl_4$

Ligand Characterisation

This was carried out as for previous ligands. Elemental analyses have been shown previously. Relevant spectroscopic data is outline below.

Infra-red Spectra (as N,N',N'',N'''-tetratosyl amines)

L_{10}.4Ts 3090. 3070, 3050(wsh), 3020(msh), 2980, 2960(wsh), 2930 (ssh), 2850(msh), 2805(wsh), (1675 occluded DMF), 1600 (ssh), 1495(ssh), 1460(sb), 1390, 1380(wsh), 1335(sb), 1315, 1310(wsh), 1285, 1265, 1245(msh), 1220(msh), 1200 (wsh), 1155(sb), 1120(msh), 1085(ssh), 1140(ssh), 1115 (msh), 970, 910(ssh), 865(msh), 845(wsh), 820, 800(ssh), 760(sb), 710, 695(ssh), 655(ssh), 645, 630(wsh), 580(ssh), 545(sb), 485, 480(wsh), 450, 425(msh).

L_{11}.4Ts 3080-3020(wshm), 2920(mb), 2860(msh), 1600(ssh), 1495 (msh), 1460(mb), 1400, 1375(wb), 1335(sb), 1305, 1290 (wsh), 1250(wb), 1210, 1200(wsh), 1155(sb), 1120, 1105 (wsh), 1085(ssh), 1015(mb, shoulder at 1035), 990(wsh), 970(wsh), 950(mb), 920(msh), 855, 840(wsh), 870(ssh), 800, 780(wsh), 740(wsh), 725, 710(ssh), 695(msh), 650 (ssh), 580, 565(wsh), 550(ssh), 480, 450(wsh).

L_{12}.4Ts 3060, 3040, 3020, 3000(wsh), 2970(wsh), 2930(mb), 2860 (msh), (1675 occluded DMF), 1600(ssh), 1495(msh), 1460 (mb), 1425, 1400, 1385, 1370(wsh), 11340(wsh), 1310,

$L_{12}.4Ts$ 1300, 1290(wsh), 1260(wsh), 1225(wsh), 1205(wb), 1185 (wsh), 1160(sb), 1110(wb), 1090(msh), 1060(wsh), 1040 (mb), 1020, 1000(wsh), 950, 920(ssh), 870, 840(wsh), 815(ssh), 800(msh), 770(mb), 715(ssh), 700(wsh), 655 (ssh), 645, 630(wsh), 585(wsh), 570(msh), 550(sb), 510, 485, 455(wsh), 410(wb).

Spectra recorded as KBr discs on a Perkin-Elmer 577 spectrometer.

^{1}H N. M. R. Spectra(as tetrahydrochloride salts)

Chemical shifts in ppm relative to NaTMS. Spectra recorded on a Perkin-Elmer R32 spectrometer, 90 MHz ^{1}H, D_2O solvent.

$L_{10}.4HCl$ 6.86(12H, m), 7.25(6H, s), 7.85(4H, m), 8.20(4H, qi)

$L_{11}.4HCl$ 6.85(12H, m), 7.25(6H, m), 7.85(4H, m), 8.30(6H, m)

$L_{12}.4HCl$ 6.85(12H, m), 7.25(6H, m), 7.90(4H, m), 8.30(4H, m), 8.55(4H, m)

^{13}C N. M. R. Spectra(as tetramine tetrahydrochloride salts)

Chemical shifts in ppm relative to NaTMS. Spectra recorded on a Bruker WP 80 spectrometer, 80MHz ^{13}C, D_2O solvent.

$L_{10}.4HCl$ 25.18(2C), 25.38(2C), 35.54(2C), 47.12(2C), 48.47(2C), 49.68(2C)

$L_{11}.4HCl$ 25.08(2C), 25.45(1C), 27.63(2C), 35.50(2C), 47.01(2C), 48.47(2C), 50.04(2C)

$L_{12}.4HCl$ 25.04(2C), 27.73(4C), 35.41(2C), 46.92(2C), 48.40(2C), 50.22(2C)

(b) Diethylated Ligands (L_{13}-L_{16})

The ligands L_{13}-L_{16} were synthesised using the general procedure outlined below for L_{16}.

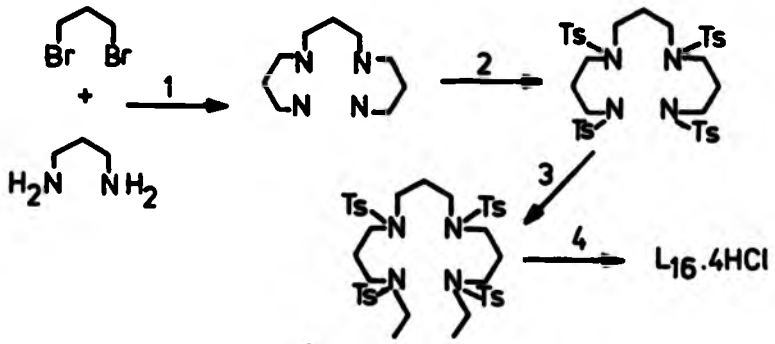

Step 1

The tetramines 1,10-diamino-4,7-diazaoctane (triethylenetetramine, $L_{(VIII)}$) and 1,12-diamino-5,8-diazadecane ($L_{(X)}$) were bought commercially and used without further purification. However 1,11-diamino-4,8-diazanonane ($L_{(IX)}$) and 1,13-diamino-5,8-diazaundecane ($L_{(XI)}$) were synthesized in the laboratory under existing literature conditions using the method described previously (see page 19).

1,13-diamino-5,8-diaminoundecane ($L_{(XI)}$): 67.3 g (0.033 mol) dibromopropane, 222.4 g (3 mol) 1,3-diaminopropane

Yield: 23.5 g (0.125 mol, 38%)

b.pt. 125 °C (0.3 mm Hg)

^{1}H nmr and infra-red spectra were consistent with the expected product.

Step 2

The tetratosylated tetramines were synthesized using the method described previously for the synthesis of $L_{(IX)}$.4Ts and $L_{(X)}$.4Ts (page).

$L_{(VIII)}$.4Ts: 14.6 g (0.1 mol) $L_{(XVIII)}$, 17 g (0.43 mol) NaOH, 78 g (0.41 mol) tosyl chloride.

The product was a brown sticky solid, which was purified by suspension in boiling methanol (~7 ml per gram) giving an off white, semi crystalline solid. ^{1}H nmr and infra-red spectra were consistent with the expected product.

Yield: 64.5 g (0.085 mol, 85%)

$L_{(XI)}$.4TS: 11.9 g (0.07 mol) $L_{(IX)}$, 12 g (0.3 mol) NaOH, 55g (0.28 mol) tosyl chloride.

The product was a white semi-crystalline solid which gave satisfactory ^{1}H nmr and infra-red spectra and was used without further purification.

Yield: 40.3 g (0.051 mol, 73%)

Step 3[8]

The synthetic details for this step are typified by the synthesis of L_{14}.4Ts as described below. 3.36 g (0.14 mol) of dry (98%) NaH was added in small portions to a stirred solution of 30.6 g (0.039 mol)

$L_{(IX)}$.4Ts in 300 ml dry DMF. Once the effervescence had subsided, the mixture was filtered directly into a 1 litre round bottomed flask fitted with a dropping funnel and condenser and drying tube. The pale green solution was heated to 120 °C and 21.9 g (0.14 mol) of ethyl iodide added dropwise with stirring, during which time, the solution became very dark in colour. After the addition was complete, the reaction mixture was stirred at 120 °C for a further 2 hours, cooled, and added directly to 900 ml of ice/water with vigorous mechanical stirring, giving a sticky yellow precipitate, which became a brown glassy solid when oven dried (80 °C). No suitable solvent for recrystallisation was found. Infra-red and ^1H nmr spectra were consistent with the expected product.

Yield: 24.0 g (0.028 mol, 71%)

L_{13}.4Ts: 52 g (0.069 mol) $L_{(VIII)}$.4Ts, 7.6 g NaH, 43 g (0.28 mol) ethyl iodide.

The product was a slightly sticky, yellow solid which was purified by suspension in boiling methanol (~ 10 ml per gram) followed by drying in vacuo over P_2O_5, giving an off-white semi-crystalline solid. Infra-red and ^1H nmr spectra were consistent with the expected product.

Yield: 28.0 g (0.034 mol, 49%)

Elemental Analysis: C: 55.95%(55.72), H: 5.95%(6.15), N: 6.92%(6.84)
( ) calculated as $C_{38}H_{50}N_4S_4O_8$

$L_{15}.4Ts$: 54 g (0.068 mol) $L_{(X)}.4Ts$, 7.6 g NaH, 43 g (0.28 mol) ethyl iodide.

As with $L_{13}.4Ts$ this was a yellow, slightly sticky solid which was purified by suspension in boiling methanol (~10 ml per gram) and drying in vacuo over P_2O_5, giving a very pale yellow, semi-crystalline solid. Infra-red and ^1H nmr spectra were consistent with the expected product.

Yield: 32.6 g (0.038 mol, 57%)

Elemental Analysis: C: 56.60%(56.72), H: 6.38%(6.42), N: 6.52%(6.61) ( ) calculated as $C_{40}H_{54}N_4S_4O_8$

$L_{16}.4Ts$: 55 g (0.068 mol) $L_{(XI)}.4Ts$, 7.6 g NaH, 43 g (0.28 mol) ethyl iodide.

As with $L_{14}.4Ts$, the product was a very sticky yellow solid which became a dark brown glassy solid when oven dried (80 °C). No suitable solvent was found for re-crystallisation. Infra-red and ^1H nmr spectra were consistent with the expected product.

Yield: 48.3 g (0.036 mol, 82%)

Step 4

The cleavage of the sulphonamide protecting groups was accomplished using the method outlined previously for L_1 - L_{12}, using 80% H_2SO_4 at 150-160 °C for 1 hour. During this period, any iodine adsorbed onto the product in the previous step was evolved as iodine vapour. As with previous ligands, double re-crystallisation from aqueous EtOH gave analytically pure tetrahydrochloride salts.

$L_{13}.4HCl$: 27.5g (3.4×10^{-2}mol) $L_{13}.4Ts$, 70 ml acid

Yield: 6.7g (1.9×10^{-2}mol), 57%)

Elemental Analysis: C: 34.52%(34.50), H: 8.76%(8.68), N: 16.02%(16.07)

( ) calculated as $C_{10}H_{30}N_4Cl_4$

$L_{14}.4HCl$: 24.0g (2.8×10^{-2}mol) $L_{14}.4Ts$, 70 ml acid

Yield: 6.1g (1.7×10^{-2}mol, 60%)

Elemental Analysis: C: 36.65%(36.48), H: 9.00%(8.90), N: 15.53%(15.45)

( ) calculated as $C_{11}H_{32}N_4Cl_4$

$L_{15}.4HCl$: 32.0g (3.8×10^{-2}mol) $L_{15}.4Ts$, 90 ml acid

Yield: 7.3g (1.9×10^{-2}mol, 51%)

Elemental Analysis: C: 38.40%(38.31), H: 9.29%(9.11), N: 15.00%(14.89)

( ) calculated as $C_{12}H_{34}N_4Cl_4$

$L_{16}.4HCl$: 45.0g (5.2×10^{-2}mol) $L_{16}.4Ts$, 120 ml acid

Yield: 11.3g (2.9×10^{-2}mol, 56%)

( ) calculated as $C_{13}H_{36}N_4Cl_4$

Ligand Characterization

Chemical analyses have already been discussed. Relevant spectroscopic data is outlined below.

Infra-red Spectra(As N,N',N'',N'''-tetratosyl amines)

$L_{13}.4Ts$: 3020(wsh), 2960(msh), 2925, 2860(wsh), 1600(ssh) 1490(msh), 1460(ssh), 1400, 1380(wb), 1340(sb),1330 1305(wsh), 1290, 1260(msh), 1195(ms), 1185(wsh), 1155 (sb), 1120, 1090(ssh), 1040(wsh), 1020(wsh), 1005(ssh), 920(msh), 820, 810(ssh), 785(wsh), 750(wsh),725,695 (ssh), 645(ssh), 605(wsh), 550(ssh), 540, 480(wsh), 430(wb)

L_{14}.4Ts 3050(wsh), 2980(ssh), 2920, 2860(ssh), 1600(ssh), 1495 (msh), 1470(msh), 1400(wsh), 1340, 1330(wsh), 1310(wb), 1280, 1250(msh), 1180, 1160(wsh), 1120(wsh), 1090(ssh), 1050(wsh), 1020(wsh), 1000(msh), 970–950(wb), 820, 805 (ssh), 775, 750(msh), 720, 700(ssh), 650(ssh), 550(ssh), 490(msh), 440(mb).

L_{15}.4Ts 3060, 3025(wsh), 2980(msh), 2920, 2860(mb), 1600(ssh), 1495(ssh), 1470(ssh), 1400(msh), 1340(ssh), 1310(wb), 1300(wsh), 1275, 1250(msh), 1220(wsh), 1180(wsh), 1160 (sb), 1135, 1120(wsh), 1090(ssh), 1060(msh),1040(wb), 1020, 1000(msh), 985(ssh), 940(msh), 890(wsh), 860(msh), 850(wsh), 820(ssh), 800(msh), 770(wsh), 745(wsh), 720 (ssh), 700(msh), 650(sb), 575(mb), 550(ssh), 510, 490 (wsh), 450(msh), 415(wsh).

L_{16}.4Ts 3050–3020(wbmu), 2960, 2920, 2860(wsh), (1675 occluded DMF), 1600(ssh), 1495(msh), 1470–1450(mbmu), 1400(wsh), 1380(wsh), 1330(sb), 1300, 1285(wsh), 1235(wb), 1155 (sb, shoulder at 1185), 1115(wb), 1090(msh), 1020(wsh), 995(wb), 925(mb), 845(wb), 815(ssh), 800(wsh), 770(wb), 780,760, 740(msh), 650(sb), 570(wsh), 550(ssh), 480(wb).

Spectra recorded as KBr discs on a Shimadzu IR-43T spectrometer.

^{1}H N. M. R. Spectra (as tetrahydrochloride salts)

Chemical shifts in ppm relative to NaTMS. Spectra recorded on a Perkin-Elmer R32 spectrometer, 90 MHz ^{1}H, D_2O solvent.

$L_{13}.4HCl$ 6.45(12H, d), 6.80(4H, qu), 8.70(6H, t)

$L_{14}.4HCl$ 6.50(12H, s), 6.75(6H, m), 8.70(6H, t)

$L_{15}.4HCl$ 6.50(12H, s), 6.80(8H, m), 8.70(6H, t)

$L_{16}.4HCl$ 6.80(20H, m), 8.70(6H, t)

^{13}C N. M. R. Spectra (as tetrahydrochloride salts)

Chemical shifts in ppm relative to NaTMS. Spectra recorded on a Bruker WP 80 specrometer, 80 MHz ^{13}C, D_2O solvent.

$L_{13}.4HCl$ 13.13(2C), 44.97(2C), 46.18(6C)

$L_{14}.4HCl$ 13.13(2C), 25.24(2C), 45.03(2C), 45.84(2C), 46.25(2C),47.52(2C)

$L_{15}.4HCl$ 13.15(2C), 25.32(2C), 45.80(4C), 46.41(2C), 47.80(2C)

$L_{16}.4HCl$ 13.13(2C), 25.30(3C), 45.70(2C), 46.42(2C), 47.27(4C)

1,14- diamino-5,10-diazadodecane (Spermine. L_{17})

This ligand was purchased commercially from "Fluka" and was purified by short path "bulb-to-bulb" distillation under reduced pressure(rotary oil pump). The analytically pure tetrahydrochloride salt was obtained by the addition of an excess of hydrochloric acid (AnalAr grade) to an ethanolic solution of the free amine, followed by a double recrystallisation from aqueous ethanol.

Ligand Characterisation $L_{17}.4HCl$

Relevant spectroscopic and gravimetric data are outlined below.

^{1}H N. M. R. Spectrum (as tetrahydrochloride salt)

Chemical shift in ppm relative to NaTMS. Spectrum recorded on a Perkin-Elmer R32 spectrometer, 90 MHz ^{1}H, D_2O as solvent.

6.85(12H, m), 8.20(8H, m)

^{13}C N. M. R. Spectrum (as tetrahydrochloride salt)

Chemical shift in ppm relative to NaTMS. Spectrum recorded on a Bruker WP 80 spectrometer, 80 MHz ^{13}C, D_2O as solvent.

25.45(2C), 26.39(2C), 39.24(2C), 47.19(2C), 47.68(2C)

Elemental Analysis: C: 34.66%(34.70), H: 8.25%(8.15), N: 16.01%(16.19)

( ) calculated as $C_{10}N_4H_{30}Cl_4$

Isolation and Purification of free amines

The free amines L_1-L_{16} were liberated from the corresponding tetrahydrochloride salts by the addition of the salt to a strong (approximately 15M) solution of NaOH. The amines are insoluble in this medium, and float to the surface. It was found most convenient to recover the amines by extraction from the NaOH solution into chloroform. The chloroform layer was then separated and left standing over anhydrous $MgSO_4$ for 24 hours to remove excess water. After removing the $MgSO_4$ by filtration at the pump, the chloroform was evaporated under reduced pressure on a rotary evaporator, leaving the impure amine.

Amine Purification

a) Macrocyclic Ligands

The macrocyclic ligands L_1-L_5 were purified by fusion with KOH followed by vacuum sublimation. This procedure was carried out three times, giving rise to the white, solid, analytically pure macrocycles. Melting ranges, determined on a Perkin-Elmer DSC II, were of the order of 1 °C in all cases. Unlike L_1-L_5, L_6 proved to be a very viscous liquid, and was purified using the method outlined below for the acyclic ligands. The macrocyclic ligands proved to be reasonably stable when exposed to the atmosphere for a short period of time, but absorbed water to become sticky and opalescent if left exposed to the atmosphere for long periods.

Physical Characteristics

L_1 white, solid, m.pt. 99 °C, Sublimes at (45 ± 5) °C at approximately 0.3 mm Hg.

L_2 white, solid, m.pt. 85 °C. Sublimes at (50 ± 5) °C at approximately 0.3 mm Hg.

L_3 white, solid, m.pt. 57 °C. Sublimes at (60 ± 5) °C at approximately 0.3 mm Hg.

L_4 white, solid, m.pt. 46 °C. Sublimes at (65 ± 5) °C at approximately 0.3 mm Hg.

L_5 white, solid, m.pt. 69 °C. Sublimes at (75 ± 5) °C at approximately 0.3 mm Hg.

L_6 colourless, liquid, b.pt. (120 ± 5) °C at approximately 0.3 mm Hg.

b) Non-cyclic ligands(Plus L_8 and L_{17})

Purification of the above amines was achieved by careful repeated short path bulb-to-bulb distillation from Na metal under reduced pressure (rotary oil pump). All necessary handling of the amines was carried out in a glove box with an N_2 atmosphere. On exposure to the atmosphere, the acyclic liganda (L_7-L_{17}) underwent rapid hydration, forming solid, crystalline hydrates.

Physical Characteristics

L_7 Colourless liquid, b.pt.(115 ± 5) °C at approximately 0.5 mm Hg.

L_8 Colourless liquid, b.pt. (135 ± 5) °C at approximately 0.5 mm Hg.

L_9 Colourless crystalline solid, m.pt. 41 °C, b.pt. (150 ± 5) °C at approximately 0.5 mm Hg.

L_{10} Colourless liquid, b.pt. (145 ± 5) °C at approximately 0.5 mm Hg.

L_{11} Colourless liquid, b.pt. (155 ± 5) °C at approximately 0.5 mm Hg.

L_{12} Colourless crystalline solid, m.pt. 36 °C, b.pt. (165 ± 5) °C at approximately 0.5 mm Hg.

L_{13} Colourless liquid, b.pt. (115 ± 5) °C at approximately 0.5 mm Hg.

L_{14} Colourless liquid, b.pt. (130 ± 5) °C at approximately 0.5 mm Hg.

L_{15} Colourless liquid, b.pt. (140 ± 5) °C at approximately 0.5 mm Hg.

L_{16} Colourless liquid, b.pt. (150 ± 5) °C at approximately 0.5 mm Hg.

L_{17} Colourless crystalline solid, m.pt. 39 °C (lit 40 °C) b.pt. (155 ± 5) °C at approximately 0.5 mm Hg.

Synthesis of N-methyl-3-aminopropan-1-ol

Unlike the other starting materials for synthesis of the ligands L_1-L_{17}, N-methyl-3-aminopropan-1-ol was not available commercially. The synthesis was carried out as outlined below, using a variation on the procedure used by J S Pierce.[16]

$$Cl(CH_2)_3OH \xrightarrow{COCl_2} Cl(CH_2)_3CO_2Cl \quad (1)$$

$$Cl(CH_2)_3CO_2Cl \xrightarrow{MeNH_2} Cl(CH_2)_3CO_2HNMe \quad (2)$$

$$Cl(CH_2)_3CO_2HNMe \xrightarrow{xs\ KOH} HO(CH_2)_3HNMe \quad (3)$$

Step 1: γ-chloropropyl chloroformate

This is readily obtained in high yield by the careful addition with stirring (under a fume hood) of 1 mole of phosgene (20% w/v in toluene) to 1 mole of ice/salt cooled 3-chloropropan-1-ol in a three necked two litre round bottomed flask fitted with dropping funnel, condenser and mechanical stirrer. The solution was then allowed to warm to room temperature, and was left standing for 12 hours. After washing with H_2O and dilute Na_2CO_3 solution, the excess toluene was removed under reduced pressure on a rotary evaporator, and the resulting oil distilled at atmospheric pressure to give a colourless oil.

Yield: 96.4 g (0.62 mol, 62%), b.pt. 180 °C (literature 177 °C)

Product Characterisation

^{1}H N. M. R. Spectrum

Chemical shifts in ppm relative to TMS. Spectrum recorded on a Perkin-Elmer R24 spectrometer. ^{1}H 60 MHz, $CDCl_3$ solvent.

5.20(2H, t), 6.00(2H, t), 7.45(2H, qi)

Infra-red Spectrum

Spectrum recorded as a thin film on a Perkin-Elmer 577 spectrometer using NaCl plates.

2950(msh), 1760(ssh), 1440(msh), 1415(wsh), 1365(msh) 1290(msh), 1145(sb, shoulder at 1220), 990(msh), 875(mb) 810(ssh, shoulder at 775), 720(wsh), 680, 650(msh), 570 (sb).

Step 2: ɣ -chloropropyl methylcarbamate

96.4 g (0.62 mol) of ɣ -chloropropyl chloroformate was added dropwise to a stirred solution of methylamine (100 mls of 40% w/v solution, 1.2 moles methylamine) in a 500 ml two necked round bottomed flask fitted with mechanical stirrer and dropping funnel. After two hours stirring, the resulting product, an oil immiscible with water, was extracted with several portions of diethyl ether. The diethyl ether solution was then washed with several portions of 1:3 HCl solution and with water, and was dried over anhydrous $MgSO_4$. Removal of the diethyl ether under reduced pressure on a rotary evaporator gave the product, ɣ -chloropropyl methylcarbamate in good yield.

Yield: 75 g (0.495 mol, 81%)

Product Characterisation

^{1}H N. M. R. Spectrum

Chemical shifts in ppm relative to TMS. Spectrum recorded on a Perkin-Elmer R24 spectrometer, ^{1}H 60 MHz, $CDCl_3$ solvent.

5.85(2H, t), 6.45(2H, t), 7.30(3H, s), 8.00(2H, qi)

Infra-red Spectrum

Spectrum recorded as a thin film on a Perkin-Elmer 577 spectrometer using NaCl plates.

3310(sb), 2930(sb), 1680(sb), 1515(sb, shoulder at 1440), 1320(wsh), 1240(sb), 1125(ssh), 1100(wsh), 1000(msh), 945 (msh), 865(wb), 765(msh), 710(wb), 640, 600(wb).

Step 3: ɣ -methylaminopropan-1-ol

ɣ -chloropropyl methylcarbamate (75 g, 0.495 mol) was added to a solution of 4 equivalents of KOH (112 g, 2 mols) in 400 mls ethanol in a one necked, 1L round bottomed flask fitted with a condenser. The two phase mixture was then heated to reflux on a steam bath for two hours, cooled, and filtered at the pump to remove inorganic solids. A considerable excess of K_2CO_3 was then added to the ethanolic solution which was left standing for two hours with occasional stirring. The resulting inorganic solids were removed by filtration at the pump, and the ethanol removed under reduced pressure on a rotary evaporator, leaving a slightly yellow oil. This oil was purified by distillation under reduced pressure to give a colourless, sweet smelling viscous oil.

Yield: 10.6 g (0.12 mol, 24%), b.pt. 84-86 °C (approximately 3 mm Hg)

Product Characterisation

^{1}H N. M. R. Spectrum

Chemical shifts in ppm relative to TMS. Spectrum recorded on a Perkin-Elmer R32 spectrometer, ^{1}H 90 MHz, $CDCl_3$ solvent.

6.10(2H, s(OH + NH)), 6.35(2H, t), 7.30(2H, t), 7.60(3H, s), 8.30(2H, qi)

Infra-red Spectrum

Spectrum recorded as a thin film on a Perkin-Elmer 577 spectrometer using NaCl plates.

3500-3200(sb), 2940, 2860(sb), 2800(msh), 1515, 1495(wsh), 1480(sb), 1450(ssh), 1380(sb), 1295(wb), 1260(msh), 1110 (ssh, shoulder at 1140), 1065(sb, shoulder ar 1040), 800, 790(wsh).

Elemental Analysis: C: 53.71%(53.90), H: 12.29%(12.44), N: 15.93%(15.71)
( ) calculated as $C_4H_{11}ON$

Copper(II) Complex Formation

$[CuL_1](ClO_4)_2$

25 ml of a methanolic copper(II) perchlorate hexahydrate solution (0.4M, 2 mmol) was added slowly to a stirred solution of L_1 (0.43 g, 2 mmol) in 75 ml of ethanol. After a few minutes of gentle stirring, the finely divided purple product crystallised, leaving a pale purple mother liquor. The product was filtered at the pump and washed liberally with 2-propanol, ethanol, and finally with diethyl ether. Drying in vacuo over P_2O_5 gave an analytically pure, purple microcrystalline product.

Yield: 0.76 g (1.6 mmol, 80%)

Infra-red Spectrum:

3500(mb), 3180(msh), 2910, 2860(msh), 1830(mb), 1475, 1435(mb), 1380(wsh), 1300(wb), 1140, 1090 (sb), 1030(wsh), 960(wsh), 885(msh), 625(ssh), 560(wb).

Visible Spectra:

Aqueous solution, 5.36×10^{-3}M, λ_{max} = 536 nm, ε = 107 $mol^{-1}dm^3cm^{-1}$

Diffuse reflectance, λ_{max} = 520 nm

Elemental Analysis: C: 27.20%(27.11), H: 5.56%(5.50), N: 11.63%(11.75)

( ) calculated as $Cu(C_{11}H_{26}N_4)(Cl_2O_8)$

$[CuL_2](ClO_4)_2$

L_2 (0.46 g, 2 mmol) was treated in the same manner as L_1. The resulting solids were filtered at the pump, washed with 2-propanol, ethanol and diethyl ether, and dried in vacuo over P_2O_5. This yielded an analytically pure finely divided, purple crystalline product.

Yield: 0.75 g (1.5 mmol, 76%)

Infra-red Spectrum:

3410(msh), 3200(ssh),2910, 2860(msh), 2000(wb), 1660(wsh), 1615(wsh), 1490(wsh), 1445, 1435(msh), 1370(wsh), 1340(wsh), 1300(wsh), 1250, 1230(wsh), 1140, 1080(sb), 1020(wsh), 990(wsh), 950(msh), 890(msh), 865(wsh), 820(wsh), 795(wsh),625(ssh), 540(wb).

Visible Spectra:

Aqueous solution, 5.12×10^{-3}M, λ_{max} = 547 nm, ε = 114 $mol^{-1} dm^3 cm^{-1}$

[lit. value, λ_{max} = 524 nm ε = 90 mol^{-1} dm^3 cm^{-1} [17]]

Diffuse reflectance, λ_{max} = 524 nm

Elemental Analysis: C: 29.51%(29.37), H: 6.00%(5.75), N: 11.37%(11.42)

( ) calculated as $Cu(C_{12}H_{28}N_4)(Cl_2O_8)$

$[CuL_3](ClO_4)_2$

L_3 (0.48 g, 2 mmol) was also treated like L_1. The resulting solids were recrystallised from ethanol, filtered at the pump, and washed liberally with 2-propanol, ethanol, and finally with diethyl ether. Drying in vacuo over P_2O_5 yielded an analytically pure, finely divided, purple crystalline product.

Yield: 0.70 g (1.4 mmol, 69%)

Infra-red Spectrum:

3240(ssh), 3100(ssh), 2910, 2860(ssh), 2810(wsh), 2000(wb), 1630(wb), 1465(sb), 1430(ssh), 1385, 1360(wb), 1300(msh), 1265(wsh), 1240, 1220(wsh), 1140, 1080(sb), 930(wsh), 905(msh), 880(msh), 845 (msh), 820(wsh), 795(msh), 620(ssh), 600(wsh),580 (wsh), 560(wsh), 520(wsh), 425(wb).

Visible Spectra:

Aqueous solution, 5.10×10^{-3}M, λ_{max} = 549 nm, ε= 145 $mol^{-1}dm^3\ cm^{-1}$

[lit. value, λ_{max} = 568 nm, ε= 213 $mol^{-1}\ dm^3\ cm^{-1}$ [17]]

Diffuse reflectance, λ_{max} = 517 nm

Elemental Analysis: C: 31.10%(30.93), H: 6.21%(5.99), N: 10.97%(11.10)

( ) calculated as $Cu(C_{13}H_{30}N_4)(Cl_2O_8)$

$[CuL_4](ClO_4)_2$

L_4 (0.46 g, 2 mmol) was treated in the same manner as L_1. The resulting solids were filtered at the pump, washed with 2-propanol, ethanol and diethyl ether, and dried in vacuo over P_2O_5. This procedure yielded an analytically pure, finely divided purple crystalline product.

Yield: 0.80 g (1.6 mmol, 81%)

Infra-red Spectrum:

3400(mb), 32400(ssh), 3100(ssh), 2910, 2860(ssh), 2000(wb), 1630(wb), 1440(sb), 1390(mb), 1335(wsh), 1310, 1295, 1280(msh), 1240(wsh), 1120, 1080(sb), 950, 940(wsh), 930(wsh), 900(wsh), 890, 885(msh), 810(wb), 780(msh), 620(ssh), 560(wsh), 540, 520 (wb), 430(wb).

Visible Spectra:

Aqueous solution, 5.20×10^{-3}M, λ_{max} = 543 nm, ε = 172 $mol^{-1}dm^3cm^{-1}$

Diffuse Reflectance, λ_{max} = 514 nm

Elemental Analysis: C: 29.27%(29.37), H: 5.90%(5.75), N: 11.34%(11.42)

( ) calculated as $Cu(C_{12}H_{28}N_4)(Cl_2O_8)$

$[CuL_5](ClO_4)_2$

L_5 (0.48 g, 2 mmol) was treated in the same manner as L_1. The resulting solids were filtered at the pump, washed with 2-propanol, ethanol and diethyl ether and dried in vacuo over P_2O_5. This procedure yielded an analytically pure, finely divided, purple crystalline product.
Yield: 0.81 g (1.6 mmol, 80%)

Infra-red Spectrum:

3400(mb), 3220(ssh), 3120(msh), 2910, 2860(ssh), 2000(wb), 1630(wb), 1440, 1430(sb), 1360, 1350(msh), 1280(msh), 1265(msh), 1250, 1230(vsh), 1120, 1080 (sb), 950(vsh), 930(vsh), 920(msh), 870(msh),835 (vsh), 815(vsh), 795(vsh), 760(vsh), 620(ssh), 560 (wb).

Visible Spectra:

Aqueous solution, 4.60×10^{-3}M, λ_{max} = 533 nm, ε = 181 $mol^{-1}dm^3cm^{-1}$
Diffuse reflectance, λ_{max} = 514 nm

Elemental Analysis: C: 31.88%(31.93), H: 6.01%(5.99), N: 10.87%(11.10)
( ) calculated as $Cu(C_{13}H_{30}N_4)(Cl_2O_8)$

$[CuL_6](ClO_4)_2$

L_6 (0.5 g, 2 mmol) was treated in the same manner as L_1. The resulting solids were recrystallised from ethanol, filtered at the pump, and washed liberally with small portions of 2-propanol, ethanol and diethyl ether. Drying in vacuo over P_2O_5 gave an analytically pure, purple crystalline product.

Yield: 0.76 g (1.5 mmol, 73%)

Infra-red Spectrum:

3420(ssh), 3260(msh), 3140(ssh), 2900, 2860(ssh), 2000(wsh), 1610(wsh), 1500, 1490(wsh), 1450, 1425 (msh), 1390(wsh), 1360(wb), 1330(wsh), 1290, 1280 (wsh), 1140, 1090(sb), 1005(wsh), 990(ssh), 960 (msh), 940(wsh), 905(wsh), 890(msh), 870(wsh), 850 (wsh), 830(wsh), 810(msh), 760(wsh), 625(ssh), 540 (sb), 425(mb).

Visible Spectra:

Aqueous solution, 5.06×10^{-3}M, λ_{max} = 546 nm, ε = 108 $mol^{-1}dm^3cm^{-1}$

Diffuse reflectance, λ_{max} = 518 nm

Elemental Analysis: C: 32.51%(32.40), H: 6.30%(6.22), N: 10.95%(10.80)

( ) calculated as $Cu(C_{14}H_{32}N_4)(Cl_2O_8)$

$[CuL_7](ClO_4)_2$

5 ml of methanolic copper(II) perchlorate hexahydrate solution (0.4M, 2 mmol) was added slowly to a stirred solution of L_7 (0.40 g, 2 mmol) in 25 ml of methanol. The resulting blue-purple solution was then reduced carefully to a small volume (1-2 ml), and 10 mls of 1:1 methanol: diethyl ether added. On standing, the resultant solution yielded a small amount of blue-purple crystals. These were filtered at the pump and washed with ice cooled methanol and diethyl ether before drying in vacuo over P_2O_5. This procedure yielded analytically pure blue-purple crystalline product in a moderate yield.

Yield: 0.32 g (0.7 mmol, 34%)

Infra-red Spectrum:

3400(mb), 3210, 3160(ssh), 2910, 2860(ssh), 2000 (wsh), 1620(wb), 1440(sb), 1360(wsh), 1290(wsh), 1265(wsh), 1120, 1080(sb), 990, 970, 955(ssh), 890 (msh), 860(ssh), 625(ssh), 560(wsh).

Visible Spectra:

Aqueous solution, 5.11×10^{-3}M, λ_{max} = 560 nm, ε = 120 $mol^{-1}dm^3cm^{-1}$

Diffuse reflectance, λ_{max} = 532 nm

Elemental Analysis: C: 25.70%(25.84), H: 5.66%(5.64), N: 12.12%(12.05)

( ) calculated as $Cu(C_{10}H_{26}N_4)(Cl_2O_8$

$[CuL_8](ClO_4)_2$

L_8 (0.45 g, 2 mmol) was treated with 5 ml of a methanolic copper(II) perchlorate hexahydrate solution (0.4M, 2 mmol) in the same manner as L_7. The resulting solids were filtered at the pump and washed with ice cooled methanol and diethyl ether before drying in vacuo over P_2O_5. This procedure yielded an analytically pure, blue-purple crystalline product in moderate yield.

Yield: 0.35 g (0.7 mmol, 37%)

Infra-red Spectrum:

3420(mb), 3280(msh), 3230(msh), 2910, 2860(msh), 2000(wb), 1640(mb), 1460(mb), 1380(wsh), 1350(wb), 1275(wsh), 1140, 1080(sb), 860(wb), 730(wb), 625 (ssh), 520(wb).

Visible Spectra:

Aqueous solution, 6.00×10^{-3}M, λ_{max} = 586 nm, ε = 77 $mol^{-1}dm^3cm^{-1}$

Diffuse reflectance, λ_{max} = 538 nm

Elemental Analysis: C: 27.64%(27.59), H: 5.72%(5.89), N: 11.63%(11.70)

( ) calculated as $Cu(C_{11}H_{28}N_4)(Cl_2O_8)$

$[CuL_9](NO_3)_2$

5 ml of a methanolic solution of copper(II) nitrate (0.4M, 2mmol) was added to an equimolar amount of L_9 in 25 ml of water (0.46 g), slowly with stirring. The resulting blue solution was carefully evaporated to a small volume (1-2 mls), and 25 ml of hot ethanol added. On cooling, crystallisation of a blue product took place. The product was recrystallised from ethanol, washed with ethanol and diethyl ether, and dried in vacuo over P_2O_5. The resulting blue crystalline product was analytically pure and was formed in moderate yield.

Yield: 0.43 g (1 mmol, 51%)

Infra-red spectrum:

3400(mb), 3180(mb), 2910, 2860(msh), 1765(wsh), 1635(mb), 1480, 1460(sb), 1270(wsh), 1085(wsh), 1060(msh), 1020(wb), 965(msh), 860, 835(msh), 730 (wb), 595, 540(wb).

Visible Spectra:

Aqueous solution, 4.88×10^{-3}M, λ_{max} = 570 nm, ε = 127 $mol^{-1}dm^3cm^{-1}$

Diffuse reflectance, λ_{max} = 554 nm

Elemental Analysis: C: 34.61%(34.48), H: 7.20%(7.23), N: 13.37%(13.41)

( ) calculated as $Cu(C_{12}H_{30}N_4)(N_2O_6)$

$[CuL_{13}](NO_3)_2$

5 ml of a methanolic solution of copper(II) nitrate (0.4 M, 2 mmol) was added to 1 equivalent (0.40 g, 2 mmol) of L_{13} in 25 ml of ethanol. The solution was evaporated to dryness on a steam bath, leaving a pale blue, very sticky mass. Numerous attempts at recrystallisation from various solvents proved unsuccessful. Drying in vacuo over P_2O_5 gave a blue glassy solid which quickly became a sticky gum again on exposure to the atmosphere. However, the infra-red spectrum is consistent with the expected product.

Yield: (approximately) 0.7 g (0.18 mmol, 90%)

Infra-red Spectrum:

(thin film, NaCl plates)

3400(sb), 3200(ssh), 2920, 2880(msh), 2410(wsh), 2350(wb), 2050(wsh), 1785(wsh), 1740(wb), 1650(mb), 1350(sb), 1160(wb), 1120(wb), 1080(msh), 1040(wsh), 1000(mb), 920(wb), 840, 830(msh), 780(wb).

Visible Spectrum:

Aqueous solution, 7.6×10^{-3}M, λ_{max} = 590 nm, ε = 160 $mol^{-1}dm^3cm^{-1}$

$[CuL_{14}](ClO_4)_2$

L_{14} (0.43 g, 2 mmol) was treated in the same manner as L_1. The resulting solids were recrystallised from a small quantity of ethanol, washed with ethanol and diethyl ether, and dried in vacuo over P_2O_5, giving an analytically pure purple crystalline product in moderate yield.

Yield: 0.58 g (1.2 mmol, 61%)

Infra-red Spectrum:

3420(ssh), 3180(ssh), 2910, 2860(msh), 2000(wsh), 1625(wb), 1460, 1445, 1420(msh), 1380(msh), 1295 (wsh), 1260(wsh), 1140, 1085(sb), 1980(msh), 940 (wsh), 915(wsh), 880(wsh), 845, 835(wsh), 800(wb), 625(ssh), 560(wb).

Visible Spectra:

Aqueous solution, 4.95×10^{-3}M, λ_{max} = 542 nm, ε = 117 $mol^{-1}dm^3cm^{-1}$

Diffuse reflectance, λ_{max} = 525 nm

Elemental Analysis: C: 27.68%(27.59), H: 5.86%(5.89), N: 11.82%(11.70)

( ) calculated as $Cu(C_{11}H_{28}N_4)(Cl_2O_8)$

$[CuL_{15}](NO_3)_2$

5 ml of a methanolic solution of copper(II) nitrate (0.4M, 2 mmol) was added slowly with stirring to one equivalent of L_{15} (0.46 g, 2 mmol) in water. The resulting purple solution was evaporated to dryness on a water bath, and the resulting purple solids recrystallised from ethanol. The purple crystalline product was filtered at the pump, washed with ethanol and diethyl ether, and dried in vacuo over P_2O_5. The analytically pure product was formed in moderate yield.

Yield: 0.66 g (1.3 mmol, 67%)

Infra-red Spectrum:

3410(mb), 3120(ssh), 2910, 2860(msh), 1760(wsh), 1625(wb), 1380(sb), 1275(wsh), 1240(wb), 1200 (wsh), 1160(wsh), 1140, 1120(wsh), 1080(msh), 1020(msh), 920(wsh), 900(wsh), 880, 860(wsh), 825(msh), 800(wsh), 770(wb), 565(wb).

Visible Spectra:

Aqueous solution, 7.54×10^{-3}M, λ_{max} = 554 nm, ε = 158 $mol^{-1}dm^3cm^{-1}$

Diffuse reflectance, λ_{max} = 536 nm

Elemental Analysis: C: 29.19%(29.24), H:6.18%(6.14), N: 11.30%(11.37)

( ) calculated as $Cu(C_{12}H_{30}N_4)(N_2O_6)$

$[CuL_{16}](ClO_4)_2$

5 ml of a methanolic solution of copper(II) perchlorate hexahydrate (0.4M, 2 mmol) was added slowly with stirring to one equivalent of L_{16} (0.49 g, 2 mmol) in 25 ml of methanol. The resulting blue solution was evaporated to a small volume (1-2 ml) on a water bath, and 25 ml cold ethanol added to precipitate the product. The resulting blue solids were recrystallised from ethanol. The product was filtered at the pump, washed with ethanol and diethyl ether and dried in vacuo over P_2O_5, giving an analytically pure purple crystalline product in moderate yield.

Yield: 0.70 g, (1.4 mmol, 69%)

Infra-red Spectrum:

3400(mb), 3200(ssh), 2910, 2860(msh), 1620(wb), 1450(mb), 1380(wsh), 1300(wb), 1260(wb), 1140, 1080(sb), 920(wsh), 880(wsh), 800(wsh), 625(ssh), 560(wb).

Visible Spectra:

Aqueous solution, 5.03×10^{-3}M, λ_{max} = 623 nm, ε = 251 $mol^{-1}dm^3cm^{-1}$

Diffuse reflectance, λ_{max} = 595 nm

Elemental Analysis: C: 30.82%(30.87), H: 6.41%(6.36), N: 10.98%(11.05)

( ) calculated as $Cu(C_{13}H_{32}N_4)(Cl_2O_8)$

$[CuL_{17}](ClO_4)_2$

L_{17} (0.40 g, 2 mmol) was treated in the same manner as L_1. The resulting solids were recrystallised from a small quantity of ethanol, filtered at the pump, washed with ethanol and diethyl ether, and dried in vacuo over P_2O_5. This procedure gave an analytically pure blue/purple crystalline product in good yield.

Yield: 0.79 g (1.7 mmol, 85%)

Infra-red Spectrum:

3440, 3380(msh), 3290(ssh), 3150, 3100(ssh), 2910, 2860(msh), 1600(ssh), 1445(mb), 1390(wsh, mu), 1300(wsh), 1285(wsh), 1255(wsh), 1140, 1105 1085(sb), 1020(wsh), 920, 900(wsh), 830(wsh), 800(wb), 700(wb), 625(ssh), 560, 530(wb), 470(wb).

Visible Spectra:

Aqueous solution, 6.75×10^{-3}M, λ_{max} = 560 nm, ε = 142 $mol^{-1}dm^3cm^{-1}$

Diffuse reflectance, λ_{max} = 538 nm

Elemental Analysis: C: 25.81%(25.84), H: 5.68%(5.64), N: 12.17%(12.08)

( ) calculated as $Cu(C_{10}H_{26}N_4)(Cl_2O_8)$

Chapter 3

POTENTIOMETRY

Apparatus and Methodology

The stepwise protonation constants (log K_{1-4}) of L_1-L_{17}, and the copper(II) complex formation constants (log K_{CuL}) for L_{1-9} and L_{13}-L_{17} were measured potentiometrically using a commercial automatic titrator with an integral pH - mv meter, burette and printer. Due to precipitation problems, attempts to measure log K_{CuL} for L_{10}-L_{12} by this method proved unsuccessful.

Determination of log K_{1-4} for L_1-L_{17} involved the alkimetric titration of a known weight of the hydrochloride salt of the appropriate ligand and measured weight of a standard HCl solution of known molality. The hydrogen ion concentration was followed throughout the titration using a suitably calibrated glass electrode. To measure the log K_{CuL} values, a known weight of a standard $CuNO_3$ solution of known molality[18] was added to the ligand and acid prior to titration.

The titration system used at Stirling has as its basis the Mettler DL40 Memotitrator, which has a wide variety of pre-programmed analytical and titration facilities, and the ability to store and operate user defined titration procedures. This makes the system relatively easy to operate and reduces the opportunity for operator dependent error. The Stirling titration system is shown schematically in figure 3:1.

The resolution of the Mettler DL40 is $\pm$ 0.2 mV compared to $\pm$ 0.1 mV found in other systems.[19] However, this lower resolution does not appear to lead to any loss in accuracy or precision in calculated

log K_{1-4} and log K_{CuI} values. Indeed, rather surprisingly, the lower resolution seems to be an advantage rather than a disadvantage, for the reasons outlined below.

When a titration is in the region of an endpoint, the potential of the system tends to be less stable than at other regions where the change in potential with each added increment of titrant will be relatively small. The potential will tend to fluctuate around the equilibrium value leading to long delays before the next increment of titrant is added. The lower resolution of the Mettler DL40 memotitrator seems to have a damping effect on these fluctuations, without any concomitant effect on the recorded potential, thus resulting in much shorter titration times. In addition, this increased speed of titration minimises possible changes in E^o during a titration and makes such titrations considerably more convenient.

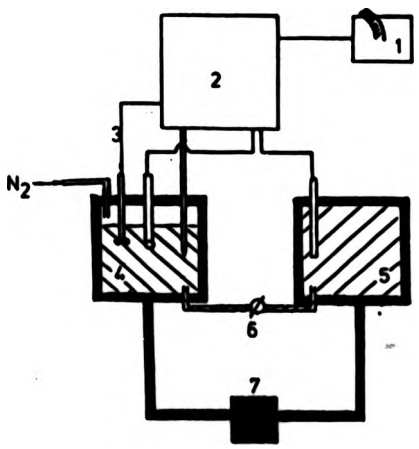

1. Mettler GA40 printer
2. Mettler DL40 memotitrator
3. Mettler DV70 stirrer
4. Titration Vessel
5. Reference cell
6. Salt bridge
7. Haake D3 circulating water bath

Figure 3:1

In keeping with similar systems previously studied, the titrations were carried out in 0.5M KNO_3 solution, using an Orion 91-01 glass electrode and an Orion 90-01 Ag, AgCl reference electrode, in the cell;

Salt Bridge

Ag, AgCl(s) | NaCl (1.0M) || KNO_3 (0.5M) | Glass electrode

(Orion 90-01) (Sat Ag^+) (titration solution) (Orion 91-01)

Liquid-liquid contact was maintained using a Wilhelm-type salt bridge containing 0.5M KNO_3 solution, as outlined schematically in figure 3:2. This will be discussed in detail later on. Both the titration vessel and reference cell were kept at a temperature of 25.0 $\pm$ 0.1 °C using a thermostatically controlled water bath. The contents of the titration vessel were stirred mechanically throughout each titration to prevent the formation of a H^+ ion depletion layer around the glass electrode. All titrations were carried out under a stream of nitrogen which was pre-saturated with water vapour by bubbling through a 0.5M KNO_3 solution.

The water used to make up all solutions was prepared by boiling de-ionised water and allowing it to cool while protected from atmospheric carbon dioxide. The 0.5M KNO_3 used in both the salt bridge, and in the titration vessel as the constant ionic strength medium for the titration, was prepared by weight to a known density using Fisons analytical reagent grade KNO_3.

The 0.1M HCl solution was made from constant boiling, analytical reagent grade, hydrochloric acid, and was standardised by potentiometric titration against high purity (analytical reagent grade) Tris (tris-(hydroxymethyl)aminomethane) using Grans method[20] to determine the end point.

The sodium hydroxide solution (approximately 0.5M) used as the main titrant was prepared from analytical reagent grade potassium hydrogen phthalate, again using Grans method to determine the endpoint. These solutions were routinely standardised once a week.

Figure 3:2

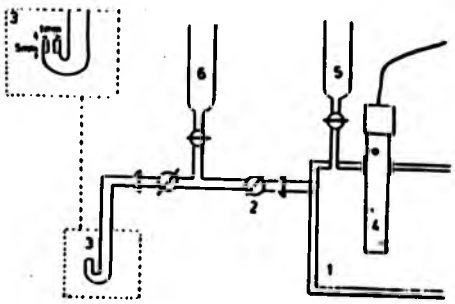

1. Reference cell
2. Junction 1
3. Junction 2
4. Reference electrode
5. 1.0M NaCl solution
6. 0.5M KNO_3 solution

Figure 3:3

The liquid junction 1 between the reference cell and the bridge solution was formed by flushing fresh solution through the tap from both sides of the junction, using the drain tube. The drain tube was then emptied and the junction allowed to form with the three way tap closed to all three openings. This junction is of the constrained leakage type, where the liquid junction is actually formed by the slow leakage of electrolyte solution around the tap. The bridge and reference solutions diffuse together within the confines of the tap to produce a steady state potential.

It was found in practice that after renewing the solutions on either side of the tap, the system stabilised to give a steady value within one hour of the tap being closed. This junction remained stable for up to six hours, even when junction 2 had been renewed several times during that period. It was found that satisfactory results were obtained by renewing junction 1 by the above method, once at the start of each day.

Junction 2 was formed of a 5mm length of 1mm diameter precision capillary tubing, as shown in figure 3:3. This junction was renewed before every titration by flushing with 0.5M KNO_3 solution. This design of junction is recommended as being a very stable and reproducable junction between the bridge and test solutions. The resulting repeated flushing of the bridge solution over a series of measurements may have helped to minimise the drift in potential at junction 1 by keeping the area of liquid contact well defined. In effect, the region of liquid contact in this system is held within the confines of the three way tap, a structurally well defined area. This results in a well defined and reproducible junction potential.

In order that the Gran function is linear with respect to pH, the standard potential of the cell assembly $E^{o'}$, including the junction potential described above, must be constant over the pH range under examination.[20] This type of dependence was found between pH 2.5 and pH 10.8. Outside these limits, a small departure from linearity was observed. It is therefore reasonable to use titration data obtained within these limits without having to correct for changes in junction potential. Confirmation of the reproducibility of the junction potentials was gained by determining $E^{o'}$ by Grans method[20,21] at regular intervals.

Over each day, a small change in $E^{o'}$ (~0.5 mV) was observed, and was thought to be mainly due to ageing of the glass electrode. $E^{o'}$ was also found to change slowly from day to day in the same direction as the observed daily drift, confirming electrode ageing as the major cause of drift. After a time, usually 2-3 months, this drift became unacceptably high and the electrode was replaced. The length of time between replacements varied depending on the history of each particular electrode.

Using standard buffer solutions of pH 4.0, 7.0 and 9.2, the pH response of the glass electrode was checked and was found to be close to the theoretical value of 59.16 mV pH^{-1} (usually 58.9-59.1 mV pH^{-1}). At worst, this would result in a difference of 0.02 pH units at pH 4.0 if the electrode had been calibrated at pH 9.0 and had shown the theoretical response. As this difference is of the order of resolution of the Stirling system, it is probably unimportant and therefore no correction was made for this effect.

The standard potential of the cell, $E^{o'}$, was measured experimentally by the application of Grans method to the titration of the standard HCl solution against the standard NaOH solution immediately before and after each titration to determine a set of constants. This procedure also served as a check on the titrant concentration, and was used to determine log K_w.

The equilibrium constants for each titration were calculated using the programme MINIQUAD[22] from the potential data and titrant volume obtained from that titration. For each of the systems investigated in this study, the calculation procedure outlined below was followed.

a) Determination of log K_{1-4} Values (Titrations with no metal ion added) Titrations were carried out in duplicate, but processed individually to yield two sets of log K_{1-4} results. If suitable agreement was observed between these two sets of results, the titration data were combined and processed simultaneously, yielding the final refined values of log K_{1-4}. If suitable agreement was not achieved between the two sets of results, then both sets of titration data were discarded and the titrations repeated using a freshly purified batch of ligand hydrochloride.

b) Determination of log K_{CuL} Values (Titrations with added metal ion) As in a) above, titrations were carried out in duplicate. Using the values obtained above in a), and with data from each titration in the presence of added metal ion, values of log K_{CuL} were evaluated. Firstly, each titration was processed individually, with log K_{1-4} held constant, to provide a series of log K_{CuL} values. If these values were in suit-

able agreement, the titration data were combined to yield the final K_{CuL} values as in a), again with the log K_{1-4} values held constant. Finally, the simultaneous refinement of log K_{1-4} and log K_{CuL} was carried out to check for the presence of errors between titrations, particularly those titrations with added metal ion and those without. It was usually found that the values obtained from the sequential refinement of log K_{1-4} and log K_{CuL} were in reasonable agreement with those obtained from simultaneous refinement, differing only in the first or second decimal places.

The values obtained from simultaneous refinement were not used as the final values, as they were thought to be less reliable than results obtained from the sequential treatment of titration data, for two main reasons:

1. The data used to obtain values of refinement is solely from titrations carried out with added metal ion, rather than from data obtained under two sets of conditions. This data is therefore liable to be subject to systematic errors.
2. Simultaneous refinement of the titration data tends to disperse uncertainties in the log K_{CuL} values throughout all of the calculated formation constants. As it is possible to determine the protonation constants with a higher level of precision than the corresponding complex formation constants, this simultaneous refinement almost certainly affects the accuracy of the log K_{1-4} values adversely, and therefore leads to over-estimation of the accuracy and precision of the log K_{CuL} values.

Using the above treatment of titration data, it was found that the values obtained from individual titrations were usually in good agreement with those from the combined refinement, differing only in the second decimal place. Estimated standard deviations in log K_{1-4} and log K_{CuL} values from the combined refinement of titration data were usually in the second, or more commonly the third, decimal place.

Experimental details of potentiometric titrations for the evaluation of log K_{1-4} and log K_{CuL} (L_1-L_6).

Curve	System	Ligand	Total Acid	Cu^{2+}	Data Points
1	L_1-H^+	0.2140	1.3646	0	51
2	L_1-H^+	0.2203	1.3893	0	52
3	L_1-Cu^{2+}	0.2021	1.3856	0.0997	42
4	L_1-Cu^{2+}	0.2238	1.4728	0.1028	42
5	L_2-H^+	0.2229	1.3999	0	43
6	L_2-H^+	0.2219	1.3958	0	44
7	L_2-Cu^{2+}	0.2240	1.4043	0.1056	57
8	L_2-Cu^{2+}	0.2150	1.3684	0.1046	57
9	L_3-H^+	0.1961	1.3620	0	45
10	L_3-H^+	0.2125	1.3563	0	40
11	L_3-Cu^{2+}	0.1904	1.3389	0.1045	38
12	L_3-Cu^{2+}	0.1969	1.3651	0.1039	41
13	L_4-H^+	0.2720	1.5810	0	43
14	L_4-H^+	0.2585	1.5265	0	41
15	L_4-Cu^{2+}	0.2265	1.3985	0.1038	43
16	L_4-Cu^{2+}	0.2555	1.5143	0.1032	45
17	L_5-H^+	0.2309	1.4171	0	35
18	L_5-H^+	0.2118	1.3393	0	39
19	L_5-Cu^{2+}	0.2205	1.3752	0.1034	39
20	L_5-Cu^{2+}	0.2338	1.4284	0.1020	38
21	L_6-H^+	0.2498	1.4917	0	36
22	L_6-H^+	0.2190	1.3686	0	33
23	L_6-Cu^{2+}	0.2052	1.3131	0.1042	33
24	L_6-Cu^{2+}	0.2382	1.4453	0.1036	36

Experimental details of potentiometric titrations for the evaluation of log K_{1-4} and log K_{CuL} (L_7-L_{12}).

Curve	System	Ligand	Total Acid	Cu^{2+}	Data Points
25	L_7-H^+	0.2187	1.3884	0	33
26	L_7-H^+	0.2219	1.4006	0	34
27	L_7-Cu^{2+}	0.2345	1.4306	0.1062	38
28	L_7-Cu^{2+}	0.2137	1.3471	0.1058	36
29	L_8-H^+	0.2264	1.3979	0	36
30	L_8-H^+	0.2195	1.3706	0	35
31	L_8-Cu^{2+}	0.2120	1.3406	0.1085	38
32	L_8-Cu^{2+}	0.2273	1.4020	0.1071	41
33	L_9-H^+	0.2069	1.3410	0	33
34	L_9-H^+	0.2268	1.4209	0	36
35	L_9-Cu^{2+}	0.2201	1.3939	0.1064	47
36	L_9-Cu^{2+}	0.2150	1.3733	0.1076	47
37	L_{10}-H^+	0.2101	1.3491	0	34
38	L_{10}-H^+	0.2019	1.3163	0	33
39	L_{11}-H^+	0.2011	1.3131	0	33
40	L_{11}-H^+	0.2168	1.3758	0	35
41	L_{12}-H^+	0.1997	1.3070	0	34
42	L_{12}-H^+	0.1999	1.3065	0	39

Experimental details of potentiometric titrations for the evaluation of log K_{1-4} and log K_{CuL} (L_{13}-L_{17}).

Curve	System	Ligand	Total Acid	Cu^{2+}	Data Points
43	L_{13}-H^+	0.2045	1.3953	0	42
44	L_{13}-H^+	0.2221	1.4659	0	41
45	L_{13}-Cu^{2+}	0.2136	1.4318	0.1043	40
46	L_{13}-Cu^{2+}	0.2021	1.3858	0.1045	38
47	L_{14}-H^+	0.2145	1.3717	0	34
48	L_{14}-H^+	0.2206	1.3962	0	33
49	L_{14}-Cu^{2+}	0.2166	1.3992	0.1027	35
50	L_{14}-Cu^{2+}	0.2213	1.3992	0.1041	43
51	L_{15}-H^+	0.2191	1.3904	0	35
52	L_{15}-H^+	0.2292	1.4307	0	36
53	L_{15}-Cu^{2+}	0.1944	1.2919	0.1034	49
54	L_{15}-Cu^{2+}	0.1958	1.2970	0.1038	49
55	L_{16}-H^+	0.1981	1.3699	0	35
56	L_{16}-H^+	0.1854	1.3190	0	33
57	L_{16}-Cu^{2+}	0.1877	1.3284	0.1048	34
58	L_{16}-Cu^{2+}	0.1933	1.3507	0.1050	35
59	L_{17}-H^+	0.2219	1.3963	0	37
60	L_{17}-H^+	0.2220	1.3968	0	37
61	L_{17}-Cu^{2+}	0.2303	1.4300	0.1056	54
62	L_{17}-Cu^{2+}	0.2104	1.3505	0.1055	41

Cumulative protonation and complex formation constants at 25 °C in 0.5M KNO_3 (L_1-L_6).

System	$\log \beta_{101}$	$\log \beta_{102}$	$\log \beta_{103}$	$\log \beta_{104}$	R
L_1-H^+	10.903(5)	21.434(2)	25.280(8)	28.670(6)	0.0015
L_2-H^+	10.296(2)	19.957(1)	25.818(2)	29.646(3)	0.0004
L_3-H^+	10.29(1)	19.832(6)	26.52(2)	31.11(2)	0.0030
L_4-H^+	10.931(3)	20.917(2)	27.807(3)	31.768(5)	0.0005
L_5-H^+	10.78(2)	21.000(9)	28.66(2)	33.22(4)	0.0042
L_6-H^+	10.724(4)	20.760(2)	28.767(4)	33.252(5)	0.0007

	$\log \beta_{110}$	$\log \beta_{111}$	$\log \beta_{112}$	$\log \beta_{210}$	
L_1-Cu^{2+}	22.03(2)	-	26.66(4)	-	0.0034
L_2-Cu^{2+}	21.602(9)	-	26.1(1)	-	0.0032
L_3-Cu^{2+}	19.358(6)	-	25.68(9)	-	0.0017
L_4-Cu^{2+}	21.78(2)	23.84(5)	-	-	0.0030
L_5-Cu^{2+}	18.75(2)	23.03(7)	-	-	0.0060
L_6-Cu^{2+}	16.13(2)	23.670(6)	-	18.88(3)	0.0011

For all titrations, $pK_w = 13.695(5)$

Note, for the reaction:-

$$aL + bCu^{2+} + cH^+ \longrightarrow (L_aCu_bH_c)^{(2b+c)+}$$

$$\beta_{abc} = \frac{[L_aCu_bH_c]^{(2b+c)+}}{[L]^a.[Cu^{2+}]^b.[H^+]^c}$$

Also, R is the crystallographic factor, and is a measure of the difference between observed and calculated titration curves. Values in parentheses are estimated standard deviations in the least significant figure.

Cumulative protonation and complex formation constants at 25 °C in 0.5M KNO_3 (L_7-L_{12}).

System	$\log \beta_{101}$	$\log \beta_{102}$	$\log \beta_{103}$	$\log \beta_{104}$	R
L_7-H^+	10.393(2)	20.051(1)	27.450(2)	33.890(2)	0.0004
L_8-H^+	10.391(3)	20.161(1)	27.7000(3)	34.524(3)	0.0006
L_9-H^+	10.473(2)	20.293(1)	27.890(3)	34.827(2)	0.0005
L_{10}-H^+	10.993(2)	21.294(1)	30.374(2)	38.560(3)	0.0006
L_{11}-H^+	11.058(1)	21.468(1)	30.672(2)	39.187(2)	0.0004
L_{12}-H^+	11.103(1)	21.588(1)	30.863(2)	39.507(2)	0.0005
	$\log \beta_{110}$	$\log \beta_{111}$	$\log \beta_{112}$	$\log \beta_{210}$	
L_7-Cu^{2+}	17.25(2)	21.85(4)	-	-	0.0024
L_8-Cu^{2+}	14.64(3)	-	27.00(2)	17.25(6)	0.0034
L_9-Cu^{2+}	14.57(2)	-	27.16(1)	16.25(8)	0.0014

Cumulative protonation and complex formation constants at 25 °C in 0.5M KNO_3 (L_{13}-L_{17}).

System	$\log \beta_{101}$	$\log \beta_{102}$	$\log \beta_{103}$	$\log \beta_{104}$	R
L_{13}-H^+	10.251(3)	19.864(2)	26.753(4)	30.316(5)	0.0007
L_{14}-H^+	10.352(3)	20.027(2)	27.268(3)	32.970(4)	0.0007
L_{15}-H^+	10.873(2)	21.105(1)	29.560(2)	35.282(3)	0.0003
L_{16}-H^+	10.969(3)	21.300(2)	30.256(4)	37.744(6)	0.0011
L_{17}-H^+	11.43(1)	21.818(6)	31.15(1)	39.49(1)	0.0032

	$\log \beta_{110}$	$\log \beta_{111}$	$\log \beta_{112}$	$\log \beta_{210}$	
L_{13}-Cu^{2+}	18.63(2)	23.291(5)	-	-	0.0009
L_{14}-Cu^{2+}	21.45(2)	-	-	-	0.0067
L_{15}-Cu^{2+}	17.00(5)	23.78(2)	-	18.4(7)	0.0028
L_{16}-Cu^{2+}	12.89(4)	20.54(3)	27.28(4)	15.57(7)	0.0033
L_{17}-Cu^{2+}	16.12(2)	-	28.99(6)	19.71(4)	0.0047

DISCUSSION

The Stirling titration system has previously been compared with the system in use at the University of Florence in Italy, a system which is known to produce reliable results.[23] The results obtained from this comparison indicated that the Stirling titration system was capable of producing results comparable both in accuracy and precision to a more dedicated system.

Some of the protonation data obtained from this study has been compared with the values available in the literature, as shown in table 3:1. Results obtained for L_1 and L_4 compare favourably with values obtained by Bartolini et al[24] using the Florence titration system, despite the physical differences between these systems.

Table 3:1 Comparison of pK_a values with literature

	pK_1	pK_2	pK_3	pK_4
L_1(This work)	10.90	10.53	3.85	3.39
(a)	11.04	10.47	3.98	3.41
L_4(This work)	10.93	9.99	6.89	3.96
(a)	10.73	9.85	6.83	3.96
(b)	10.04	9.69	6.80	3.54
L_{17}(This work)	11.43	10.39	9.34	8.34
(c)	10.80	10.02	8.85	7.96

(a) Bartolini,[24] (b) Kimura and Yatsunami,[25] (c) Palmer and Powel[26]

The same cannot be said however when comparing results from this work with those obtained by Palmer and Powel (L_4)[26] or Kimura and Yatsunami(L_{17}).[25] Table 3:2 further shows the poor agreement between results obtained by Bartolini[24] et al and Kimura and Yatsunami[25] for the ligand $L_{(VII)}$.

Table 3:2 Protonation data for $L_{(VII)}$

	pK_1	pK_2	pK_3	pK_4
(a)	11.20	10.13	7.96	6.30
(b)	10.23	9.66	7.40	5.31

The validity of the protonation data reported by Palmer and Powel for L_{17}[26] and Kimura and Yatsunami for L_4 and $L_{(VII)}$[25] must be placed in some doubt in view of the observed differences between these results and results obtained from this work and from the Florence titration system. Further evidence supporting this viewpoint is the good correlation of experimentally determined overall protonation constants calculated using the procedure describe by Clark and Perrin,[27] as is illustrated later in this chapter.

When comparing individual evaluations of a series of log K values, several possible sources from which differences in results may arise must be considered. These are:-

(i) Temperature

(ii) Ionic medium

(iii) Operator error

(iv) Purity and Standardisation of reagents

(v) Types of electrode

(vi) Electrode calibration

(vii) Calculation methods

(viii) Titration procedures

(ix) Liquid-liquid junction potentials

The major source of differences in results between the Stirling and Florence titration systems has been shown to be the purity and standardisation of the complexing system, despite the physical differences between the two titration systems. In view of this, it is reasonable to assume that (v), (vi), (vii), and (viii) are comparable between any two systems. In addition (i) is the same for all systems considered in this study, and (ix) has previously been shown to be constant over the pH range used. Thus differences between results obtained from the Stirling (and Florence) titration systems and the systems operated by Palmer and Powel and Kimura and Yatsunami are most likely to have arisen from (1) operator error, (2) differences in the complexing system, and (3) differences in ionic media. Of these possible reasons, (1) is highly unlikely to be an important factor. It is most likely that observed differences in the reported values of protonation constants are due to a combination of (2) and (3). Macrocyclic and acyclic ligands of the type studied in this work are very difficult to obtain in a pure form, contamination by small amounts of synthetic intermediates being commonly found and extremely difficult to remove. In the systems studied by Palmer and Powel and Kimura and Yatsunami, all measurements were carried out using 0.2 mol dm^{-3} $NaClO_4$ as a constant ionic strength buffer. This contrasts markedly with

the 0.5 mol dm^{-3} KNO_3 used both at Stirling and Florence. In addition to differences resulting from the lower ionic strength of the buffering system used by Palmer and Powel and Kimura and Yatsunami, there will also be an alkaline error in the measured potential due to the presence of a relatively high concentration of $Na^+(aq)$ ions. This error will be more significant at high pH.

Due to these differences, results obtained by Palmer and Powel and Kimura and Yatsunami have been used only as a qualitative or semi-quantitative comparison while results obtained by the Florence titration system have been assumed to be comparable to results obtained at Stirling and have therefore been employed in a direct comparison.

Protonation Behaviour

Protonation constants obtained for the tetraaza macrocyclic ligands and their acyclic analogues indicate that a similar trend in overall basicity is observed for each series i.e. an increasing log β_4 with increasing methylene bridge length/ring size. This trend is apparent as a function of individual methylene bridge length and as a function of overall chain length/macrocyclic ring size. These trends are clearly shown in figure 3:4 and in table 3:3-3:4. Note that analogous members of each series of acyclic ligands have similar overall basicities, implying that the structure of the terminal alkyl groups has little or no influence on the overall basicity of the ligand, and that the overall basicity of the acyclic ligand is significantly higher than that of the analogous macrocycles.

Table 3:3 Protonation and Complexation Data - Acyclic Ligands

	pK_1	pK_2	pK_3	pK_4	$\log\beta_4$	$\log\beta_{CuL}$	$\log\beta_{CuLH}$	$\log\beta_{CuLH_2}$	$\log\beta_{CuL_2}$
$L_{(VIII)}$ [a,i]	9.95	9.31	6.86	3.66	29.78	20.2	-	24.12	-
$L_{(II)}$ [d,e]	10.25	9.50	7.20	6.02	33.05	23.9	-	-	-
$L_{(III)}$ [f,g]	10.40	9.68	7.60	6.80	34.48	19.34	-	27.50	-
$L_{(IIII)}$ [f]	10.47	9.79	7.89	7.01	34.96	-	-	-	-
$L_{(IIV)}$ [f]	10.60	9.93	7.76	7.13	35.41	-	-	-	-
$L_{(IV)}$ [h]	10.75	9.88	7.50	4.08	32.10	20.9	25.35	-	-
$L_{(VI)}$ [h]	10.30	9.57	7.18	5.66	32.71	21.89	-	-	-
L_7 [a]	10.380(2)	9.658(1)	7.398(2)	6.440(2)	33.89	17.25(2)	21.85(4)	-	-
L_8 [a]	10.391(3)	9.770(2)	7.537(3)	6.825(3)	34.52	14.64(4)	-	27.03(3)	16.25(8)
L_9 [a]	10.473(3)	9.821(2)	7.569(3)	6.937(3)	34.83	14.57(3)	-	27.16(2)	16.25(8)
L_{13} [a]	10.251(3)	9.644(2)	6.888(4)	3.584(5)	30.32	18.63(2)	23.291(5)	-	-
L_{14} [a]	10.353(3)	9.675(2)	7.241(3)	5.702(4)	32.97	21.45(2)	-	-	-
$L_{(I)}$ [i,j]	10.67	9.96	8.34	5.84	34.99	21.8	-	-	-
$L_{(II)}$ [k]	10.45	9.88	8.34	7.22	36.03	17.3	-	-	-
L_{17} [a]	11.43	10.39	9.34	8.34	39.49	16.12(2)	-	28.99(6)	19.71(4)
$L_{(VII)}$ [h]	10.84	10.12	8.44	5.89	35.10	18.50	24.33	-	-
$L_{(VIII)}$ [h]	10.95	10.25	8.89	7.43	37.49	14.62	20.97	27.01	-
L_{10} [a]	10.910(2)	10.331(1)	9.080(3)	8.186(3)	38.56	-	-	-	-
L_{11} [a]	11.088(2)	10.480(1)	9.040(2)	8.515(2)	39.19	-	-	-	-
L_{12} [a]	11.103(2)	10.488(1)	9.275(2)	8.644(2)	39.51	-	-	-	-
L_{15} [a]	10.873(3)	10.232(1)	8.458(2)	5.721(3)	35.28	17.03(5)	23.78(2)	-	18.9(2)
L_{16} [a]	10.969(3)	10.331(2)	8.938(4)	7.488(7)	37.76	12.88(4)	20.54(3)	27.28(4)	15.57(2)

(a). This work

(b). Reference 35

(c). Reference 36

(d). Reference 37

(e). Reference 38

(f). Reference 39

(g). Reference 40

(h). Reference 8

(i). Reference 41

(j). Reference 42

(k). Reference 43

These observations can be explained in terms of the enhanced inductive effects due to the increase in size of the methylene bridges, and to charge repulsion effects.

Table 3:4 Protonation and Complexation Data - Macrocyclic Ligands

	pK_1	pK_2	pK_3	pK_4	$\log\beta_4$	$\log\beta_{CoL}$	$\log\beta_{CoLH}$	$\log\beta_{CoLH_2}$	$\log\beta_{CoL_2}$
$L_{(I)}$ [b,c]	10.7	9.7	1.73	0.97	23.1	24.8	-	-	-
$L_{(II)}$ [b,d]	11.13	10.00	2.30	1.30	24.81	29.1	-	-	-
$L_{(VI)}$ [e]	10.98	9.75	4.86	2.00	27.59	22.36	25.44	-	-
$L_{(III)}$ [f,d]	11.59	10.62	1.61	2.42	26.2	27.2	-	-	-
L_1 [a]	10.903(5)	10.532(3)	3.846(9)	3.39(1)	28.83	22.0 (1)	-	26.1(1)	-
L_2 [a]	10.296(2)	9.660(1)	5.861(2)	3.828(2)	29.65	21.60(1)	-	26.1(1)	-
L_3 [a]	10.29(1)	9.593(6)	6.75(2)	4.52(2)	31.11	19.358(7)	-	25.7(1)	-
$L_{(IV)}$ [h,j]	11.08	10.38	5.28	3.60	30.36	24.4	-	-	-
L_4 [a]	10.931(3)	9.986(2)	6.893(2)	3.963(5)	31.77	21.78(2)	23.84(5)	-	-
L_5 [a]	10.78(2)	10.22(1)	7.46(2)	4.58(4)	33.22	18.75(4)	23.03(8)	-	-
L_6 [a]	10.724(4)	10.036(2)	8.038(4)	4.484(6)	33.25	16.13(2)	23.670(6)	-	18.88(3)
$L_{(V)}$ [i,k]	10.85	9.80	7.21	5.69	33.25	20.9	-	-	-
$L_{(VII)}$ [l]	11.20	10.13	7.96	6.30	35.59	-	-	-	-

(a). This work

(b). Reference 23

(c). Reference 6, 28

(d). Reference 5, 29

(e). Reference 30

(f). Reference 23

(g). Reference 31

(h). Reference 23

(i). Reference 32

(j). Reference 33

(k). Reference 34

(l). Reference 24

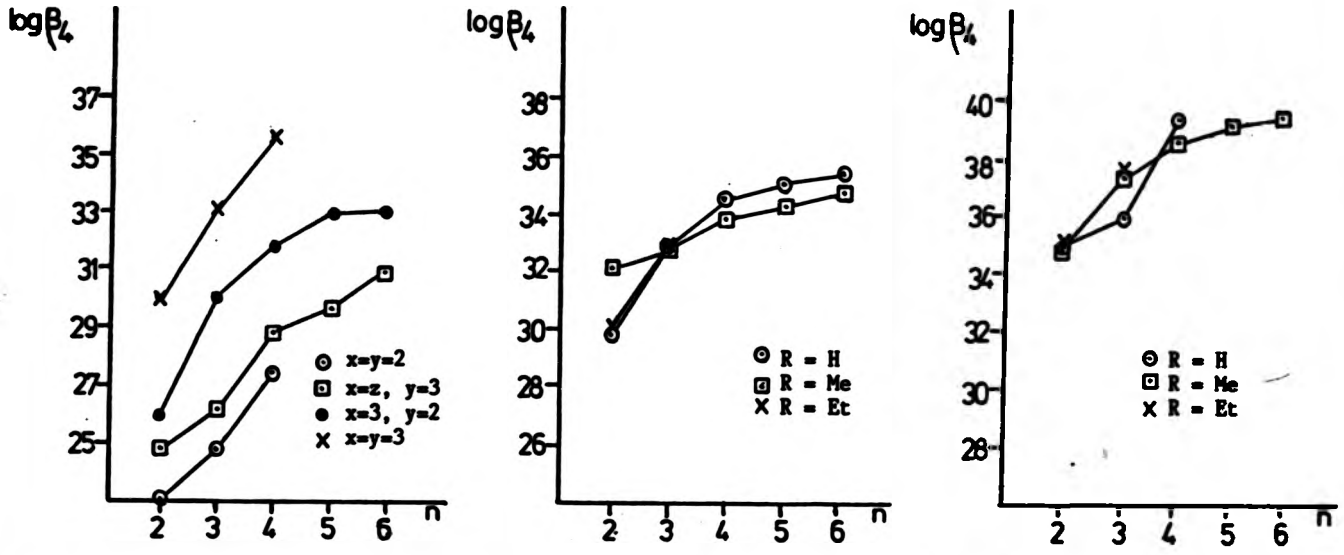

a) $NH\text{-}(CH_2)_x\text{-}NH(CH_2)_yNH\text{-}(CH_2)_x\text{-}NH$ with $(CH_2)_n$ bridge

b) $R\text{-}NH(CH_2)_2NH\text{-}(CH_2)_n\text{-}NH(CH_2)_2NH\text{-}R$

c) $R\text{-}NH(CH_2)_3NH\text{-}(CH_2)_n\text{-}NH(CH_2)_3NH\text{-}R$

Figure 3:4 Overall Protonation Constants (log β_4)

The $R\text{-}\overset{+}{N}H_2\text{-}R'$ groups in the protonated macrocyclic species are held in close proximity due to the cyclic nature of the ligand, making the addition of each successive proton more difficult. Conversely, the acyclic ligand can adopt a conformation which minimises the interaction between non-adjacent $R\text{-}\overset{+}{N}H_2\text{-}R'$ groups. Due to this, the macrocyclic ligands have a lower overall basicity than analogous acyclic ligands. As the overall macrocyclic ligand ring size increases, so does the intramolecular distance between the amine functions, leading to a higher overall basicity. The overall basicity of the larger macrocyclic ligands shows some convergence with the overall basicity of analogous acyclic ligands (i.e. $\Delta(\log \beta_4)$ for $L_{(XVI)}$-$L_{(II)}$ = 7.9 log units while $\Delta(\log \beta_4)$ for L_9-L_3 = 3.7 log units). Broadly speaking, the overall basicity of the macrocyclic ligands increases with ligand atomicity. The overall basicity of the macrocycle is also influenced by the relative sequence and size of the methylene bridges such that, in general, macrocycles with a more symmetric structure have a higher overall basicity. The only exception to this appears to be $L_{(III)}$ (cyclam). However, it has often been stated that cyclam behaves in an exceptional way and is in many respects atypical.

The stepwise protonation constants of the ligands considered in this work are tabulated in table 3:3 - table 3:4 and are represented graphically in figures 3:5-3:7.

The variation in pK_{1-4} within each series of acyclic ligands is illustrated in figures 3:5 and 3:6. Within each series of acyclic ligands, $pK_1 - pK_3$ increases only slightly (0.5-0.9 log units), as the N_2-N_3

methylene bridge length is increased from two to six methylene units (four methylene units in the case of the series $H_2N-(CH_2)_3-NH-(CH_2)_n-NH-(CH_2)_3-NH_2$). This small increase can be largely attributed to the increasing inductive effect as the N_2-N_3 methylene bridge becomes longer. The magnitude of the charge repulsion effects for the first three protonation steps will be only minimally affected by alteration of the size of the N_2-N_3 methylene bridge, as the acyclic tetraaza ligands may adopt a linear structure in solution, thus minimising the interaction between protonated nitrogen groups. As has been demonstrated by Clay et al,[8] the terminal nitrogens of these ligands are almost certainly protonated first, meaning that the nitrogens at N_2 and N_3 must be protonated during the third and fourth protonation steps. Thus, during the third protonation step, the basicity constant of the nitrogen being protonated (either N_2 or N_3) will not be strongly affected by the nitrogen at the other end of the N_2-N_3 methylene bridge (i.e. N_3 or N_2) which will still be unprotonated. However, the basicity constant of the last protonation will be strongly dependent on the effect of both the nitrogen groups adjacent to it. This explains the relatively large increase in pK_4 as the N_2-N_3 methylene bridge length is increased from two to six methylene units.

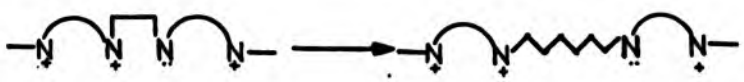

As the N_2-N_3 methylene bridge length is increased, the charge repulsion interaction between N_2 and N_3 diminishes in magnitude, with a concomitant increase in the value of the fourth basicity constant (and hence an increase in the basicity of the ligand).

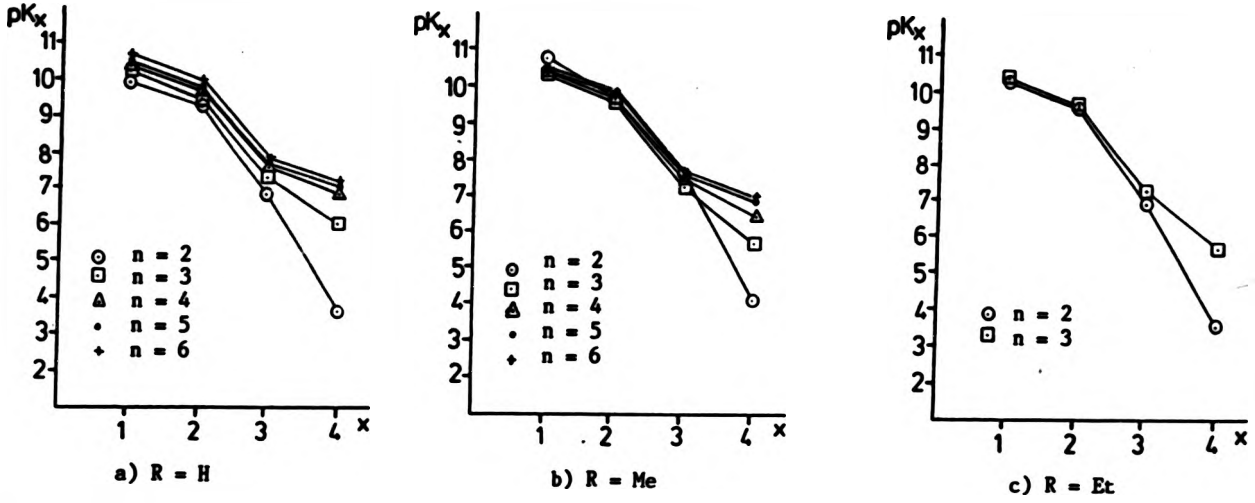

Figure 3:5 Stepwise Protonation constants of the ligands R-NH-$(CH_2)_2$-NH-$(CH_2)_n$-NH-$(CH_2)_2$-NH-R

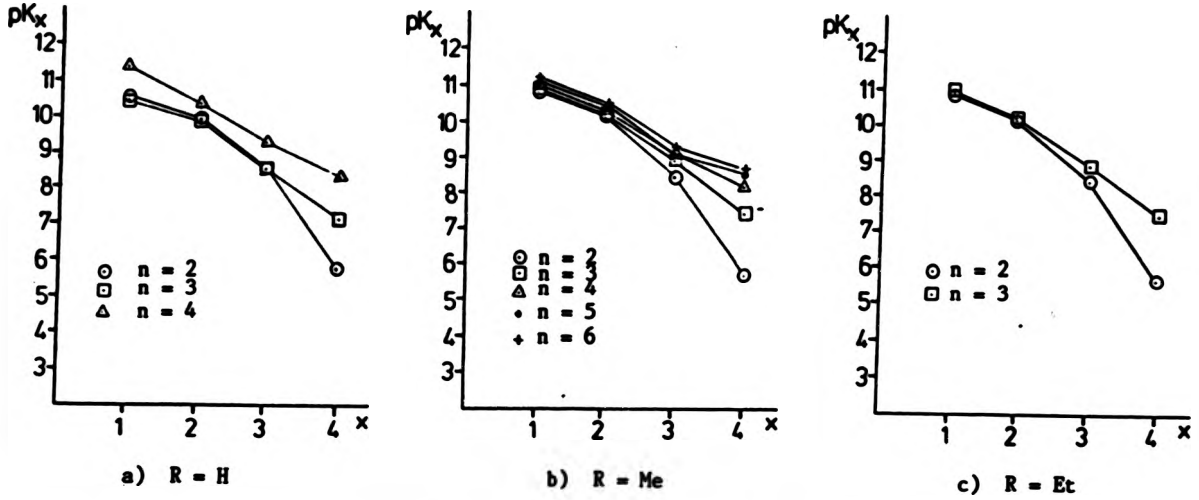

Figure 3:6 Protonation Constants of the ligands R-NH-$(CH_2)_3$-NH-$(CH_2)_n$-NH-$(CH_2)_3$-NH-R

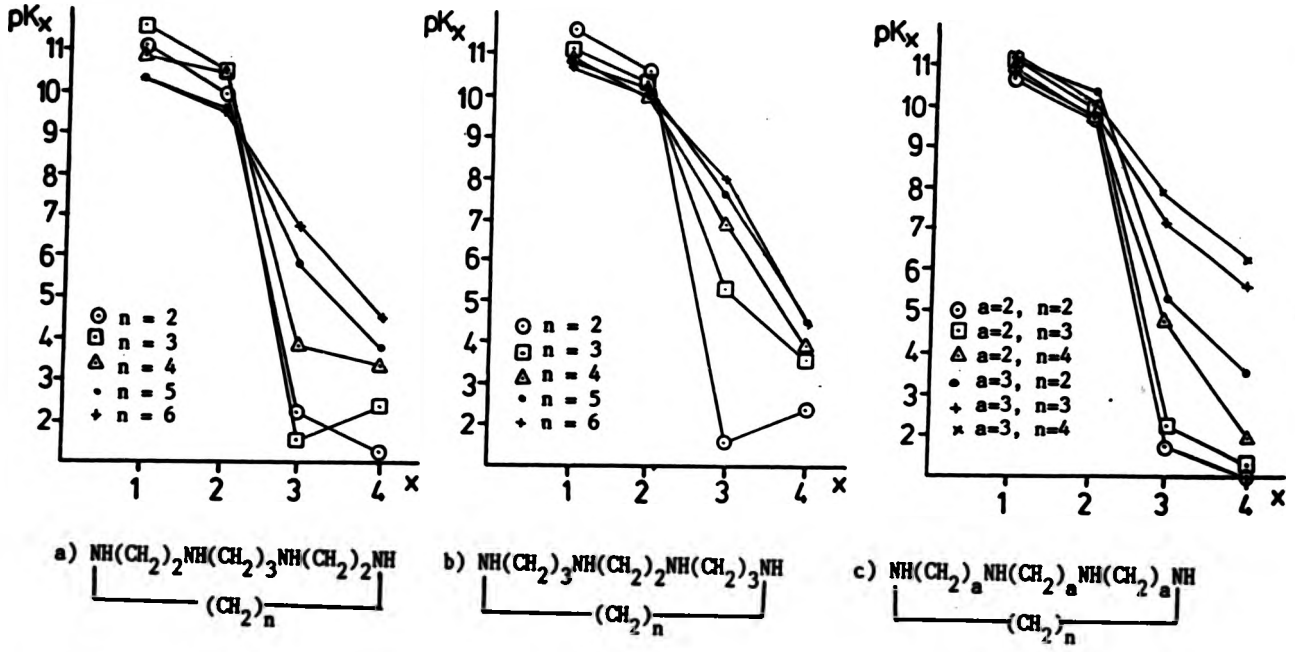

Figure 3:7 Stepwise Protonation Constants of the Macrocyclic Ligands

In the case of the macrocyclic ligands, (fig 3:7), the situation is somewhat different, due to the structural and conformational constraints placed on these ligands by their cyclic nature.

In general, the first two basicity constants of the macrocylic ligands are much higher that the third and fourth basicity constants. This means that the diprotonated macrocyclic species is important over a wide pH range. This behaviour is modified to a certain extent as the ligand ring size increases. This behaviour can be rationalised as follows: when a macrocyclic tetraaza ligand such as those considered here, is in the diprotonated form, the two protonated nitrogen groups will be structurally far removed from one another and there will be little or no interaction between the two protonated sites. This in turn implies that the second protonation constant, pK_2, should be similar to pK_1, much of the difference being due to statistical factors. The diprotonated species LH_2^{2+} will be further stabilised by the presence of intramolecular hydrogen bonding (i.e. N—H·····N) between adjacent protonated and unprotonated nitrogen atoms.

In order that the third and fourth protonation steps may take place, these intramolecular hydrogen bonds must be broken, an energetically unfavourable process. In addition, the third and fourth protonation steps will take place at nitrogen atoms which are structurally close to other protonated nitrogen groups, further decreasing the basicity of the group being protonated. This is reflected in the values obtained for pK_3 and pK_4. Before the fourth protonation can take place, the tetraaza macrocylic ligands will have to undergo and endo → exo trans-

formation to relieve the high charge density inside the triprotonated macrocyclic species.

an endo ⟶ exo transformation

Due to the nature of the tetraaza macrocyclic ligands, the basicities of the third and fourth nitrogens to be protonated are dependent on the size of the macrocyclic ring and methylene bridges. This is illustrated in figure 3:7. This figure illustrates the large difference between the second and third stepwise protonation constants of the smaller macrocycles (ie~9 log units difference between pK_2 and pK_3 for $L_{(III)}$), and the modulation of this effect by increasing size (~3 log units difference between pK_2 and pK_3 for L_3). This increase in pK_3 and pK_4 can be explained by the increased size and conformational flexibility of the larger macrocyclic ligands, leading to an increase in the distance between the adjacent nitrogen groups and hence reducing the magnitude of the charge repulsion effects between the protonated nitrogen groups.

Comparison of figures 3:5 and 3:6 with figure 3:7 illustrates that as the macrocyclic ring size is increased, the protonation behaviour of the macrocyclic ligands is modified in such a way that it becomes similar to the protonation behaviour exhibited by analogous acyclic tetraaza ligands.

Enthalpies of Protonation (Macrocyclic Ligands)

The stepwise enthalpies and entropies of protonation of some of the macrocyclic ligands studied in this work have been determined by a group at the University of Florence.[24] The enthalpies were determined in 0·5M KNO_3 using an LKB 8700 calorimeter employing a continuous titration technique. Available results are summarised in table 3:5.

The major factors determining the magnitude of the enthalpy and entropy of protonation of a polyamine ligand, and their contribution to the overall enthalpy and entropy of protonation, can be summarised as shown below.

	Contribution	
Process	H	S
(i) Desolvation of R_3N	large, +ve	+ve
(ii) Desolvation of H^+	large, +ve	+ve (constant)
(iii) Formation of N-H bond	large, -ve	-ve
(iv) Solvation of $\overset{+}{N}$-H species	large, -ve	-ve
(v) Charge repulsion	+ve	0
(vi) Internal H-bond cleavage prior to protonation	+ve	+ve
(vii) Inversion of nitrogen followed by hydration	-ve	-ve

The last two points ((vi),(vii)) are not expected to be important in non cyclic systems. Point (vii) in fact corresponds to the endo-exo

transformation discussed previously.

The results in table 3:5 indicate that the overall enthalpy of protonation of the macrocyclic ligands is primarily a function of ring size, and not of chelate ring sequence, as macrocycles with the same ring size but different chelate ring sequences have similar overall enthalpies of protonation (ie $L_{(IV)}/L_1$, $L_{(V)}/L_4$). The macrocyclic ligands show a steady increase in overall enthalpy of protonation with increasing macrocyclic ring size, ΔH_{prot} increasing by approximately 10 kJ mol^{-1} for each additional methylene group. As with $\log \beta_4$ values, this general increase can be attributed to charge repulsion effects and to the increasing inductive effect of the methylene bridges (a contributing factor in (iii) above).

It should be noted that unlike the overall protonation enthalpy, the stepwise protonation enthalpies are dependent on chelate ring sequence as is seen by a comparison of the stepwise protonation enthalpies of L_4 and $L_{(V)}$.

Using the data available in the form of stepwise protonation enthalpies and entropies and stepwise protonation constants it is possible to propose mechanisms for the protonation of the macrocyclic tetraaza ligands for which data is available. These proposed mechanisms are described below.

For the ligand L_1, the first protonation step invloves the protonation of a nitrogen atom in an exo configuration, with no internal hydrogen

Table 3:5 Enthalpies and Entropies of Protonation

	$L_{(III)}$[b]	$L_{(IV)}$[b]	$L_{(V)}$[c]	L_1[d,e]	L_4[d,e]	$L_{(VII)}$[d]
$-\Delta H_1$	51·5	45·2	42·0	46·4	46·4	43·5
$-\Delta H_2$	53·6	51·5	44·8	51·5	47·7	46·4
$-\Delta H_3$	11·7	30·2	43·0	27·2	42·7	45·6
$-\Delta H_4$	32·2	32·3	44·2	30·5	33·5	45·6
$-\Sigma\Delta H$	149·0	159·1	173·9	155·6	170·3	181·1
$-\Delta S_1$[a]	49·1	60·4	67·4	53·0	53·7	68·8
$-\Delta S_2$[a]	23·9	26·7	37·9	9·7	31·2	37·9
$-\Delta S_3$[a]	-8·4	0·0	-5·6	-17·4	-11·4	0·0
$-\Delta S_4$[a]	-63·4	-39·3	-39·3	-37·4	-36·6	-32·2
$-\Sigma\Delta S$	1·4	47·8	60·4	7·9	36·9	74·5

a Entropy values (J K^{-1} mol^{-1}) calculated from the corresponding ΔG (kJ mol^{-1}) and ΔH (kJ mol^{-1}) values.

b Micheloni et al JCS Perkin (II), 945,(1978).[44]

c Gallori et al JCS Dalton, 1722,(1980).[45]

d Bartolini et al JCS Perkin (II), 1345,(1982).[24]

e ΔS_{1-4} calculated using ΔG values from this work.

bond formation. The nitrogen which is protonated will probably be bridged by the tetramethylene bridge, as one of these two nitrogens is probably in an exo configuration.

The second protonation step involves protonation of the nitrogen atom furthest away from the nitrogen which is already protonated, i.e. the nitrogen at the "far end" of the trimethylene bridge, followed by the formation of an intramolecular hydrogen bond bridging the trimethylene chain. This explains the large exothermic value for this step (51.5 $kJmol^{-1}$).

The third protonation will occur at the other nitrogen atom bridged by the tetramethylene bridge. This process will be energetically unfavourable due to the increase in positive charge density without nitrogen inversion.

In the final protonation step, the intramolecular hydrogen bond is broken, and the inversion of all the nitrogens occurs to relieve the charge repulsion due to the high charge density. On inversion, the tetraprotonated species is strongly hydrated, leading to a large decrease in entropy.

The ligand L_4, however, behaves differently. In this case, the first three protonation enthalpies are similar in magnitude (with smaller macrocycles there is a large difference between second and third protonation enthalpies). Behaviour of a similar kind has been ex-

plained for $L_{(V)}$[24] by the ability of the lone pairs of electrons on the nitrogen atoms to point in different directions, possibly due to some of the nitrogens being in an exo configuration (presumably this is not likely for L_1 due to the two ethylenic bridges) and thus to act independently of one another. Unlike $L_{(V)}$ however, the fourth stepwise protonation enthalpy of L_4 is less exothermic than the other three. This is possibly due to the endo to exo inversion which occurs when the fourth protonation step takes place. Possible protonation mechanisms for L_1 and L_4 are illustrated in figure 3:9

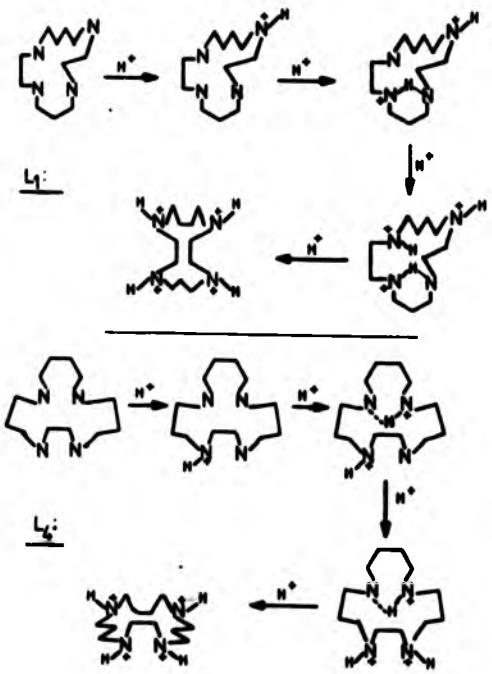

figure 3:9

For the ligands $L_{(V)}$, and $L_{(VII)}$ all four stepwise protonation enthalpies are similar. This implies that in large macrocycles (i.e. with all methylene bridges at least three units in length), all four nitrogens can act independently of one another.

If we consider this data in conjunction with the protonation data previously discussed, and in particular the effect of macrocyclic ring size on $\log K_3$ and $\log K_4$, it can reasonably be stated that macrocyclic ligands with more than two methylene groups in each methylene bridge exhibit protonation behaviour similar to that of the corresponding acyclic tetramines.

Empirical Calculation of pK_n Values

It was previously noted that the stepwise protonation constants of the acyclic tetramine ligands could be estimated with some success if it was assumed that the terminal nitrogens were protonated first. This estimation was carried out using an empirical method described by Clark and Perrin in a review on ligand protonation.[27] Using this method, $\log K_n$ values are estimated on a group additivity basis. In polybasic systems, the effect of other basic sites must be taken into account. Stepwise protonation constants are calculated as shown below:

Starting $\log K_n$ values:

primary - N = 10.77 log units

secondary-N = 11.15 log units

(= 10.95 log units if one alkyl group is $-CH_3$)

Substituents	Contribution to $\log K_n$
$-RNH_2$	-0.8
NHR_2, NR_3	-0.9
RN^+H_3, N^+R_3H	-3.6

The above contributions to $\log K_n$ apply to the stated group situated two carbons distant from the nitrogen atom of interest. For each additional atom spacing, the group contribution is halved. In a polyamine with n groups, each with an identical probability of protonation, the observed $\log K_n$ will be greater by a factor of log(n), as there are n ways in which the proton can add, but only one way in which it may subsequently be removed. Conversely, the last of n equivalent sites to be protonated will have a statistical contribution of -log(n) to $\log K_n$, as the proton may only add in one way, but may subsequently be lost in n ways.

The method is best illustrated using an example. Consider then the system $L_{(XVI)}$:

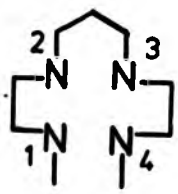

Assuming, as previously proposed, that the terminal nitrogens are protonated first, the protonation constants can be calculated as follows:

Log K_1 (N_1)

(i)	Secondary R-NH-CH_3	(N_1)	10.95	
(ii)	effect of NHR_2	(N_2)	-0.9	$\log K_1$ = 10.3
(iii)	effect of NHR_2	(N_3)	-0.06	
(iv)	statistical factor		0.30	

Log K_2 (N_4)

(i)	Secondary R-NH-CH_3	(N_4)	10.95	
(ii) and (iii) above			-0.96	$\log K_2$ = 9.7
(v)	effect of $-N^+H_2-CH_3$	(N_1)	-0.03	
(vi)	statistical factor		-0.30	

Log K_3 (N_2)

(vii)	Secondary R-NHR'	(N_2)	11.15	
(viii)	effect of $R-N^+H_2-CH_3$	(N_1)	-3.6	
(ix)	effect of $R-N^+H_2-CH_3$	(N_4)	-0.23	$\log K_3$ = 7.2
(x)	effect of R-NHR	(N_3)		
(xi)	statistical factor		0.30	

Log K_4 (N_3)

(vii)	Secondary R-NH-R'	(N_3)	11.15	
(viii) and (ix) above			-3.85	$\log K_4$ = 5.2
(xii)	effect of $R-N^+H_2-R'$	(N_2)	-1.8	
(xiii)	statistical factor		-0.30	

	$\log K_1$	$\log K_2$	$\log K_3$	$\log K_4$	$\log \beta_4$
Calculated	10.3	9.7	7.2	5.2	32.4
Observed[θ]	10.3	9.6	7.2	5.6	32.7

These calculated values are in good agreement with the observed stepwise protonation constants and overall protonation constant obtained for $L_{(XVI)}$. Stepwise and overall protonation constants were similarly calculated for the ligands L_7 - L_{17}. Values obtained are detailed in table 3:6.

The good agreement observed between the calculated $\log K_n$ values and the observed values, tends to confirm the proposed theory that the initial protonation steps occur mainly at the terminal nitrogens. Allowing for differences in temperature and ionic strength the observed and calculated overall protonation constants are in excellent agreement (with the exception of L_{17}, see later), differing generally by only 0.1-0.2 log units, and at most by 0.4 log units.

The good agreement between observed and calculated protonation constants indicates that it is likely that the systems under consideration are influenced by a similar combination of group effects as the wider range of systems on which this empirical method is based. Substantial differences between observed and calculated values, as in the case of L_{17}, may reflect unusual solvation, hydrogen bonding, or steric effects not normally observed in polyamine systems such those on which this method is based.

Table 3:6 Calculated Stepwise and Overall Protonation Constants

	pK_1	pK_2	pK_3	pK_4	$\log \beta_4$ (calc)	$\log \beta_4$ (obs)
L_7	10.3	9.7	7.5	6.2	33.7	33.9
L_8	10.3	9.7	7.7	6.7	34.4	34.5
L_9	10.4	9.8	7.3	7.0	35.0	34.8
L_{10}	10.8	10.2	9.4	8.1	38.5	36.6
L_{11}	10.8	10.2	9.5	8.6	39.1	39.2
L_{12}	10.8	10.2	9.6	8.8	39.4	39.5
L_{13}	10.4	9.8	6.5	3.2	29.9	30.3
L_{14}	10.5	9.9	7.2	5.2	32.8	33.0
L_{15}	10.9	10.3	8.5	5.2	34.9	35.3
L_{16}	11.0	10.4	9.1	7.1	37.6	37.7
L_{17} (a)	10.6	10.0	9.4	8.1	38.1	39.5

Calculated values refer to I = 0 and 20 °C

(a) See text

To conclude, several points have been demonstrated:

1. In the case of all the non-cyclic tetraaza ligands studied, it is almost certain that the terminal nitrogens are the first to be protonated.
2. There is almost certainly some proton exchange between the basic sites.
3. Within each series of macrocyclic and acyclic ligands, the trends in $\log K_{1-4}$ and $\log \beta_4$ can be explained in terms of charge repulsion and inductive effects.
4. The observed $\log K_{1-4}$ and $\log \beta_4$ values of the acyclic ligands can be predicted with good accuracy using the method of Clark and Perrin.
5. The protonation behaviour of the macrocyclic ligands becomes more similar to that of analogous acyclic ligands as the macrocyclic ligand ring size is increased.

Trends in Copper(II) Complex Formation

The values obtained for the copper(II) complex formation constants of the macrocyclic ligands under consideration in this study indicate that with one notable exception, the stability of the macrocyclic complex decreases as the length of any one methylene bridge is increased (figure 3:8). This decrease in complex stability can be attributed to the increasing size of the macrocyclic aperture (macrocyclic "hole") as the ligand ring size is increased. This in turn may lead to successively weaker Cu-N interactions (i.e. longer Cu-N bonds) and to an increase in the strain in the complex as the macrocyclic ligand distorts to form a more favourable environment for the Cu(II) ion. This ligand distortion leads to a larger loss in conformational entropy and, as will be seen later, to progressively less exothermic enthalpies of complex formation with increasing ligand ring size.

The ligand $L_{(III)}$ has a macrocyclic aperture with an "ideal" M-N bond length of 2.07 Å,[46] which corresponds very well with the "experimental" Cu(II)-N average bond length of 2.02 -2.07 Å obtained from x-ray analysis of tetragonal Cu(II) polyamine complexes.[47,48]

The ligand $L_{(IV)}$, which differs in size from $L_{(III)}$ by only one methylene unit, has a macrocyclic hole with an ideal M-N bond length of 2.22 Å.[46] This is seemingly too large to encompass a copper(II) ion in a strain free environment. The complex $[CuL_{(IV)}][ClO_4]_2$ has been shown by x-ray crystallography to have a planar CuN_4 arrangement with a bond length of 2.03 Å.[49] The distortion of the macrocycle $L_{(IV)}$ to

accommodate the copper(II) ion places significant steric constraints on the complex, decreasing its stability.

Conversely, the ligand $L_{(I)}$ (ideal M-N distance 1.82 Å)[46] has a macrocyclic hole size much too small to co-ordinate the copper(II) ion in a co-planar tetragonal arrangement. This ligand, which is the exception mentioned above, has been shown to form penta-coordinate square pyramidal copper(II) complexes, unlike other (larger) ligands of this type which form planar, tetragonally distorted copper(II) complexes. X-ray analysis of the complex $[CuL_{(I)}(NO_3)][NO_3]$ has shown that the copper(II) ion is removed from the N_4 plane by approximately 0.4 Å.[50] This explains the relatively low copper(II) complex stability constant observed for this complex. .

A similar trend is observed for the series of acyclic ligands of general formula R-NH-$(CH_2)_2$-NH-$(CH_2)_n$-NH-$(CH_2)_2$-NH-R (R = H, Me, Et) where the general trend is for log K_{CuL} to decrease as n increases, but log K_{CuL} for n = 2 is lower than for n = 3 (figure 3:8).

It has been shown by x-ray crystallography that as with $L_{(I)}$, copper(II) complexes of $L_{(VIII)}$ are five co-ordinate in the solid state,[51] with the copper(II) ion approximately 0.4-0.5 Å above the N_4 plane. In aqueous solution, copper(II) complexes of both $L_{(I)}$ and $L_{(VIII)}$ form 2:1[9] electrolytes, presumably by substitution of the co-ordinated anionic species by a water molecule. Although it is not known whether these complexes retain their penta-coordinate structure in aqueous solution,

the similarity between the electronic spectra of the solid and the aqueous solution suggests that similar chromophores are involved.

Comparing acyclic tetraaza ligands with the same skeletal structure but different terminal R groups (figure 3:10), it is found that although the protonation behaviour is essentially independent of the nature of the R groups (figures 3:4-3:6), these groups have a significant influence on the complexation behaviour of the ligand.

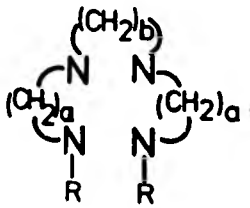

a = constant = 2, 3

b = constant = 2, 3, 4, 5, 6

R = H, Me, Et

Figure 3:10

As the terminal R groups became larger (H - Me - Et) the magnitude of $\log K_{CuL}$, the copper(II) complex formation constant decreases (figure 3:8). As the only difference between analogous ligands is the nature of the terminal R groups, it is probable that this loss of stability is due to the increased steric interaction of the nore bulky Me and Et groups, leading to distortion of the complex species to minimise this interaction. It is possible that this is the reason why no copper(II) complex formation was detected for L_{10}, L_{11} and L_{12} using the Stirling titration system. Indeed, molecular models of all

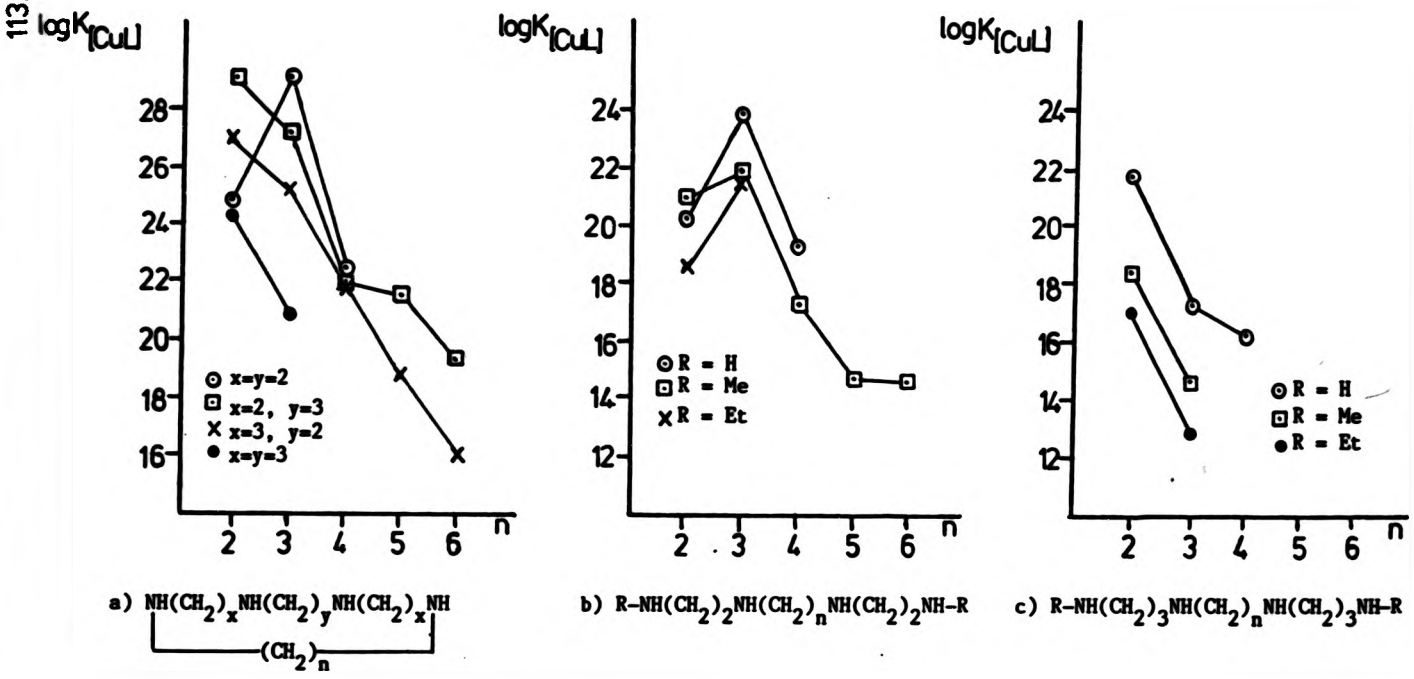

Figure 3:8 Copper(II) Complex Formation Constants

possible conformational isomers of these complexes show significant steric interaction which may inhibit or even prevent complex formation under the conditions used. It has previously been shown that $L_{(XVIII)}$ (and to a lesser extent $L_{(XVII)}$) has an appreciable degree of steric hindrance associated with the terminal methyl groups.[8] With this ligand, any attempt to achieve the maximum M-N interaction results in severe intra-ligand interactions. The complex is therefore assumed to distort from its ideal geometry to relieve these steric effects.

The distortion of these ligands is almost certainly reflected in the magnitude of the copper(II) complex formation constant (figure 3:8) and the enthalpy of complex formation (see later), and as such, models the distortion effects found in the macrocyclic ligands.

The presence of protonated complexes may well be an indication of the presence of adverse steric effects associated with co-ordination, more strained systems being more readily protonated. Such mono- and di-protonated species have been observed for copper(II) complexes of many if the ligands studied in this work (tables 3:3, 3:4). There appear to be two distinct cases where the formation of protonated copper(II) complexes of this type of ligand occurs.

1. In the case of both the macrocyclic and acyclic ligands, when the chelate ring sequence deviates from the ideal of alternating five and six membered chelate rings.

   (a) When the ligand is too small to accommodate the copper(II) ion in a tetragonally distorted coplanar CuN_4 arrangement (i.e. in the case of $L_{(VIII)}$).

(b) When the ligand is larger than the ideal size, it must adopt a less favourable conformation in order to accommodate the copper(II) ion in the ideal coplanar CuN_4 arrangement.

2. In the case of the acyclic ligands as the terminal R groups become bulkier, they are associated with an increase in steric hindrance, forcing the complex to distort from its ideal geometry to relieve the strain (i.e. L_{15}).

Unusual Complex Species

In calculating the copper(II) complex formation constants using the computer programme MINIQUAD,[22] it was discovered that the best refinement of experimental data for some of the ligands studied required the inclusion of the species $[CuL_2]^{2+}$. The ligands for which this was the case are: L_6, L_8, L_9, L_{15}, L_{16} and L_{17}. For each of these ligands, the species $[CuL_2]^{2+}$ was formed only in small amounts (less than 2% of the total complex formation). This unusual complex species only appears to have been formed in cases where the ligand involved is large and/or has bulky terminal R groups.

It is possible that in these cases, steric and conformational restrictions allow the nitrogen groups on the ligand to act independently or in pairs. This is supported by the formation of the diprotonated $[CuLH_2]^{4+}$ species by many of the ligands studied.

Evidence to support the existence of these species is limited to that obtained from the potentiometric data, and thus it is not possible to prove that these unusual species are in fact present in aqueous solution without further investigation.

Chapter 4

COPPER COMPLEX FORMATION ENTHALPIES

Until 1977, it was not possible to determine the enthalpies of complexation of tetraaza macrocyclic ligands directly, although calorimetric titration and flow calorimetry[42] and isoperibolic calorimetry[36] had previously beeen used successfully for most non-cyclic systems. The problems associated with macrocyclic systems were overcome by the use of 1M NaOH as the reaction medium (ensuring complete deprotonation of the ligand), dilute solutions of both metal ion and ligand, and the advent of very sensitive microcalorimeters.[52]

In this study, the enthalpies of complex formation of ligands L_1-L_9, L_{13}-L_{17} with Cu^{2+} were determined in 1M NaOH using a batch microcalorimeter as described below.

The calorimeter used for these determinations was an LKB 10 700-2 Batch Microcalorimeter, fitted with gold reaction cells. The voltages generated by the thermopiles surrounding the cell were amplified by a Kiethley 150B Microvolt amplifier and recorded as a function of time using a Philips 8000 potentiometric chart recorder. The area under the resulting voltage - time curve is directly proportional to the heat output of the reaction. This area was determined as the mean of six measurements using an accurate planimeter. Each heat of reaction was determined at least four times and the mean value reported. The copper solutions were introduced to one half of the calorimeter cell by weight using a syringe and an excess of the ligand in (approximately two equivalents) 1M NaOH introduced by syringe to the other half of the cell.

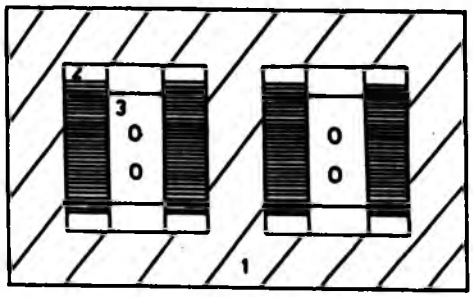

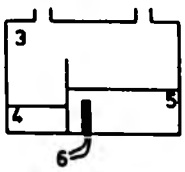

1. Heating block
2. Thermopiles
3. Reaction cell
4. Copper(II) solution
5. ligand solution (1M NaOH)
6. Calibration heater (not used)

Figure 4:1

The reaction enthalpy of interest is that between the $Cu^{2+}(aq)$ ion and the aqueous non-protonated ligand i.e.

$$Cu^{2+}(aq) + L(aq) \xrightarrow{\Delta H_{ML}} [CuL]^{2+}(aq)$$

This was obtained from the thermochemical cycle illustrated below:

Scheme 1:

$$\begin{array}{ccccc} Cu(aq) & + & L(aq) & \xrightarrow{\Delta H_{CuL}} & [CuL]^{2+}(aq) \\ & & \downarrow \Delta H_3 & & \downarrow \Delta H_2 \\ Cu^{2+}(aq) & + & L(1M\ NaOH) & \xrightarrow{\Delta H_1} & [CuL]^{2+}(1M\ NaOH) \end{array}$$

$\Delta H_1 = \Delta H_{obs} - \Delta H_{dil}$ (ΔH_{dil} = dilution correction)

$\Delta H_3 = 0$

As there is a fault in the calibration circuit of the calorimeter, the heat outputs corresponding to ΔH_1 and ΔH_2 were determined by comparison of the area under the voltage - time graph with that of a similar reaction of known heat output. The reaction chosen was the formation of $[CuL_{(X)}]^{2+}$.[42] This system was chosen for several reasons:

1. The reaction is simple and well defined.
2. The reaction enthalpy is well known.
3. The ligand $L_{(X)}$ is commercially available and is relatively easy to purify to an acceptable level.
4. The $[CuL_{(X)}]^{2+}$ system is chemically similar to those under consideration. This should reduce the influence of systematic errors between the standard system and the systems of interest.
5. ΔH_2 was found to be negligible, therefore $\Delta H_4 = \Delta H_1$.
6. By using the same Cu^{2+} solution and the same concentration of ligand, and the same experimental conditions, any error in the determination of $[Cu^{2+}]$ should cancel since:

$$\frac{\Delta H_{ML\ 2+(CuL)}}{\Delta H_{ML\ 2+\ (CuL')}} = \frac{\text{Area (CuL)}}{\text{Area (CuL')}}$$

Area = area per gramme of Cu^{2+} solution, corrected for dilution and ΔH_2 terms.

This means that the accurate determination of $[Cu^{2+}]$ is required only to calculate the concentration of complex solution needed for the determination of ΔH_2.

As ΔH_2 is generally very small in comparison to ΔH_1 in the case of copper(II) complexes, small errors in $[Cu^{2+}]$ could reasonably be expected to result in negligible errors in the calculation of ΔH_{ML}.

Results

All heats of reaction were corrected directly for both ΔH_2 and dilution effects before ΔH_1 was calculated. As a check on the accuracy of this method of calculation and calibration, the enthalpy of formation of $[CuL_{(IX)}]^{2+}$ was determined. Results obtained are in good agreement with existing literature values (observed: 115.5(6), literature: 115.9(4) $kJmol^{-1}$).

Experimental results for L_1-L_{17} are given in table 4:1. All values quoted are the mean of four determinations as previously stated. All ΔH_1 values were obtained using an accurately standardised solution of $Cu(ClO_4)_2.6H_2O$.

Copper complex solutions were made up using the bis-perchlorate salt except in those cases specified in table 4:1, where the bis-nitrato salt had to be used as it was not possible to crystallize bis-perchlorate salts of these copper complexes (see chapter 2). As both these counter ions are non-complexing, it is not thought that this will greatly affect the overall complexation enthalpy.

No attempt was made to correct results for the presence of unusual species such as CuL_2 etc (see chapter 3), as stability constant results and uv/vis spectra indicate that these are only present in small concentrations

Table 4:1 Calorimetric Terms Relating to Scheme 1 (This work)

Ligand	$[ML]^{2+}$ ($molkg^{-1}$)	$-\Delta H_1$	$+\Delta H_2$	$+\Delta H_3$	$-\Delta H_{ML}$	ν(d-d) ($cm^{-1} \times 10^3$)
L_1	5.37×10^{-2}	108.4(1.8)	-0.4(1)	2.1	108.0(1.9)	18.66
L_2	5.30×10^{-2}	81.5(1.8)	0.2(1)	2.1	81.7(1.9)	18.28
L_3	1.04×10^{-2}	84.4(8)	-2.6(1)	2.1	81.8(9)	18.22
L_4	5.30×10^{-2}	96.9(2.0)	-1.4(1)	2.1	95.5(2.1)	18.42
L_5	4.68×10^{-2}	79.8(1.7)	8.5(2)	2.1	88.3(1.9)	18.08
L_6	5.20×10^{-2}	84.8(1.5)	6.0(1)	2.1	90.8(1.6)	18.32
L_7	5.17×10^{-2}	66.9(5)	8.6(3)	2.1	75.5(9)	17.86
L_8	1.22×10^{-2}	60.6(7)	5.5(2)	2.1	66.1(9)	17.07
L_9 (a)	4.99×10^{-2}	59.6(1.2)	19.2(5)	2.1	78.8(1.7)	17.54
L_{13} (a)	3.3×10^{-2}	76.8(0.5)	-10.8(0.5)	2.1	66.0(1.0)	16.95
L_{14}	5.29×10^{-2}	100.2(1.2)	2.8(0.2)	2.1	103.0(1.4)	18.45
L_{15} (a)	7.48×10^{-2}	76.4 (1.1)	6.0(0.2)	2.1	82.4(1.3)	18.05
L_{16} (a)	5.14×10^{-2}	55.0(0.5)	-2.1(0.1)	2.1	53.9(0.6)	16.05
L_{17}	6.86×10^{-2}	54.8(9)	23.9(9)	2.1	78.7(1.8)	17.86

(a) ΔH_2 determined using $[CuL][NO_3]_2$ complex.

and are thus unlikely to have any significant effect on ΔH_{ML}, especially as the bonds being formed are still Cu-N bonds.

Trends in Copper(II) complex formation enthalpies

The experimental values for the copper(II) complex formation enthalpies ($-\Delta H_{ML}$) of the tetraaza macrocyclic and acyclic ligands under consideration in this work are shown graphically in figure 4:2. From these graphs, it is evident that within each series of macrocyclic or acyclic ligands, $-\Delta H_{ML}$ is at a maximum when the copper(II) complex contains a sequence of alternating five and six membered chelate rings (or as close as possible to this sequence within the structural limitations of each series). That the alternating sequence of five and six membered chelate rings is enthalpically preferred can be further proven by the comparison of ligands with the same molecular formulae but slightly different structural formulae. For example, both L_4 and $L_{(V)}$ have the same molecular formula ($C_{12}H_{28}N_4$) but have different structural formulae leading to different chelate ring sequences (6,5,6,7 for L_4, 6,6,6,6 for $L_{(V)}$). The formation of $[CuL_{(V)}]^{2+}$ is less exothermic than $[CuL_4]^{2+}$ by c.a. 11.8 $kJmol^{-1}$. Similarly, the formation of $[CuL_{(XII)}]^{2+}$ (chelate ring sequence 5,5,5,7) is less exothermic than the formation of $[CuL_{(III)}]^{2+}$ (chelate ring sequence 6,5,6,5) by 48.1 $kJmol^{-1}$.

As has been discussed in the previous chapter, the ligands distort on complexation with a copper(II) ion to accommodate the copper(II) ion in a planar CuN_4 arrangement with the preferred Cu-N distance of 2.02-2.07 Å. In those ligands containing a fused sequence of five membered chelate rings (i.e. $L_{(I)}$, $L_{(II)}$, $L_{(VI)}$, $L_{(VIII)}$, L_{13}) the ligand is unable to accommodate the Cu(II) ion in such an arrangement.

Table 4:2 ΔH_{ML} Values of Some Tetra-aza Liganda

Ligand	$-\Delta H_{CuL}$ ($kJmol^{-1}$)	ν (d-d)($cm^{-1} \times 10^3$)
$L_{(I)}$ [a,b]	95.0	16.95
$L_{(II)}$ [b,c]	107.1	18.32
$L_{(III)}$ [b,d]	135.6	19.88
$L_{(IV)}$ [b,e]	110.9	17.61
$L_{(V)}$ [b,f]	83.7	-
$L_{(VI)}$ [g]	87.5	17.61
$L_{(VIII)}$ [h]	90.4	17.39
$L_{(IX)}$ [i]	115.9	19.08
$L_{(X)}$ [j]	108.4	18.48
$L_{(XI)}$ [k]	81.6	16.75
$L_{(XII)}$ [l]	86.2	18.22
$L_{(XV)}$ [m]	88.3	17.27
$L_{(XVI)}$ [n]	108.4	18.66
$L_{(XVII)}$ [n]	93.1	18.35
$L_{(XVIII)}$ [n]	62.3	15.90

(a). Reference 28
(b). Reference 52
(c). Reference 53
(d). Reference 7
(e). Reference 32
(f). Reference 45
(g). Reference 30
(h). Reference 36
(i). Reference 38
(j). Reference 42
(k). Reference 43
(l). Reference 40
(m). Reference 9
(n). Reference 8

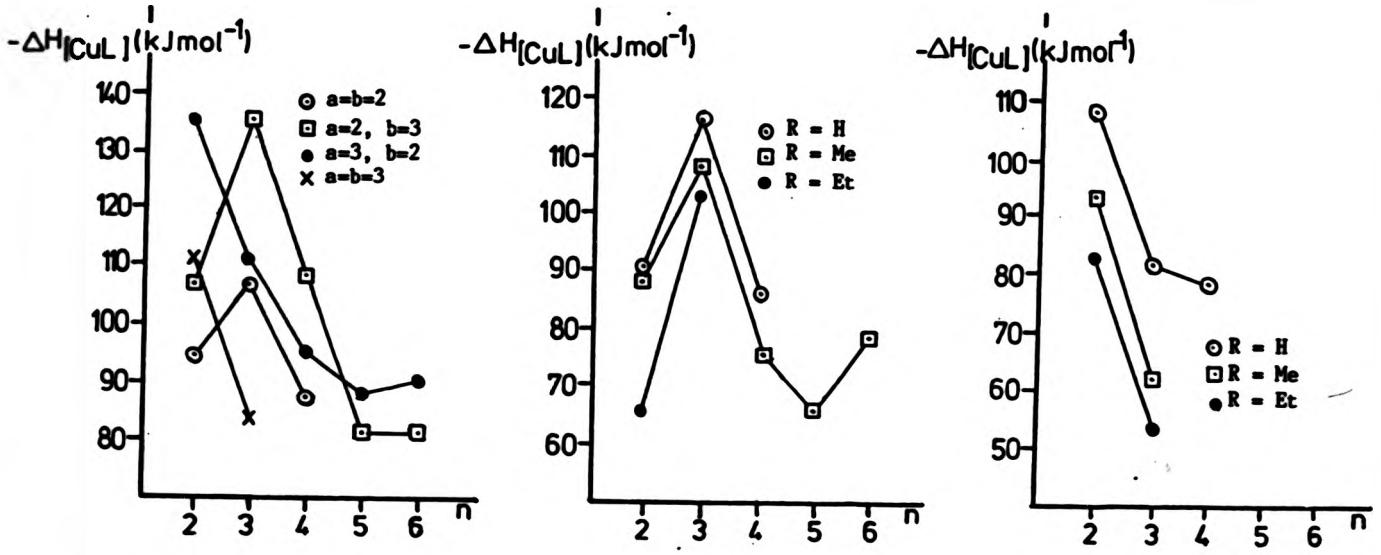

a) $NH(CH_2)_aNH(CH_2)_bNH(CH_2)_aNH$ with $(CH_2)_n$ bridge

b) $R\text{-}NH(CH_2)_2NH(CH_2)_nNH(CH_2)_2NH\text{-}R$

c) $R\text{-}NH(CH_2)_3NH(CH_2)_nNH(CH_2)_3NH\text{-}R$

Figure 4:2 Enthalpies of Copper(II) Complex formation $-\Delta H_{ML}$

As a result, these complexes tend to exist with a pentaco-ordinate square pyramidal structure, with the copper(II) ion removed above the N_4 plane. This type of structure will possess a relatively large cumulative ring strain, making the complex formation less enthalpically favourable.

Ligands which are larger than the ideal size for complexation with copper(II) must also distort significantly to accommodate the copper(II) ion in its preferred geometry. This distortion induces a large configurational strain on the complex, again lowering the enthalpy of complex formation. As the chelate ring size is increased, the enthalpy of complex formation decreases, implying that configurational strain is also increasing. However, once a chelate ring size of eight is achieved, there does not appear to be any additional configurational strain with further increases in chelate ring size.

Ligands containing the preferred sequence of chelate rings can accommodate the copper(II) ion in a CuN_4 plane with the ideal Cu-N bond length of between 2.02 and 2.07 Å. This means that the copper(II) complexes of these ligands contain a minimum of both cumulative ring strain and configurational strain, making complex formation more enthalpically favourable.

A comparison of the macrocyclic ligands with analogous acyclic ligands shows that the complexation of the macrocyclic ligand is always more exothermic than that of the analogous acyclic ligand(s). This observation has been explained by the fact that the macrocyclic ligands are "synthetically preoriented" for complexation.

As a result, they do not have to expend configurational energy in wrapping themselves around the metal ion as is the case with the acyclic ligands.

From figure 4:2 it is evident that the complexation of the N, N''' alkylated ligands is energetically less favourable than that of the non-alkylated ligands. It is probable that the less favourable complex formation enthalpy of the alkylated ligands is at least partly due to the adverse steric effects caused by the presence of the terminal alkyl groups (R), as ΔH_{ML} becomes less exothermic in the order of H→ Me→ Et for terminal alkyl groups. In addition, it is also obvious from figure 4:2 that for each series of acyclic ligands where the ligands differ only in the nature of the terminal R groups (R = H, Me, Et), the trends in ΔH_{ML} are parallel.

The presence of adverse steric effects due to the terminal alkyl groups is further supported by molecular models of the copper(II) complexes of these ligands. With the exception of two ligands ($L_{(XV)}$, $L_{(XVI)}$) the terminally alkylated acyclic ligands show an appreciable amount of steric hindrance. Attempts to give the maximum Cu-N interaction result in significant intraligand interactions. The copper(II) complex is therefore assumed to distort from its ideal geometry to relieve these steric effects, leading to the observed reduction in the enthalpy terms.

As was discussed previously (see chapter 3), the presence of protonated complexes may be a further reflection of the adverse steric effects associated with co-ordination to a metal ion, strained systems being more easily protonated.

Another possible reason for observed differences in the trends in copper(II) complexation enthalpies of the copper(II) complexes of the acyclic ligands is the presence of differences in ligand and/or complex solvation enthalpies due to the differences in molecular size and the nature of the amine groups caused by the terminal alkyl groups.

Relationship between electronic spectra and ΔH_{CuL} for Copper(II) Tetramine complexes

In a study by Fabbrizzi, Paoletti and Lever published in 1976,[54] an empirical linear relationship between the energy of the electronic maxima (ν(d-d)) of the visible spectra and the enthalpy of complex formation was described for a selection of copper(II) polyamine complexes. In the aforementioned study some thirty Cu(II) amine complexes ranging from simple ammonia derivatives to macrocyclic derivatives were shown to conform to similar linear relationships. The observed general relationship for copper(II) polyamine complexes is described below in equation 4:1.

$$-\Delta H_{CuL} = 18.12\ \nu(d\text{-}d) - 227.74 \qquad 4:1$$

ΔH_{CuL} in $kJmol^{-1}$ and ν(d-d) in $cm^{-1} \times 10^3$

It has been stated that this relationship is expected to be valid only for amines capable of forming tetragonal copper(II) complexes with the nitrogen atoms disposed in a quadratic plane where two molecules of water can be co-ordinated axially.[54]

In addition to providing an empirical procedure for the estimation of $-\Delta H_{ML}$ in aqueous solution, studies such as these lead to a better understanding of such factors as outer sphere solvation energy and strain energy, and may highlight unusual bonding or structural features which might otherwise remain unnoticed.

Using the ligands considered in this work, an attempt has been made to determine similar relationships to the one shown in equation 4:1 for acyclic tetramines, macrocyclic tetramines, and for tetramines in general.

Results are shown graphically in figure 4:3. For both the macrocyclic and acyclic complexes, a best fit straight line equation was calculated using only "well behaved" complexes. Those complexes which showed unusual or atypical behaviour were not included in the calculation of best fit straight lines. The best fit straight line equations obtained for macrocyclic tetramine complexes (equation 4:2), acyclic tetramine complexes (equation 4:3) and for tetramine complexes in general (equation 4:4) are described below.

$$-\Delta H_{CuL} = 24.48\,\nu(d\text{-}d) - 353.62 \quad (r = 0.875) \qquad 4:2$$

$$-\Delta H_{CuL} = 21.09\,\nu(d\text{-}d) - 291.62 \quad (r = 0.939) \qquad 4:3$$

$$-\Delta H_{CuL} = 22.40\,\nu(d\text{-}d) - 315.0 \quad (r = 0.926) \qquad 4:4$$

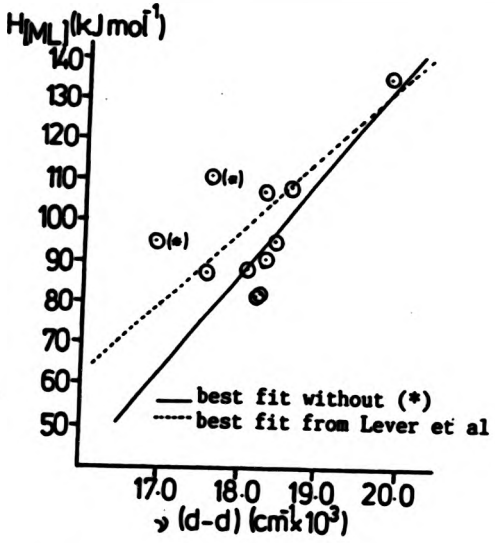

a) Macrocyclic Ligands

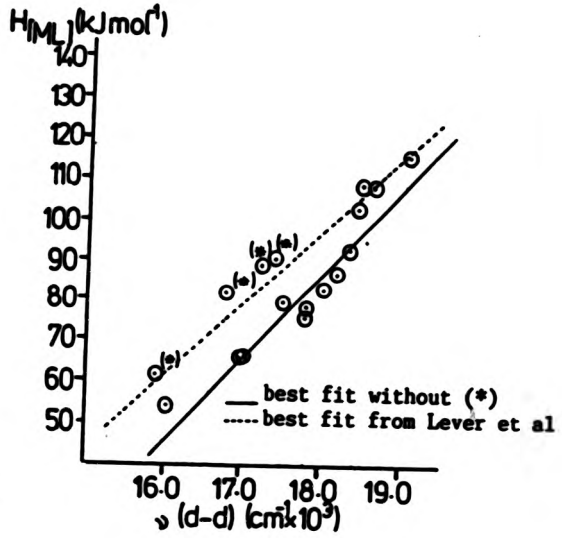

b) Non-cyclic Ligands

Figure 4:3 Relationship between ν (d-d) and $-\Delta H_{ML}$ (kJmol^{-1})

In each case, a satisfactory correlation coefficient (r) was obtained indicating a good straight line fit to the experimental data. The high correlation coefficient (r = 0.926) obtained for the equation relating the absorption maxima to the enthalpy of copper(II) complex formation of tetramines in general is indicative that similar factors are important in the structure and bonding of both the macrocyclic and acyclic copper(II) complexes.

It is evident that these equations are significantly different from the equation previously derived by Fabbrizzi et al. There are two likely reasons for this difference. Firstly, the equation derived by Fabbrizzi et al was derived using a wide range of copper(II) amine complexes with different types and numbers of amine groups, chelate rings, and substituents. This approach has given rise to a general equation covering a wide range of complexes. The equations described here however, apply solely to tetraaza macrocyclic and/or acyclic copper(II) complexes and as such might reasonably be expected to show a different relationship, particularly as some of the factors affecting copper(II) amine complexes in general will not be significant in the case of tetraaza complexes. Secondly, equation 4:1 used only smaller macrocyclic and acyclic tetraaza complexes in its derivation and as such may not adequately reflect any effects on the relationship caused by increasing chelate and macrocyclic ring size. Figure 4:4 shows that increasing chelate and macrocyclic ring size does affect the relationship between $-\Delta H_{CuL}$ and ν(d-d). With few exceptions, the smaller ligands lie above the best fit straight line while the larger ligands lie below the line.

Of the twenty seven tetraamines used to determine the relationship described in equation 4:4, six show significant deviations from the best fit straight line. The six ligands in question are $L_{(I)}$, $L_{(IV)}$, $L_{(VIII)}$, $L_{(XI)}$, $L_{(XV)}$ and $L_{(XVIII)}$.

As has previously been shown (chapter 3), $L_{(I)}$[50], $L_{(VIII)}$[51] and $L_{(XV)}$[9], with a system of fused five membered chelate rings, are too small to accommodate the copper(II) ion in a coplanar CuN_4 environment with the ideal Cu-N bond length. It has been shown that in the solid state, the copper(II) complexes of these ligands exist with a five co-ordinate square pyramidal structure, the copper(II) ion being removed approximately 0.4 Å out of the N_4 plane. In determining the relationship shown by equation 4:1, the value of $-\Delta H_{CuL}$ $(L_{(I)})$ used by Fabbrizzi was 77.5 $kJmol^{-1}$. This is significantly different from a later determination of $-\Delta H_{CuL}$ $(L_{(I)})$ by Anichini et al[52] ($-\Delta H_{CuL}$ = 95.0 $kJmol^{-1}$). If this later value of $-\Delta H_{CuL}$ is used, the point corresponding to $L_{(I)}$ would deviate significantly from the relationship determined by Fabbrizzi et al. This must throw doubt on the statement made by Fabbrizzi et al that "It is probable that five co-ordinate square pyramidal complexes with one axial water molecule will also lie on the line". Indeed, it is likely that this deviation from the more usual tetragonally distorted octahedral structure is a major reason for the deviation of these complexes from the general relationship.

The other three ligands which show unusual behaviour in terms of the relationship between $-\Delta H_{CuL}$ and ν(d-d) are $L_{(IV)}$, $L_{(XI)}$, and $L_{(XVIII)}$. These three copper(II) complexes have in common a system of three fused six membered chelate rings. Unlike the copper(II) complexes of the ligands $L_{(I)}$, $L_{(VIII)}$ and $L_{(XV)}$, there are no obvious structural or steric reasons for the unusual behaviour of copper(II) complexes with this chelate ring structure. Indeed, the ligand L_{16}, which also has a system of three fused six membered chelate rings, lies close to (but still above) the best fit straight line for this relationship. However, it is possible that the more normal behaviour of the $[CuL_{16}]^{2+}$ complex is due to a fortuitous combination of steric and structural effects, possibly caused by the presence of the relatively large terminal ethyl groups. This view is supported by the anomalous behaviour shown by the copper(II) complex of the ligand L_{13}. This complex lies below the best fit straight line correlation, unlike the other copper(II) complexes with a system of three fused five membered chelate rings.

Crystallographic data has shown that the $[CuL_{(IV)}]^{2+}$ complex species has a tetragonally distorted octahedral structure with a planar CuN_4 arrangement and a Cu-N bond length of 2.03 Å.[49] Although distortion of the macrocyle to accommodate the copper(II) ion places steric constraints on the complex, it is reasonable to assume that other large macrocycles will exhibit similar steric constraints when complexed. The fact that these complexes are well behaved with respect to the correlation between $-\Delta H_{CuL}$ and ν(d-d) suggests that steric constraints caused solely by the large ring size are not a contributing factor to the unusual behaviour

of the $[CuL_{(IV)}]^{2+}$ complex. It is probable that the system of three fused six membered chelate rings leads to unusually large cumulative ring strain in the complex and that this is a major contributing factor to the poor fit of the experimental data for this copper(II) complex to the relationship described by equations 4:2 and 4:4.

Chapter 5

SOLVATION ENTHALPIES

The enthalpy of solvation ΔH_{hyd} of a ligand is most easily and directly obtained by determination of the enthalpy of vapourisation (or sublimation) ΔH_{vap} and the enthalpy of solution, ΔH_{sol} of the ligand. These three quantities are related as shown below in figure 5:1.

Figure 5:1

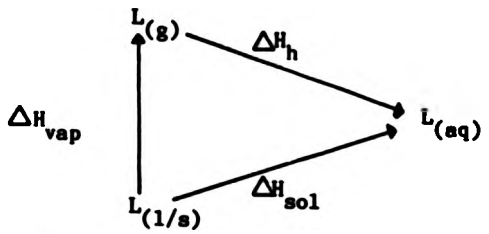

where $\Delta H_{hyd} = \Delta H_{sol} - \Delta H_{vap}$

The ligands used in this study are however extremely involatile. This precludes measurement of ΔH_{vap} by conventional techniques. For this reason, a torsion-effusion, weight loss apparatus was constructed and calibrated at Stirling.[10] This apparatus has previously been used to determine ΔH_{vap} for a number of the smaller tetraaza macrocyclic and acyclic ligands.[11]

The apparatus described in figure 5:2, allows the determination of very low vapour pressures by two independent methods, and has proved to be suitable for use with compounds having vapour pressures at room temperature in the range 0.1 to 10 Pa.

Figure 5:2

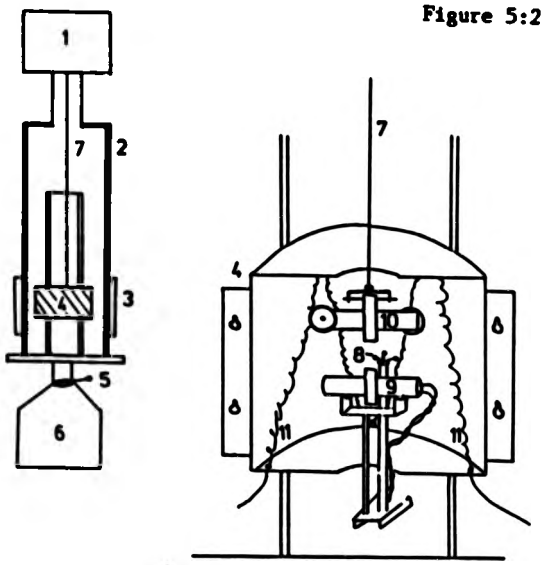

1. Electrobalance.
2. Outer jacket/Jacket heater
3. Cooling coils
4. Measurement cell
5. Butterfly valve
6. Diffusion pump
7. Fine tungsten wire
8. Temperature thermistors
9. Reference cell (Pt resistance thermometer)
10. Effusion cell
11. Heater elements

The first of these two methods, the torsion-effusion method, is independent of the molecular mass of the effusing species, whereas the Knusden, or weight loss method is not. It has been previously demonstrated for the ligands $L_{(III)}$ and $L_{(IX)}$ that similar values of ΔH_{vap} are obtained from both the above methods,[10] showing that the effusing species in this type of ligand is monomeric. This in turn means that it is reasonable to use only the experimentally more convenient weight loss technique in determining ΔH_{vap} for these ligands, and that a monomeric effusing species can be assumed.

In the weight-loss (Knusden) mode, the vapour pressure of a sample at any known temperature can be calculated if the rate of mass loss of the sample is known by using the expression:-[55]

$$P = \frac{m}{A}\cdot\left(\frac{2\pi RT}{M}\right)^{\frac{1}{2}}\cdot\frac{31 + 8r}{8r}\cdot\frac{1}{1 + 0.48r/2\lambda}$$

where P = vapour pressure (in Pa)

m = rate of mass loss (in kgs^{-1})

A = cross sectional area of effusion part (in m^2)

M = molecular mass of effusing species (in kg)

l = depth of effusion part (in m)

r = radius of effusion part (in m)

λ = mean free path of effusing species (m)

$\left(\lambda = \left(\frac{KT}{2\pi\sigma^2}\right)\cdot\frac{1}{p}\ ;\ \sigma$ = collision diameter (m)$\right)$

The dimensions of the effusion part were calculated using a travelling microscope.

The vapour pressur P was calculated using a modified version of Fortran 77 computer programme written originally by S. Corr. This programme calculated P at each temperature by a reiterative method, and determined the corresponding enthalpy of vapourisation by the application of a least squares treatment to the derived ln P vs 1/T data. Initial estimates of P were obtained from the expression:-

$$P = \frac{m}{A}\left(\frac{2\pi RT}{M}\right)^{\frac{1}{2}} \cdot \frac{31 + 8r}{8r}$$

From this estimate of P, the mean free path was then estimated. This in turn allowed a more precise estimate in the next programme cycle. This process was repeated until estimated and calculated values of P converged, usually after the second cycle.

Experimental Procedure

The purified ligand samples required for the determination of ΔH_{vap} and ΔH_{sol} were obtained either by distillation of the crude ligand from Na metal (liquid samples) or by fusion with KOH pellets and subsequent sublimation (solid samples). Liquid samples were degassed before use by repeated freezing and thawing under vacuum No degassing was carried out on solid samples. The ligands were transferred to the sample cell under dry N_2 using a syringe (liquids) or a stainless steel spatula (solids). The sample (approximately 250-300 mg) was mixed with silver turnings in a silver boat to promote thermal equilibrium. The silver boat was placed in the effusion cell which was in turn placed in the apparatus. In the weight loss mode, the apparatus was evacuated to approximately 10 Pa and the system left overnight for the balance to come to rest before measurement was started.

To ensure that the observed vapour pressure was due solely to the sample, and not to volatile impurities such as water, 15-20% of the sample was allowed to vapourize prior to results being taken.

During the experiment, the effusion cell was brought to the temperature range of interest. After equilibration at each temperature, simultaneous temperature and microbalance outputs were recorded on a 16K Commodore Pet microcomputer.

At each temperature, two groups of twenty readings were taken at ten second intervals, with ten minutes between each set of readings. The temperature readings at each temperature were averaged to give the mean temperature of each point, as there is occasionally a small temperature drift of the order of 0.1 °C over the period. The difference between the averaged microbalance outputs from each group of readings corresponds to the loss of weight from the sample over the ten minute period between each group of measurements. From this difference, the rate of weight loss of the ligand is obtained.

The enthalpy of vapourisation was determined in duplicate for each ligand system, with the sample left in the apparatus under vaccuum between runs.

Having calculated the vapour pressure at each temperature over the range of interest for each ligand, the enthalpy of vapourisation (ΔH_θ) at the mid-range temperature (θ) was calculated using a least squares fit of the calculated vapour pressures and experimental data from

duplicate runs to the Clausius-Clapeyron equation:-

$$\ln P = \frac{-\Delta H}{RT} + B$$

The enthalpy of vapourisation was then corrected to 298.15 K using the Kirchoff equation. Corrected enthalpies of vapourisation are shown in table 5:2. Previously determined enthalpies of vapourisation are shown in table 5:3.

The necessary heat capacity values for correction of vapourisation enthalpy data to 298.15 K using the Kirchoff equation were obtained using a Perkin-Elmer DSC II instrument interfaced with an Apple II microcomputer with sapphire as the heat capacity standard. Heat capacities of gaseous systems were calculated from group values as tabulated by Benson.[56] Values of calculated and experimentally obtained heat capacities are shown in table 5:1.

Enthalpies of Solution

The enthalpies of solution of the ligands L_1-L_{17} were determined using a Tronac model 450 isoperibolic calorimeter. Determinations were carried out in 0.5M NaOH to avoid the presence of protonated ligand species.

Six samples of each ligand (approximately 0.1g each, purified as described previously) were weighed into soda glass ampules under dry N_2 in a glove box. Each ampule was then sealed with paraffin tape before being removed from the glove box and flame sealed.

Figure 5:3

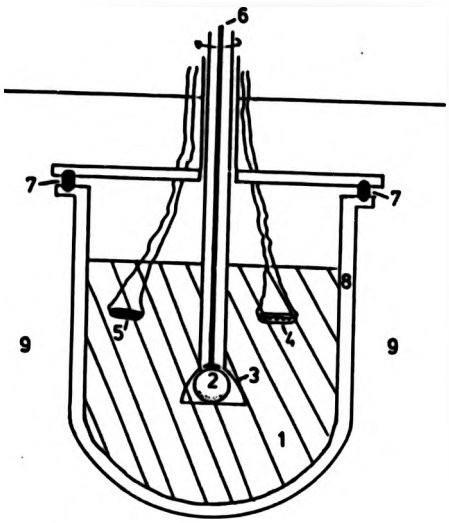

1. Reaction solvent (0.5M NaOH)
2. Soda glass ampule
3. Ampule holder/stirrer
4. Calibration stirrer
5. Temperature sensing thermistor
6. Plunger (ampule breaker)
7. Rubber O-ring
8. Dewar flask
9. Thermostatted water bath

Each ampule was then placed in the Tronac calorimeter as shown in figure 5:3 with approximately 50 ml of 0.5M NaOH solution. The solution was allowed to come to thermal equilibrium at a temperature just below 25 °C. The ampule was broken, and the resulting rise in temperature recorded as a deflection on a potentiometric recorder. Electrical calibration was carried out both before and after each ampule fracture with the mean value used to calculate the heat output of the reaction. Each run was corrected for the heat output associated with ampule fracture. This was determined as the mean of six fractures to be -0.11J per ampule.

To confirm the absolute accuracy of the system, the enthalpy of solution of KCl was determined. The result obtained, 17.3(2) kJ mol^{-1} as an average of four ampule fractures, is in excellent agreement with the literature value of 17.217 kJ mol^{-1}.[57] The experimentally determined enthalpies of solution of the liganda L_1-L_{17} are shown in table 5:2.

Table 5:1 Calculated and observed heat capacities[a]

Ligand	Cp[b]	Cp(g)[c]	Ligand	Cp[b]	Cp(g)[c]
L_1	509	315	$L_{(I)}$	338	246
L_2	430	338	$L_{(II)}$	174	269
L_3	453	362	$L_{(III)}$	374	292
L_4	518	338	$L_{(IV)}$	442	323
L_5	494	362	$L_{(V)}$	583	346
L_6	508	384	$L_{(VIII)}$	490	215
L_7	597	300	$L_{(IX)}$	548	238
L_8	640	323	$L_{(X)}$	582	261
L_9	500	346	$L_{(XI)}$	654	284
L_{16}	653	367	$L_{(XV)}$	632	254
L_{17}	239	320	$L_{(XVI)}$	690	277
			$L_{(XVII)}$	720	300
			$L_{(XVIII)}$	748	323

(a) All values are in $JK^{-1}mol^{-1}$, Cp(g) at 300 K and Cp at 320 K.

(b) Observed heat capacity of the solid or liquid sample (measured on a Perkin-Elmer DSC II with a sapphire standard).

(c) Calculated from group tables. See reference 56

Table 5:2 Vapourisation data (This work)

L	P_{298}[a] (Pa)	ΔH_{vap}[b]	$-\Delta H_{sol}$[c]	ΔH_{fus}[d]	$-\Delta H_{h}$[e]
L_1	2.04×10^{-3}	127.3	27.5	34.0	154.9
L_2	3.07×10^{-3}	129.7	24.5	36.0	154.2
L_3	1.67×10^{-2}	126.7[f]	27.5	38.5	154.2[g]
L_4	1.28×10^{-2}	123.6[f]	28.3	13.3	151.9[g]
L_5	2.50×10^{-3}	123.9	28.6	13.5	166.0
L_6	5.88×10^{-2}	70.4	70.8	-	141.2
L_7	0.111	79.0	78.8	-	157.8
L_8	3.31×10^{-2}	94.7	80.6	-	175.3
L_9	1.18×10^{-2}	124.5[f]	37.8	44.3	162.3[g]
L_{10}	-	-	89.1	-	-
L_{11}	-	-	87.5	-	-
L_{12}	-	-	69.8	-	-
L_{13}	-	-	80.5	-	-
L_{14}	-	-	84.2	-	-
L_{15}	-	-	89.5	-	-
L_{16}	2.33×10^{-2}	92.1	93.5	-	185.6
L_{17}	6.34×10^{-3}	92.1	76.9	-	169.0

a Obtained by extrapolation of lnP vs 1/T data

b $\pm$ 2 $kJmol^{-1}$

c $\pm$ 0.2 $kJmol^{-1}$

d $\pm$ 1 $kJmol^{-1}$

e $\pm$ 3 $kJmol^{-1}$

f Standard state = solid at 298 K, vapourisation data obtained above melting point. ΔH_{vap} values corrected for ΔH_{fus}.

g $\pm$ 4 $kJmol^{-1}$

Table 5:3 Other relevant Vapourisation data[10,11]

Ligand	ΔH_{vap} [a]	$-\Delta H_{sol}$ [a]	$-\Delta H_{h}$ [a]
$L_{(I)}$	121	22.1	143
$L_{(II)}$	111	26.4	137
$L_{(III)}$	134	10.5	144
$L_{(IV)}$	123	25.2	148
$L_{(V)}$	114	33.3	147
$L_{(VIII)}$	85	59.8	145
$L_{(IX)}$	100	66.2	166
$L_{(X)}$	91	71.0	162
$L_{(XI)}$	78	68.0	146
$L_{(XV)}$	87	68.9	156
$L_{(XVI)}$	83	77.4	160
$L_{(XVII)}$	85	81.8	167
$L_{(XVIII)}$	90	86.9	177

a All results in $kJmol^{-1}$ at 25 °C

Discussion of Solvation Data

A convenient way in which to discuss the available solvation data is to consider the enthalpies of vapourisation (ΔH_{vap}) and hydration (ΔH_h) separately.

The enthalpy of vapourisation (ΔH_{vap}) of each ligand should reflect the degree of intermolecular and intramolecular interactions present in the condensed phase of that ligand, assuming that these interactions will be negligible in the highly energetic gas phase.

The magnitude of ΔH_{vap} is generally much higher for the macrocyclic ligands than for the acyclic ligands. The larger positive ΔH_{vap} of the macrocyclic ligands is largely a consequence of the differing physical states of the macrocyclic and acyclic ligands at 298 K. While the macrocyclic ligands (with the exception of L_6) are solids at 298 K the acyclic ligands (with the exception of L_9) are liquids. Thus the enthalpy of vapourisation of the solid ligands contains a fusion term $-\Delta H_{fus}$, which is due to the energy required to melt the ligand. This term, which is typically of the order of 20–40 $kJmol^{-1}$, explains the significantly larger ΔH_{vap} values for the ligands which are solids at 298 K, as is shown in figure 5:5.

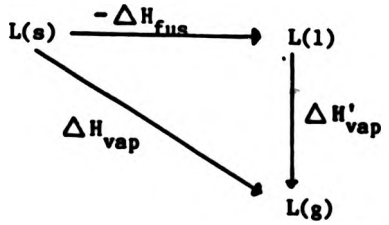

$$\Delta H_{(vap)} = \Delta H'_{vap} - \Delta H_{fus}$$

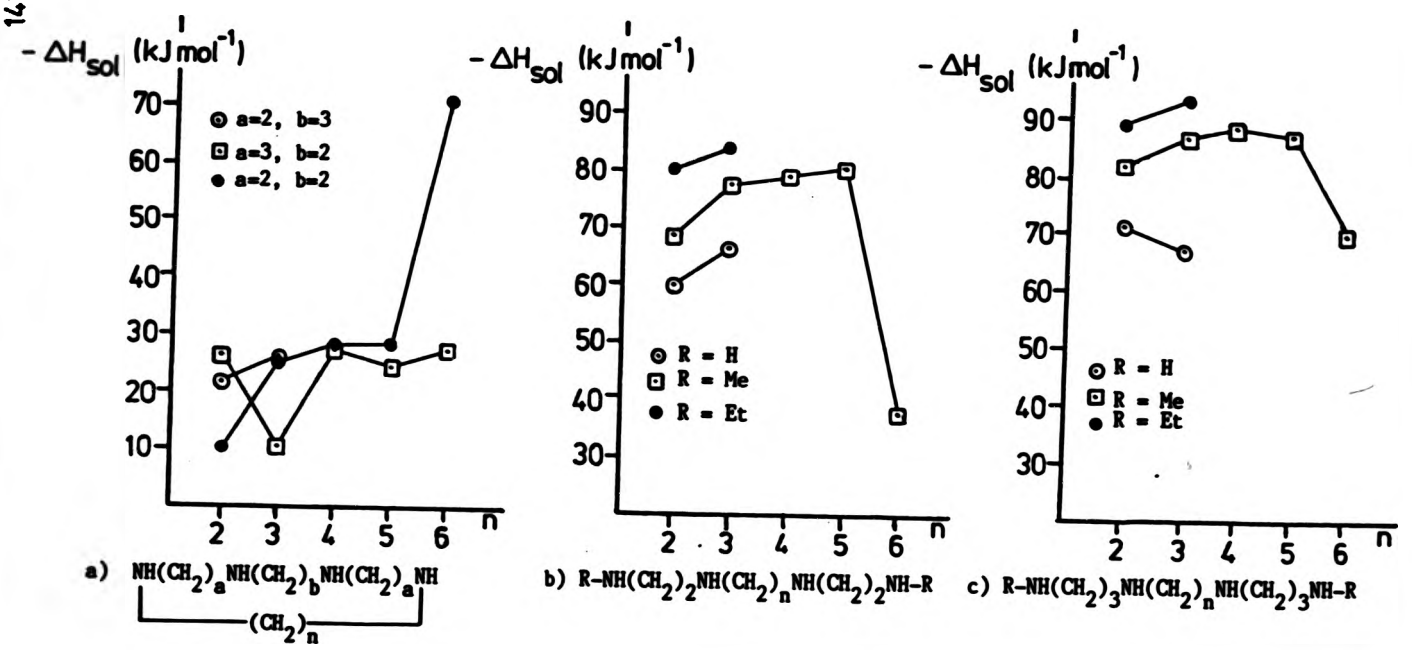

Figure 5:4 $-\Delta H_{sol}$ vs Ligand Size

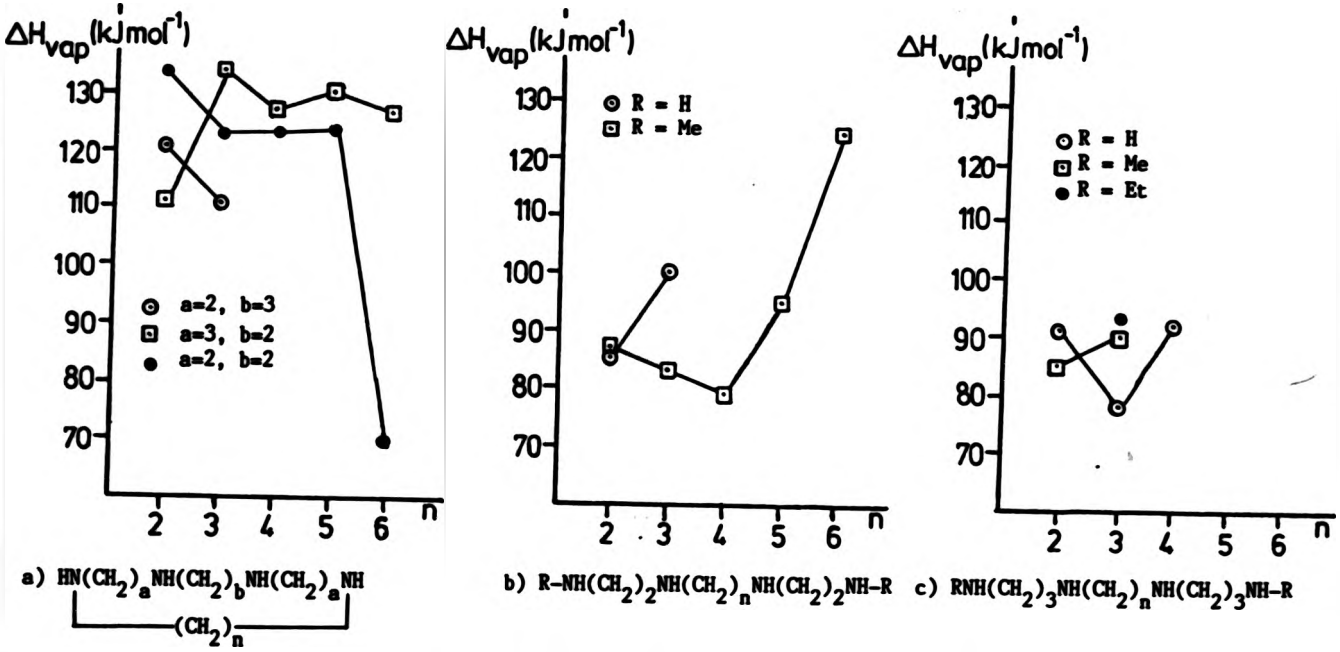

a) $HN(CH_2)_aNH(CH_2)_bNH(CH_2)_aNH$ with $(CH_2)_n$ bridge

b) $R\text{-}NH(CH_2)_2NH(CH_2)_nNH(CH_2)_2NH\text{-}R$

c) $RNH(CH_2)_3NH(CH_2)_nNH(CH_2)_3NH\text{-}R$

Figure 5:5 ΔH_{vap} vs ring size/chain length

This effect is mirrored by trends in ΔH_{sol} for these ligands, as the $-\Delta H_{fus}$ term, which is opposite in sign to the enthalpy of solution results in a less endothermic value of ΔH_{sol} being observed for the ligands which are solid at 298 K than for those which are liquid at 298 K. (Figure 5:4)

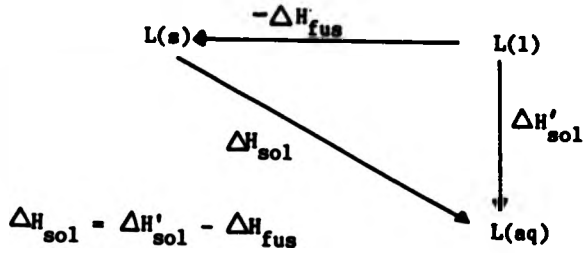

$\Delta H_{sol} = \Delta H'_{sol} - \Delta H_{fus}$

In the case of the macrocyclic ligands (excepting L_6, for the reasons previously given), a reasonable interpretation of the ΔH_{vap} results is that favourable interactions between ligand molecules are maximised for $L_{(III)}$, are at a minimum for $L_{(I)}$ and $L_{(II)}$, and at intermediate values for the other macrocyclic ligands. Assuming that dipole-dipole interactions remain approximately constant for different ligands, this implies that the ΔH_{vap} values reflect the extent of intermolecular hydrogen bonding for each ligand system, as previously suggested by Corr[11] for the smaller macrocyclic ligands.

Although the observed trend in ΔH_{vap} could also be explained by intramolecular hydrogen bonding, this seems less likely, as no intramolecular bonding was observed in the infra-red spectra of $L_{(III)}$ or $L_{(IX)}$ in $CHCl_3$ solution.[11]

It has been suggested that the highly symmetrical ligand structure of $L_{(III)}$ leads to unusually strong molecular packing through hydrogen bonding.[22] This would explain the relatively high ΔH_{vap} value observed for $L_{(III)}$ and more positive ΔH_{vap} values observed generally for tetra-aza macrocyclic ligands with the $-NH-(CH_2)_3-NH-(CH_2)_2-NH-(CH_2)_3-NH-$ structural framework. However, this does not explain the relatively low observed ΔH_{vap} value (see figure 5:5) for the ligand $L_{(II)}$. It has been suggested that $L_{(II)}$ has no intermolecular H-bonding, but no evidence is available to support this postulation.

It has been suggested that the H-bond energy between an amine and water in aqueous solution is approximately 28 $kJmol^{-1}$.[58] It is reasonable to assume that if this is a good estimate, the H-bond energy between two hindered amine molecules in the solid state would be much lower, say 10 $kJmol^{-1}$.[11] Assuming that $L_{(II)}$ has no intermolecular H-bonding, as postulated above, this would then suggest that $L_{(III)}$, L_1, L_2 and L_3 had two intermolecular H-bonds and $L_{(I)}$, L_4, L_5 and L_6 had one. Similarly, a value of 5 $kJmol^{-1}$ would double the proposed number of hydrogen bonds. It should be remembered however that these values are purely speculative and that it is not possible to quantify the level of intermolecular hydrogen bonding present from the available information.

The absolute value of ΔH_{vap} is indicative of the physical state of the ligand at 298 K and 1 atmosphere, as the ΔH_{fus} term makes a contribution of between +20 and +40 $kJmol^{-1}$ to the overall ΔH_{vap} of systems which are solid under these conditions.

From the evidence presented here, it seems likely that the trends in ΔH_{vap} for the tetraaza ligands reflect the extent of intermolecular hydrogen bonding present in the ligand in the condensed phase. This is consistent with the small decrease in ΔH_{vap} observed with increasing molecular size shown in figure 5:5, as intermolecular H-bonding might reasonably be expected to weaken as the system increases in size, primarily because of steric effects and poorer cystal packing, although the steric effects may be offset to some extent by increased inductive effects from the longer methylene bridges.

The trends evident in ΔH_h are the opposite of those observed for ΔH_{vap}, as is seen by comparing figures 5:5 and 5:6 i.e. there is a gradual increase in ΔH_h with increasing molecular size. This suggests that the factors responsible for the trends in ΔH_{vap} are not predominant in ΔH_h . If as suggested, the trends in ΔH_{vap} are due to changes in the extent of hydrogen bonding with changing molecular size, they would be extremely sensitive to changes in the crystal packing and steric effects present in each system. In aqueous solution, the interaction of interest will be that between a ligand molecule and solvent water. It is reasonable to assume that the steric hindrance for the H_2O–ligand interaction should be significantly less than for a ligand-ligand interaction.

The increasing magnitude of ΔH_h with increasing molecular size shown in figure 5:6 is most probably due to the increasing distance between the nitrogen atoms, which should lead to a greater degree of secondary ligand solvation. In the macrocyclic ligands, this effect will also

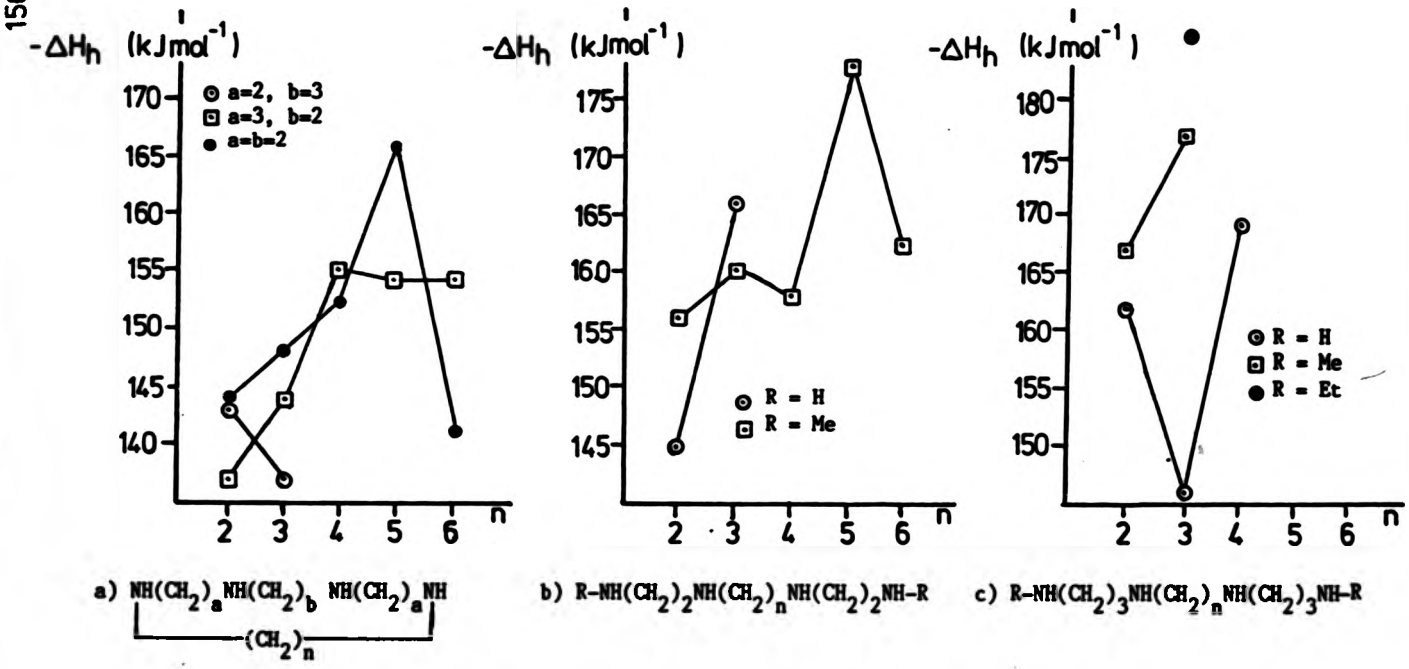

Figure 5:6 $-\Delta H_{nyd}$ vs Ligand Size

be evident. The increasing ring size will probably result in increased solvation due to both increased size and greater conformational flexibility.

A possible description of the solvation behaviour of the macrocyclic and acyclic ligands is shown below in figure 5:7.

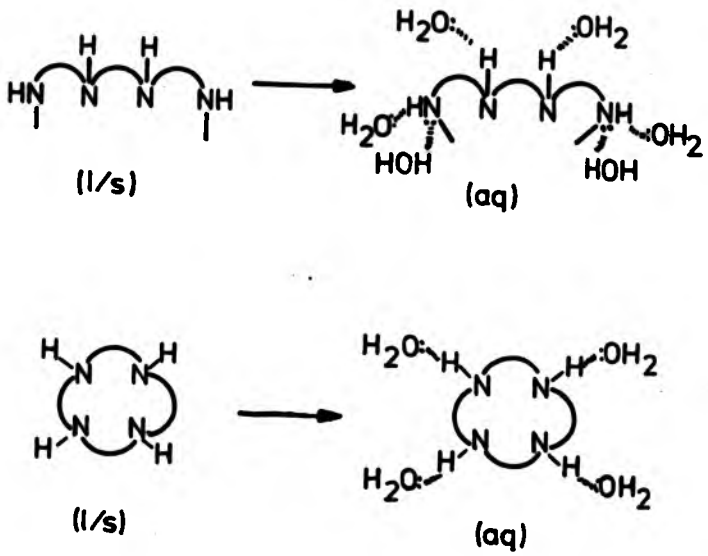

Figure 5:7

The N,N''' alkylated acyclic ligands are shown above as having a primary solvation number of six in aqueous solution, with no internal hydrogen bonding present either in the condensed phase or in solution. This proposed behaviour can be rationalised in terms of the effects of the terminal alkyl groups. Firstly, the presence of the terminal alkyl groups will reduce the probability of internal hydrogen bond

formation both in the free amine and in solution due to the steric effects associated with these groups. In addition, if intramolecular hydrogen bonding were to take place, it would almost certainly be at the expense of intermolecular hydrogen bonding, as only one hydrogen atom is available for H-bonding on each nitrogen. This would be unlikely unless intramolecular hydrogen bonding was particularly favourable. The possible inductive effect of the alkyl groups must also be taken into account. In solution, the positive inductive effect of the alkyl groups may increase the electron donating capacity of the terminal nitrogens to such an extent that solvation through N:----H-OH interactions occurs in addition to the more usual N-H------:OH_2 interactions. The additional N:-----H-OH solvation is likely to be further favoured by the N-H---:O interaction which results in an overall donation of electron density to the amine hydrogen. This would then result in two relatively strong hydrogen bonds with the solvent at each terminal nitrogen.

The observed solvation enthalpies of the N,N''' alkylated acyclic ligands shown in figure 5:6 (approximately -160 $kJmol^{-1}$) are very close to what would be expected if approximately -25 $kJmol^{-1}$[59] is assumed per mole of water bond in the primary solvation sphere (-150 $kJmol^{-1}$). The observed solvation enthalpies of the macrocyclic ligands also shown in figure 5:6 (approximately -150 $kJmol^{-1}$) are rather higher than would be expected with the proposed solvation number of four (-100 $kJmol^{-1}$). Due to the cyclic nature of the macrocyclic ligands, they might reasonably be expected to present a more compact surface to the solvent water than the N,N'''-alkylated acyclic ligands which are likely to be larger and less regular.

Consequently, the macrocyclic ligands should cause less disruption of the hydrogen bonded structure of the solvent water than the N,N'''-alkylated acyclic ligands. As this disruption of solvent structure is endothermic, it is reasonable to state that the solvation enthalpies of the macrocyclic ligands should then be more exothermic than would be expected solely from examination of the primary solvation sphere, and this is indeed what is seen.

Indeed, the reduction in the endothermic term due to solvent disruption may account for much of the difference between the observed solvation enthalpy and that calculated solely on the basis of the primary solvation sphere of the ligand.

Chapter 6

DISCUSSION

Trends in Cu^{2+} Complex solvation

Analysis of results obtained in this study shows that the behaviour of the N, N''' dimethylated ligands parallels more closely that of the macrocyclic ligands than does the behaviour of the non-alkylated acyclic ligands. This is almost certainly due to the different solvation properties of these ligands and (presumably) the solvation behaviour of the corresponding Cu^{2+} complexes. It has been suggested that within each series of ligands, the trend in solvation enthalpies of the Cu^{2+} complexes parallels that of the free ligands of the series.

In chapter 4 it was shown that with few exceptions, a linear relationship exists between H_{CuL} and (d-d) over a wide range of Cu^{2+} - tetraaza complexes.

In the thermochemical cycle outlined below,[54] it can be assumed that ΔH_g consists of two terms, E, a scalar electrostatic interaction energy term, and C, a directional crystal field term which can be assumed to be

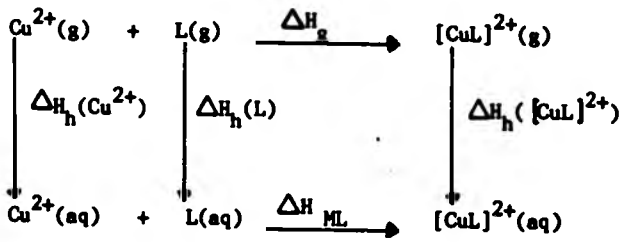

$$\Delta H_{ML} = \Delta H_g + (\Delta H_h([CuL]^{2+}) - \Delta H_h(Cu^{2+}) - \Delta H_h(L))$$

related to ν (d-d) i.e.

$$\Delta H_g = E + C$$

$$= E + f(\nu(d\text{-}d))$$

$$\Delta H_{CuL} = f(\nu(d\text{-}d)) + ((\Delta H([CuL]^{2+}) - \Delta H_h(Cu^{2+}) - \Delta H_h(L) + E)$$

The electrostatic term, E, will be dependent only on the Cu-N bond distance. It has been shown that with few exceptions, the Cu^{2+}-tetraaza systems in this study have approximately the same Cu-N bond distance, as the ligand distorts to accommodate the Cu^{2+} ion in its optimum coplanar $Cu-N_4$ configuration. Thus, E can be assumed to be approximately constant for these complexes.

In order for a linear $\Delta H_{CuL}/\nu$ (d-d) relationship to hold, the difference between the hydration enthalpies of a ligand and its Cu^{2+} complex must remain constant[54] i.e. the sum of the hydration terms must be a constant. The ligands considered in this study which deviate significantly from the derived relationship between ΔH_{CuL} and ν(d-d) are those which have a system of three or more fused five membered chelate rings ($L_{(I)}$, $L_{(VIII)}$, $L_{(XI)}$) where the macrocyclic cavity has previously been shown to be too small to accommodate a coplanar CuN_4 arrangement with the preferred Cu-N bond length, and those with a system of fused six membered chelate rings ($L_{(IV)}$, $L_{(XI)}$, $L_{(XVIII)}$). Reasons for the deviations observed for these somewhat larger copper(II) complexes are less clear, but may be due to a combination of cumulative ring strain and steric effects.

For those ligands which form Cu^{2+} complexes which deviate significantly from the derived $\Delta H_{CuL}/\nu(d\text{-}d)$ relationship, the assumption that $\Delta H_g = f(\nu(d\text{-}d))$ may not be valid. However, for the sake of convenience, four of these ligands ($L_{(I)}$, $L_{(II)}$, $L_{(XV)}$ and $L_{(XVIII)}$) are included in later discussions. It should be remembered that for these ligands the assumption that $\Delta H_g = f(\nu(d\text{-}d))$ may not be valid or that the $f(\nu(d\text{-}d))$ may be modified due to different structural and electronic effects in these complexes.

Using the experimentally determined solvation enthalpies of the tetraaza ligand systems, it should be possible to examine further the complex formation enthalpies of each series. It may also be possible, using the solvation data, to identify the origins of the observed trends. For the tetraaza ligands used in this study, the major factors to be considered are:

(i) differences in ligand solvation

(ii) differences in complex solvation

(iii) changes in chelate ring sequence

(iv) changes in the size of the macrocyclic ring cavity

As the ligand hydration enthalpies have already been experimentally determined, the difference in the Cu^{2+} complex formation enthalpies of two ligands (Δ_{ML}) can easily be corrected for the difference in the hydration enthalpies of the free ligands (ΔL_n).

A previous study[11] has shown that for copper(II) complexes of tetra-aza ligands which have a tetragonally distorted octahedral structure with a coplanar CuN_4 arrangement, differences in the solvation of the copperII) complexes are likely to be small (of the order of 4 kJ mol^{-1}). This in turn implies that when Δ_{ML} is corrected for ligand solvation it can be taken as a good approximation of ΔH_g i.e.

$$\Delta H_g' = \Delta_{ML} - \Delta L_h$$

Due to the choice of ligands, and the way in which they are compared and discussed, the chelate ring sequence remains similar along each series of ligands, the only change being in the size of one chelate ring. Differences in M–N interaction and in symmetry have thus been minimised and should remain small within any series of ligands.

Several extensive theoretical and spectroscopic studies have been carried out on the trans-octahedral complexes of various transition metal ions[59,60,61] with the smaller macrocyclic ligands ($L_{(I)}$-$L_{(V)}$), examining the effect of changing macrocyclic ring size on the ligand field strength. For each of the ligands, an ideal macrocyclic cavity size was calculated[46,59] by allowing the free ligand to adopt a minimum strain configuration while retaining a coplanar arrangement of nitrogen atoms. Similarly, each metal ion has an ideal M–N bond length.

The ligand with the macrocyclic cavity which best matches the preferred M–N bond length of the metal ion would be expected to have the most favourable complexation enthalpy with that particular metal ion.

In situations where the macrocyclic cavity is too small to accommodate the metal ion, the metal ion will be removed from the N_4 plane, possibly forcing the complex to adopt a cis-octahedral or square pyramidal geometry (as in the case of the $[CuL_{(I)}]^{2+}$ complex). When the macrocyclic ring size is larger than the ideal match for a metal ion, the ligand is able to distort to accommodate the metal ion, increasing the strain energy in the ligand framework. This increased strain energy has been discussed earlier, in chapter 3, for the complex $[CuL_{(IV)}](ClO_4)_2$ which has a mean bond length of 2.03 Å despite the ligand having an ideal macrocyclic cavity size corresponding to a Cu-N value of 2.22 Å. In this complex, the ligand framework has a significant degree of steric hindrance, reflected in a relatively low complex formation enthalpy. This implies that for ligands with a macrocyclic cavity larger than the preferred size for a metal ion, the difference between the ideal M-N value of the metal ion and the macrocyclic cavity size of the ligand is a measure of the increase in strain associated with complex formation. In general, the ligand will distort to accommodate the metal ion in its preferred geometry rather than forcing the formation of elongated M-N bonds.

Using the $\Delta H_g'$ values in table 6:1, the amount of ring strain present in the Cu^{2+} complex of the macrocyclic ligands would be in the order $L_6 > L_2 = L_3 (> L_1) > L_{(II)} > L_4 > L_5 > L_{(IV)} > L_1 > L_{(III)}$. The $[CuL_{(I)}]^{2+}$ complex, which has a square pyramidal structure, should probably not be included in this comparison.

There will probably be a slight difference in the ring strain sequence for other metal ions, primarily caused by their different ionic radii. In the case of the non-cyclic ligands, the order of ring strain for the Cu^{2+} complexes would be $L_8 > L_9 > L_{(XVIII)} > L_7 (> L_{(XV)}) > L_{(XVII)} > L_{(XVI)}$ on the basis of the H_g' values in table 6:1. In this case $L_{(XV)}$ should probably not be included as it also forms a Cu^{2+} complex with a square pyramidal structure. From figure 6:1 it is apparent that the non-cyclic ligands also show size selectivity in the gas phase. From the results in table 6:1 it would appear that the magnitude of this effect is similar for the macrocyclic and non-cyclic ligands. This is rather surprising considering the greater flexibility that the non-cyclic ligands might reasonably be expected to possess.

The Macrocyclic Effect

Choice of model complex

In order to determine the origins of the macrocyclic effect, differences between the macrocyclic and non-cyclic complexes must, as far as possible, be minimised or removed. Important characteristics of an ideal model system are:-

(i) The Cu^{2+} complexes should be as chemically similar as possible. This has been accomplished by matching the chelate ring sequences of the macrocyclic and non-cyclic ligands as closely as possible and by ensuring that the donor nitrogen atoms are all secondary (earlier comp-

Figure 6:1

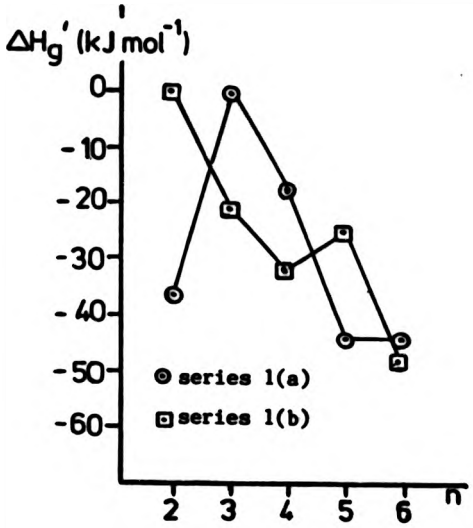

(a). H_g' relative to $CuL^{2+}_{(III)}$ for the macrocyclic ligands.

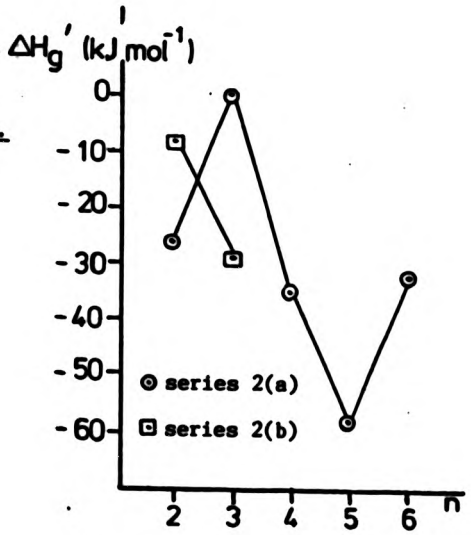

(b). H_g' relative to $CuL^{2+}_{(XVI)}$ for the non- cyclic ligands.

Table 6:1

L	Δ_{ML}	ΔL_h	$\Delta H_g'$	L	Δ_{ML}	ΔL_h	$\Delta H_g'$
$L_{(I)}$	-40.6	1	-42	$L_{(XV)}$	-20	4	-24
$L_{(II)}$	-28.5	7	-36	$L_{(XVI)}$	0	0	0
$L_{(III)}$	0	0	0	$L_{(XVII)}$	-15	-7	-8
$L_{(IV)}$	-24.7	-4	-21	$L_{(XVIII)}$	-46	-17	-29
L_1	-27.6	-11	-17	L_7	-33	2	-35
L_2	-53.9	10	-44	L_8	-42	15	-58
L_3	-53.8	10	-44	L_9	-30	2	-32
L_4	-40.1	8	-32				
L_5	-47.3	22	-25				
L_6	-44.8	-3	-48				

$$\Delta_{ML}(L) = [\Delta H_{ML}(L_{(III)}) - \Delta H_{ML}(L)]$$

$$\Delta L_h(L) = [\Delta H_h(L) - \Delta H_h(L_{(I)})]$$

$$\Delta H_g'(L) = [\Delta_{ML}(L) - \Delta L_h(L)]$$

arisons used for example $L_{(X)}$ as a model for $L_{(III)}$ rather than the more chemically similar $L_{(XVI)}$ which had not at that time been synthesised).

(ii) The macrocyclic and open-chain complexes should have ring sizes which are the same, reducing differences in internal ring strain.

(iii) The macrocyclic complex and the open-chain complex should have the same structure. In particular, both complexes should ideally have a tetragonally distorted trans-octahedral structure with a coplanar CuN_4 arrangement.

(iv) The size of the two complexes should be the same, thus minimising differences in complex solvation.

It has been argued previously that the N,N''', alkylated non-cyclic ligands meet these criteria with respect to the macrocyclic tetraaza ligands more closely than acyclic tetraaza ligands with primary terminal amine groups, and thus will be a more appropriate model for the complexation behaviour of the macrocyclic ligands.

On the basis of observed trends in $\log\beta_4$, $\log K_{CuL}$ and ΔH_{CuL}, and because of the limited choice of ligands available it was decided to compare the ligand pairs shown in figure 6:2. The pairings of the smaller ligands $L_{(III)}$ and $L_{(IV)}$ are somewhat different from previous studies[11]

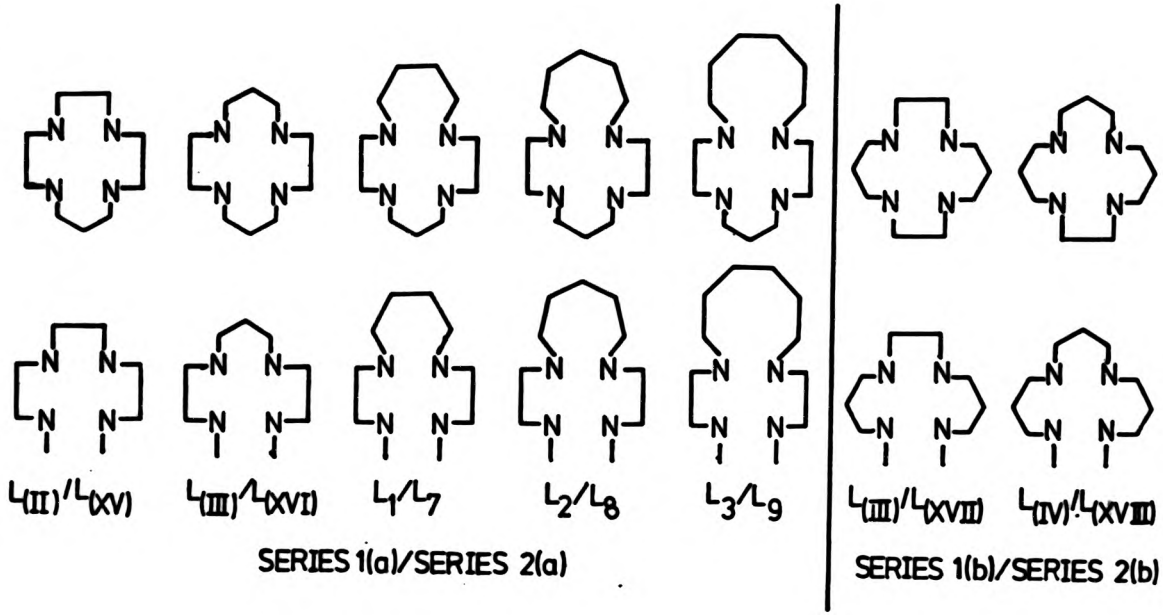

Figure 6:2 **Ligand pairings used in this work**

where $L_{(III)}$ has been compared only with $L_{(XVI)}$, and $L_{(IV)}$ has been compared with $L_{(XVII)}$. In this study, $L_{(III)}$, due to its highly symmetrical structure of alternating five and six membered chelate rings, can be considered to be a member of either series 1(a) or series 1(b) and thus can be compared with a non-cyclic ligand from either series 2(a) ($L_{(XVI)}$) or series 2(b) ($L_{(XVII)}$). This ligand has in fact been considered as a member of both series of macrocyclic ligands, offering perhaps an opportunity to determine which of the two non-cyclic ligands is a more appropriate model for $L_{(III)}$.

One of the main criteria which must be fulfilled for an open-chain complex to be a good model of a macrocyclic complex is that it should exhibit a similar amount of internal strain (due to the match of the metal ion with the ligand cavity) both in solution and in the gas phase.

Clearly, this is not the case for the $L_{(II)}/L_{(XV)}$ pairing, as $L_{(II)}$ has previously been shown to be too small to accommodate the Cu^{2+} ion in a coplanar CuN_4 arrangement whereas $L_{(XVI)}$ is able to accommodate the Cu^{2+} ion in a coplanar CuN_4 environment. This would tend to suggest that any comparison between these ligands may not be a true representation of differences in complex formation caused solely by cyclisation.

Macrocyclic free energy

The macrocyclic effect, as described in chapter 1, is the increase in stability of a macrocyclic copper(II) complex over that of the copper(II) complex of an analogous non-cyclic ligand. For Cu^{2+} complexes, the

magnitude of this effect has been expressed as the free energy change ΔG_{mac} for the metathetic reaction

$$[CuL^n]^{2+}(aq) + L^c(aq) \rightleftharpoons [CuL^c]^{2+}(aq) + L^n(aq)$$

n = non-cyclic ligand; c = macrocyclic ligand

From a comparison of the free energies of complexation of series 1(a) with series 2(a), and series 1(b) with series 2(b) as shown in figure 6:3, it is apparent that the macrocyclic ligands have a significantly larger free energy of complexation, ΔG_{CuL}, than the corresponding non-cyclic ligands. In addition, the magnitude of the macrocyclic free energy term appears to remain more or less constant for each pair of ligands. This would suggest that the factors causing the macrocyclic effect are the same and are essentially unaffected by changes in molecular size and ligand cavity size.

The macrocyclic free energy ΔG_{mac} will have associated with it a macrocyclic enthalpy ΔH_{mac} and macrocyclic entropy ΔS_{mac} such that

$$-\Delta G_{mac} = -\Delta H_{mac} + T\Delta S_{mac}$$

In order to determine the origins of the macrocyclic effect, it is more convenient to examine the macrocyolic enthalpy (ΔH_{mac}) and entropy (ΔS_{mac}) independently.

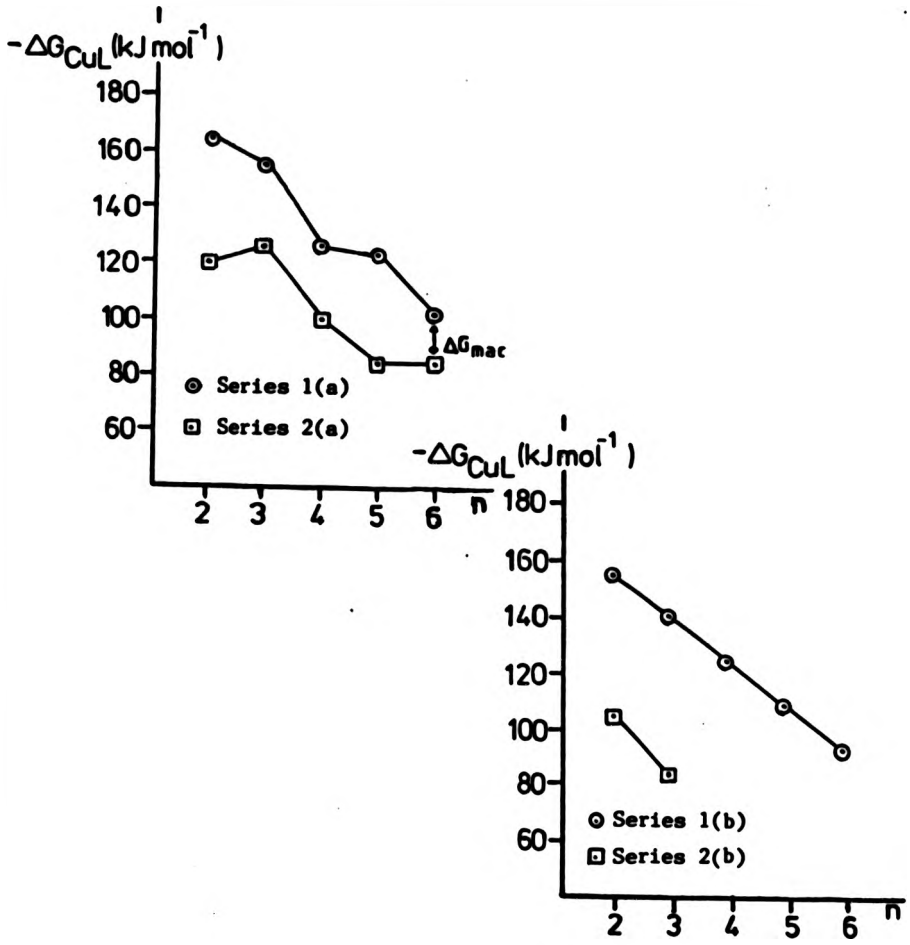

Figure 6:3 Macrocyclic free energy terms. (ΔG_{mL}, ΔG_{mac}).

Table 6:2 Summary of Thermodynamic complexation terms

Ligand	kJ mol^{-1}			
	$-\Delta G_{CuL}$ [a]	$-\Delta H_{CuL}$	$T\Delta S_{CuL}$ [b]	$-\Delta H_h$
L_1	125.7	108.0	-17.7	154.9
L_2	123.3	81.7	-41.6	154.2
L_3	110.5	81.8	-28.7	154.2
L_4	124.3	95.5	-28.8	151.9
L_5	107.0	88.3	-18.7	166.0
L_6	92.0	90.8	-1.2	141.2
$L_{(II)}$	166.0	107.1 [c]	-58.9	137 [h]
$L_{(III)}$	155.2	135.6 [d]	-19.6	144 [h]
$L_{(IV)}$	139.2	110.9 [e]	-28.3	148 [h]
L_7	98.4	75.5	-22.9	157.8
L_8	83.5	66.1	-17.4	175.3
L_9	83.1	78.8	-4.3	162.3
$L_{(XV)}$	119.3	88.3 [f]	-31.0	156 [i]
$L_{(XVI)}$	124.9	108.4 [g]	-16.5	160 [h]
$L_{(XVII)}$	105.6	93.1 [g]	-12.5	167 [h]
$L_{(XVIII)}$	83.4	62.3 [g]	-21.1	177 [h]

(a) ΔG_{CuL} values calculated from corresponding log K_{CuL} values

(b) $T\Delta S_{CuL}$ values calculated from $-\Delta G_{CuL} = -\Delta H_{CuL} + T\Delta S_{CuL}$

(c) Reference 5, 29

(d) Reference 31

(e) Reference 32

(f) Reference 9

(g) Reference 8

(h) Reference 11

(i) Reference 10

Macrocyclic enthalpy term

From the thermochemical cycle outlined in chapter 1, the macrocyclic enthalpy term ΔH_{mac} is shown to consist of three terms i.e.

$$\Delta H_{mac} = \Delta H_{mac}(g) + (\Delta H_h([ML^c]^{2+}) - \Delta H_h([ML^n]^{2+})) + (\Delta H_h(L^n) - \Delta H_h(L^c))$$

where: $\Delta H_{mac}(g)$ is the gas phase macrocyclic enthalpy.

$(\Delta H_h([ML^c]^{2+}) - \Delta H_h([ML^n]^{2+})$ is the difference in the complex solvation enthalpy of the cyclic and non-cyclic ligands.

$(\Delta H_h(L^n) - \Delta H_h(L^c))$ is the difference in ligand solvation enthalpy of the non-cyclic and cyclic ligands.

Of these four quantities, only two, the macrocyclic enthalpy ΔH_{mac} and the ligand solvation term $(\Delta H_h(L^n) - \Delta H_h(L^c))$ can at present be determined experimentally. However, it has already been shown that differences in the enthalpy of solvation of the complexes of the cyclic and non-cyclic ligands should be small due to the chemical and structural similarity of the two complexes, leaving $\Delta H_{mac}(g)$ as the only unknown quantity in the above equation.

Figure 6:4 illustrates the observed differences in complex formation enthalpy for the copper(II) complexes of the ligands in series 1 and 2. The shaded area represents the observed differences in ligand solvation enthalpies for each ligand pair. From this diagram it is evident that with the exception of the L_1/L_7 ligand pair, a large proportion of the macrocyclic enthalpy term can be accounted for by the difference in solvation enthalpy of the free ligand, particularly when it is noted that the uncertainty in the ΔL_h ($\Delta L_h = \Delta H_h(L^n) - \Delta H_h(L^c)$) term is

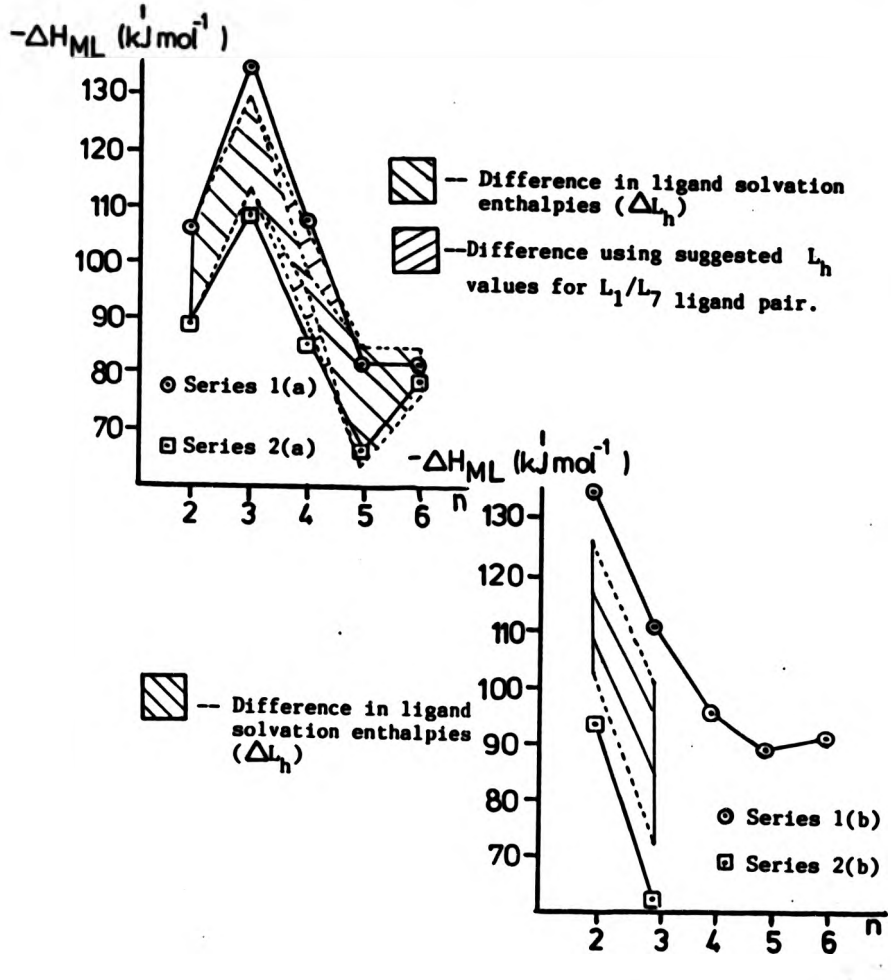

Figure 6:4 Macrocyclic enthalpy term (ΔH_{mac}).

approximately $\pm$ 6 $kJmol^{-1}$.

The ligand pair L_1/L_7 appears to be anomalous as the difference between the macrocyclic enthalpy and ΔL_h is large. In view of the magnitude and trends in solvation enthalpies observed for the other ligand pairs, this would tend to throw doubt on the validity of the solvation results for one (or both) of these ligands. Examination of trends in the solvation terms of the ligands shown in figure 5:6 would tend to suggest that the observed solvation enthalpy of L_1 was some 5 $kJmol^{-1}$ larger than might be predicted purely on the basis of observed trends. This large value of ΔH_h would appear to be due to a higher than expected enthalpy of solution ΔH_{sol} as seen in figure 5:4.

Similarly, the observed solvation enthalpy of L_7 would appear to be some 10 $kJmol^{-1}$ smaller than might be predicted. In this case however, it would appear that the smaller than expected ΔH_h value of L_4 was due principally to a lower than expected enthalpy of vapourisation ΔH_{vap}. Replacement of the observed ΔH_h values of these ligands by suggested values of -150 $kJmol^{-1}$ (L_1) and -168 $kJmol^{-1}$ (L_7) results in a difference in solvation enthalpy ΔL_h which matches more closely the observed difference in complex formation enthalpies Δ_{ML}, as is shown in figure 6:4. However, these values are purely speculative and further investigation in the form of repeat determinations of all of the solvation terms for these two ligands would be required to unequivocally identify any erroneous results.

The observation that the majority of the macrocyclic enthalpy term can be accounted for by differences in ligand solvation supports the suggestion that the complex solvation term ($\Delta H_h([ML^c]^{2+}) - \Delta H_h([ML^n]^{2+})$) must be small. If this is indeed the case, then the difference between the macrocyclic enthalpy term ΔH_{mac} and the ligand solvation term ΔL_h should be a reasonable estimate of the gas phase macrocyclic enthalpy term $\Delta H_{mac}(g)$.

$$\Delta H_{mac} = \Delta H_{mac}(g)' + \Delta L_h$$

Table 6:3 shows values of $\Delta H_{mac}(g)'$ calculated using experimentally observed values of ΔH_{mac} and ΔL_h. From the results obtained, two points are evident:-

(i) The $\Delta H_{mac}(g)'$ value for the L_1/L_7 ligand pair stands out as being significantly different from $\Delta H_{mac}(g)'$ for all other series 1(a)/ series 2(a) ligand pairs. As $\Delta H_{mac}(g)'$ values should be similar along any series, this again highlights the probable presence of inaccuracies in one or more of the experimentally determined solvation terms for this ligand pair.

(ii) When the uncertainty in the $\Delta H_{mac}(g)'$ values ($\pm$ 10 $kJmol^{-1}$) are taken into account, the value of $\Delta H_{mac}(g)'$ (with the exception of the L_1/L_7 pairing) appears to be approximately constant along each series of ligand pairs, and in the case of series 1(a)/1(b) ligand pairs, is close to zero.

Table 6:3 Calculated gas phase macrocyclic enthalpies ($\Delta H_{mac}(g)'$)

L^c/L^n	$kJmol^{-1}$		
	$-\Delta H_{mac}$(a)	$-\Delta L_h$(b)	$-\Delta H_{mac}(g)'$(c)
$L_{(II)}/L_{(XV)}$	19	19	0
$L_{(III)}/L_{(XVI)}$	27	16	9
L_1/L_7	32	3	29
L_2/L_8	16	21	-5
L_3/L_9	3	8	-5
$L_{(III)}/L_{(XVII)}$	43	23	20
$L_{(IV)}/L_{(XVIII)}$	49	29	20

(a) $\pm$ 4 $kJmol^{-1}$

(b) $\pm$ 6 $kJmol^{-1}$

(c) $\pm$ 10 $kJmol^{-1}$

The two larger ligand pairs, L_2/L_8 and L_3/L_9 have a slight negative value for $\Delta H_{mac}(g)'$. This may be indicative of slightly greater solvation of the Cu^{2+} complex of the non-cyclic ligand of these pairs, or may be a reflection of the greater conformational flexibility of the non-cyclic ligands in each pair. Equally likely is that this small endothermic $\Delta H_{mac}(g)'$ is simply an artifact due to a favourable combination of experimental errors.

The two ligand pairs of series 1(b)/series 2(b) show similar exothermic values of $\Delta H_{mac}(g)'$, suggesting that there is a small gas phase macrocyclic enthalpy for these ligands, possibly due to steric hindrance in the copper(II) complexes of the non-cyclic ligands, or that the complex solvation term ($\Delta H_h([ML^c]^{2+}) - \Delta H_h([ML^n]^{2+})$) may have a small exothermic contribution to ΔH_{mac} for these ligand pairs.

In conclusion it can be stated that, using the series 2(a) and 2(b) ligands as models for the series 1(a) and 1(b) ligands, the majority of the macrocyclic enthalpy term can be accounted for in terms of the difference in the solvation enthalpies of the free ligands. This conclusion is in agreement with Margerum's original proposition for the origins of the macrocyclic enthalpy term.[3] This is somewhat fortuitous as Margerum's original proposition was based on very inaccurate enthalpy data.

If it is assumed that the complex solvation term ($\Delta H_h([ML^c]^{2+}) - \Delta H_h([ML^n]^{2+})$) is close to zero, then $\Delta H_{mac}(g)' \simeq \Delta H_{mac}(g)$, and is thought to represent the relative ability of each ligand in a pair to adopt a conformation suitable for Cu^{2+} complex formation. This would imply that the exothermic value of $\Delta H_{mac}(g)'$ for the ligand pairs $L_{(III)}/L_{(XVI)}$, $L_{(III)}/L_{(XVII)}$ and $L_{(IV)}/L_{(XVIII)}$ reflects structural features in the macrocyclic ligands enabling them to form strain free complexes. Although this is likely for $L_{(III)}$, which has been shown to form particularly strain free complexes, it is less likely that this will be the case for $L_{(IV)}$.

For the $L_{(IV)}/L_{(XVIII)}$ ligand pair, the exothermic $\Delta H_{mac}(g)'$ is probably due to destabilisation of the Cu^{2+} complex of the non-cyclic ligand due to steric interaction of the terminal methyl groups, causing distortion of the ligand framework. Molecular models show that this steric interaction of the terminal methyl groups is much greater for the series 2(b) ligands than for the series 2(a) ligands. It is possible that the exothermic $\Delta H_{mac}(g)'$ value for the $L_{(III)}/L_{(XVII)}$ ligand pair is due to a combination of the above effects.

Macrocyclic entropy term

The origin and magnitude of the macrocyclic entropy term has been the subject of much less controversy than the macrocyclic enthalpy term. Even though early speculation was found to be based on inaccurate data, it has been generally agreed that ΔS_{mac} is small and positive, and is due primarily to the greater conformational flexibility of the non-cyclic ligands when compared to the macrocyclic ligands. The greater loss of entropy which therefore results when the Cu^{2+} complex of the non-cyclic ligand is formed leads to a positive ΔS_{mac}.

There has been much criticism of the proposal that differences in ligand solvation enthalpies accounted for the macrocyclic enthalpy term, as this solvation difference might reasonably be expected to result in a considerable loss of entropy since it is unlikely that differences in conformational flexibility would compensate for the loss of translational entropy associated with two water molecules.

In the discussion section of chapter 5, it was implied that ΔS_{hyd} was probably similar for the macrocyclic and non-cyclic ligands as the macrocycles would cause less disruption of the bulk solvent structure than the non-cyclic ligands on dissolution. If this is the case, then ΔS_{mac} for series 1 and series 2 ligands should be a measure of the difference in ligand rearrangement on complex formation. This then suggests that ΔS_{mac} should be approximately constant along a series of ligand pairs, perhaps becoming slightly less positive for larger ligands as the conformational flexibility of the macrocyclic ligand increases. Values of ΔG_{mac}, ΔH_{mac} and $T\Delta S_{mac}$ are shown in table 6:4. The calculated $T\Delta S_{mac}$ values are shown graphically in figure 6:5. From these results, it is immediately apparent that $T\Delta S_{mac}$ values for the $L_{(III)}/L_{(XVI)}$ and L_1/L_7 ligand pairs are substantially different from the other ligand pairs of that series.

Table 6:4 Macrocyclic free energy, enthalpy and entropy terms

L^c/L^n	kJmol^{-1}		
	$-\Delta G_{mac}$ (a)	$-\Delta H_{mac}$ (b)	$T\Delta S_{mac}$ (c)
$L_{(II)}/L_{(XV)}$	47	19	28
$L_{(III)}/L_{(XVI)}$	30	27	3
L_1/L_7	27	32	-5
L_2/L_8	40	16	24
L_3/L_9	27	3	24
$L_{(III)}/L_{(XVII)}$	50	43	7
$L_{(IV)}/L_{(XVIII)}$	56	49	7

(a) $\pm$ 2 kJmol^{-1}(estimated), (b) $\pm$ 4 kJmol^{-1}, (c) $\pm$ 6 kJmol^{-1}

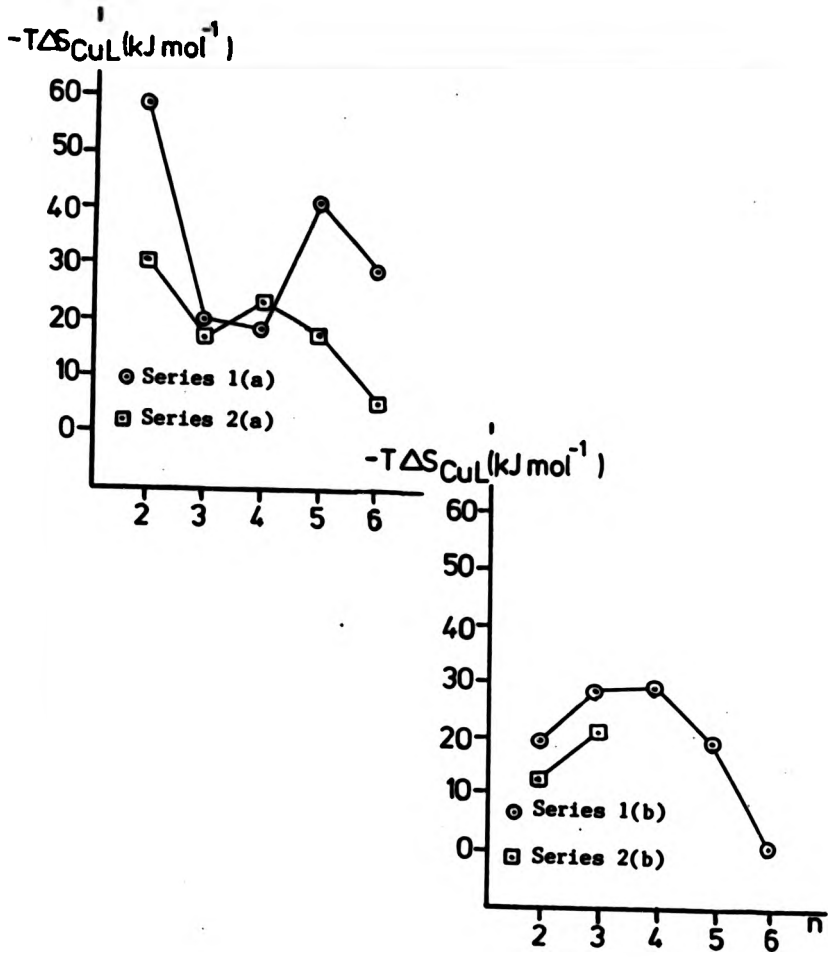

Figure 6:5 Macrocyclic entropy terms (ΔS_{rot}, ΔS_{osc}).

From previous discussions there is no obvious explanation for the observed difference in $T\Delta S_{mac}$ for these two ligand pairs.

The value of log K_{CuL} for the $[CuL_{(III)}]^{2+}$ system has been the subject of some controversy, as it has been shown to give rise to a ΔH_{ML} value some 8 $kJmol^{-1}$ less exothermic than the direct value.[6,32] Indeed, Kodama and Kimura have indicated some uncertainty in their value of log K_{CuL} for $[CuL_{(III)}]^{2+}$ and suggested that the log K_{CuL} value determined potentiometrically at low pH was a composite value for two isomers which they had detected polarographically. The presence of two isomers is observed in the copper(II) complex of "tet a", a hexamethyl derivative of $L_{(III)}$, the thermodynamically less stable isomer being converted to the more stable isomer at high pH.[50] If this also occurs for the $[CuL_{(III)}]^{2+}$, then the log K_{CuL} value for $[CuL_{(III)}]^{2+}$ obtained by Kodama and Kimura is likely to be smaller than that of the more stable isomer, for which the enthalpy of complex formation has been determined.

Assuming that $T\Delta S_{mac}$ values remain constant along any series of ligand pairs, the suggested value of log K_{CuL} for $[CuL_{(III)}]^{2+}$ is 31.0($T\Delta S_{mac}$ = 25 $kJmol^{-1}$), which corresponds reasonably well with an original estimate of 30.1.[50] If a similar situation existed for the $[CuL_1]^{2+}$ complex (although there is no evidence to support this) the revised value of log K_{ML} for $[CuL_1]^{2+}$ would be 27.3. When these values are used, as shown in figure 6:6, the trend in log K_{CuL} becomes a much better match for the trend in ΔH_{CuL}, suggesting that the above explanation may be correct. However, if this is the case, the value of $T\Delta S_{mac}$ for the $L_{(III)}/L_{(XVII)}$

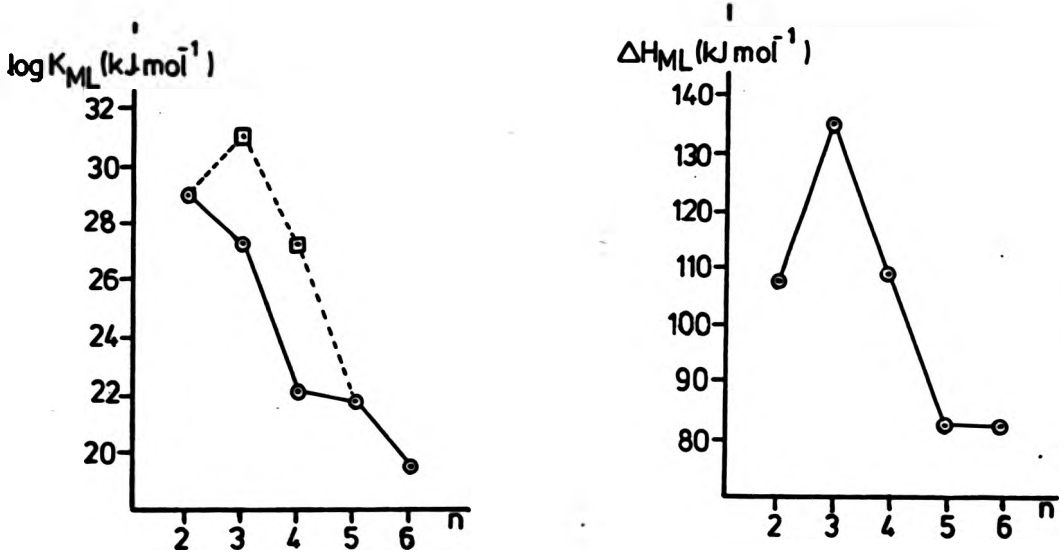

Figure 6:6 Thermodynamic parameters of Cu(II) complex formation of the series 1(a) ligands using experimental (●) and suggested values (⊡) for $\log K_{ML}$.

ligand pair would also be much larger implying that the $T\Delta S_{mac}$ value of the $L_{(IV)}/L_{(XVIII)}$ ligand pair is smaller than might be expected. This in turn implies that the $[CuL_{(IV)}]^{2+}$ complex also shows the type of isomerism which is found for $[CuL_{(III)}]^{2+}$, although there is no evidence to support this suggestion.

It is also possible that the small negative $T\Delta S_{mac}$ value for the L_1/L_7 ligand pair is simply due to impurities in one or both of the ligands, as this would also explain the unusually small difference in solvation enthalpy which was observed for these two ligands.

General Conclusions

The macrocyclic effect - is it a useful concept?

For the tetraaza ligand systems studied in this work, the macrocyclic effect would appear to be the sum of three terms:-

(i) An approximately constant, favourable entropy term due to the greater conformational flexibility of the non-cyclic ligands.

(ii) A variable favourable enthalpy term which is substantially due to differences in the hydration enthalpies of the free ligands.

(iii) A small variable gas phase enthalpy term dependent on the relative ability of the ligands in each pair to adopt the preferred configuration for Cu^{2+} complexation.

A previous study postulated that as the macrocyclic ligand size was increased, the difference in the solvation enthalpy of the non-cyclic and macrocyclic ligands in each ligand pair would decrease, leading to a decrease in the magnitude of ΔH_{mac}. Results obtained in this study, as shown in table 6:3, indicate that this is not the case, as the difference in solvation enthalpy (and ΔH_{mac}) shows no obvious signs of becoming smaller in magnitude. As expected, the macrocyclic entropy term remains favourable and approximately constant, although there are signs of a slight decrease in ΔS_{mac} as the ligand size increases. This slightly less favourable ΔS_{mac} can be explained in terms of the increased conformational flexibility of the larger macrocyclic ligands.

The systems studied in this work have hopefully emphasised the importance of choice and range of model ligand systems as this can have a significant effect on the results obtained and conclusions reached in a study such as this.

From the observed trends in log K_{ML} (chapter 3) it is apparent that as ligand size increases, the incidence of unusual complexes increases. It is likely that for ring sizes much larger than that of L_6, the formation of polymeric and/or polynuclear complexes will make ligand comparisons increasingly difficult.

The difficulty experienced in attempting to obtain information on the complexation behaviour of the ligands L_{10}-L_{12} was possibly due to a combination of the steric hindrance of the terminal methyl groups and the cumulative ring strain that would result on Cu^{2+} complexation.

This has precluded the use of these systems as models for the copper(II) complexes of the ligands L_4-L_6 respectively.

In conclusion, it appears that the concept of a macrocyclic effect is a useful one. However, this will only be the case when a suitable set of non-cyclic model complexes is available for comparison. In evaluating the macrocyclic effect, a full study of all relevant aspects of metal complex formation and of the thermodynamic properties of the free ligands must be considered.

Initially, this work was undertaken to determine the thermodynamic origins of the observed difference in stability of the copper(II) complexes of macrocyclic and non-cyclic tetraaza ligands. The most striking point which has been illustrated is that it is dangerous to assume that this difference originates in differences between the Cu^{2+} complexes, as this is clearly not the case. Indeed, the macrocyclic effect for Cu^{2+}- tetraaza complexes has little to do with the complexes as both the enthalpy and entropy contributions arise principally from differences in the properties of the uncomplexed ligands in aqueous solution.

This only serves to illustrate that in a study of any thermodynamic system, it is dangerous to make "obvious" assumptions as to the origin of any effects, and that the properties of the entire thermodynamic system (solvent, complexes, ligands etc) must necessarily be considered in any rationalisation of the process taking place if accurate conclusions are to be reached.

APPENDIX 1

Grans method of potentiometric analysis

Consider the titration of a known quantity of a strong acid of concentration H with a known volume v of a strong base of concentration B in a cell of general structure:

glass electrode | titration solution || reference half cell

The potential of this cell is given by the expression:

$$E = E' - RT/F \ln[H^+]\gamma_{H^+} + E_j \qquad (i)$$

where E' includes the potential of the reference half cell

E_j is the sum of liquid junction potentials

For the above solution, if the initial volume of the titration system is V, then for any value of v before the equivalence point ve,

$$[H^+] = \frac{VH - vB}{V + v} = \frac{VH(ve - v)}{ve(V + v)} = \frac{B(ve - v)}{V + v} \qquad (ii)$$

A function Ψ can be defined such that

$$\Psi = (V + v)\exp^{(-EF/RT)} \qquad (iii)$$

Then, from (i), (ii) and (iii)

$$\Psi = (ve - v)B\gamma_{H^+} \exp^{-(E' + E_j)F/RT} \qquad (iv)$$

Similarly, after the equivalence point,

$$[H^+] = \frac{K_w}{[OH^-]} = \frac{K_w(V + v)}{B(v - ve)} \qquad (v)$$

where K_w is the ionic product of water.

In the alkaline range, the function Ψ can be defined as:

$$\Psi = \frac{(v - ve)B \exp(E' + E_j)F/RT}{K_w \gamma_{H^+}} \qquad \text{(vi)}$$

If E_j, K_w and γ_{H^+} remain constant throughout a titration, $\Psi(v)$ and $\Psi'(v)$ should be linear functions of v such that $\Psi = \Psi' = 0$ at ve. Plotting either Ψ or Ψ' against v should thus give a straight line from which ve and B can be found. For a linear plot, γ_{H^+} and $(E' + E_j)$ are constant. If $(E' + E_j) = E^{o'}$, then from (iv):

$$\Psi = \gamma_{H^+} B \exp^{-(E^{o'}F/RT)}(ve - v) \qquad \text{(vii)}$$

i.e. $\Psi = -v\ \gamma_{H^+} B \exp^{-(E^{o'}F/RT)} + ve\ \gamma_{H^+} B \exp^{-(E^{o'}F/RT)}$ (viii)

which is a straight line equation of the form $y = mx + c$

When ve and B are both known, $E^{o'}$ can be evaluated from the linear plot of Ψ against v. Similarly, as ve, B and $E^{o'}$ can be calculated from the first half of the titration, K_w may then be evaluated using data obtained from the second half of the titration.

The Gran functions were evaluated using a modified version of a Fortran 77 computer programme specially written for this purpose. Values of ve,

B, $E^{O'}$ and K_w were calculated by least squares treatment of the data.

A more thorough discussion and description of Grans method and of possible reasons for the deviation of the Gran function from linearity can be found in reference (19) and reference (20).

APPENDIX 2

Sample potentiometric titration data

(L_1-H^+)

$E^{o'}$ = 350.9 mV [NaOH] = 0.4831M V_i = 49.87 ml

L_{tot} = 0.2141 m equiv H_i^+ = 1.3646 m equiv

V(ml)	E(mV)	V(ml)	E(mV)	V(ml)	E(mV)
0.55	215.0	1.40	144.0	2.25	-263.0
0.60	212.8	1.45	139.2	2.30	-267.8
0.65	210.2	1.50	134.4	2.35	-272.2
0.70	207.4	1.55	129.4	2.40	-276.4
0.75	204.4	1.60	124.2	2.45	-280.2
0.80	201.0	1.65	118.4	2.50	-283.8
0.85	197.4	1.70	111.8	2.55	-287.2
0.90	193.2	1.75	104.0	2.60	-290.4
0.95	188.8	1.80	93.8	2.65	-293.6
1.00	184.0	1.85	78.2	2.70	-296.6
1.05	178.8	1.90	41.4	2.75	-299.6
1.10	173.6	1.95	-184.6	2.80	-302.4
1.15	168.4	2.00	-218.0	2.85	-305.0
1.20	163.2	2.05	-233.0	2.90	-307.6
1.25	158.2	2.10	-243.4	2.95	-310.0
1.30	153.4	2.15	-251.2	3.00	-312.4
1.35	148.6	2.20	-257.4	3.05	-314.6

(L_1-Cu(II))

$E^{o'}$ = 362.4 [NaOH] = 0.4926M V_i = 52.20 ml

L_{tot} = 0.2021 m equiv H_1^+ = 1.3856 m equiv

V(ml)	E(mV)	V(ml)	E(mV)	V(ml)	E(mV)
0.55	237.6	1.35	217.4	2.15	147.2
0.60	236.4	1.40	216.0	2.20	136.4
0.65	235.0	1.45	214.4	2.25	123.0
0.70	233.8	1.50	212.6	2.30	101.4
0.75	232.4	1.55	210.6	2.35	-20.2
0.80	231.0	1.60	208.2	2.40	-209.6
0.85	229.4	1.65	206.6	2.45	-231.8
0.90	227.8	1.70	204.0	2.50	-245.0
0.95	226.2	1.75	201.4	2.55	-254.6
1.00	224.8	1.80	197.4	2.60	-262.2
1.05	223.4	1.85	193.2	2.65	-268.8
1.10	222.4	1.90	187.6	2.70	-274.6
1.15	221.4	1.95	181.0	2.75	-279.6
1.20	220.4	2.00	173.6	2.80	-284.2
1.25	219.4	2.05	165.4	2.85	-288.2
1.30	218.4	2.10	156.6	2.90	-292.0

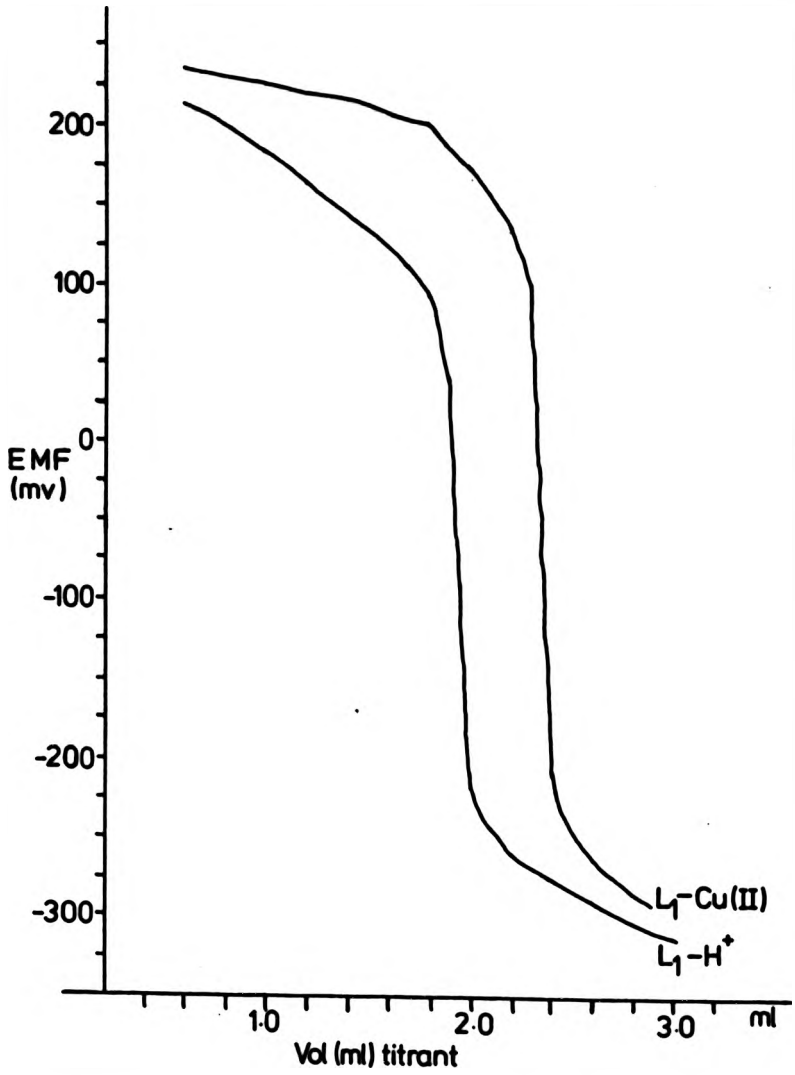

Plot of potential (mv) vs added titrant (ml)

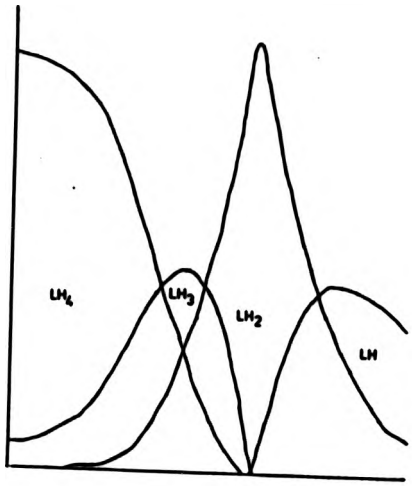

L_1-H^+

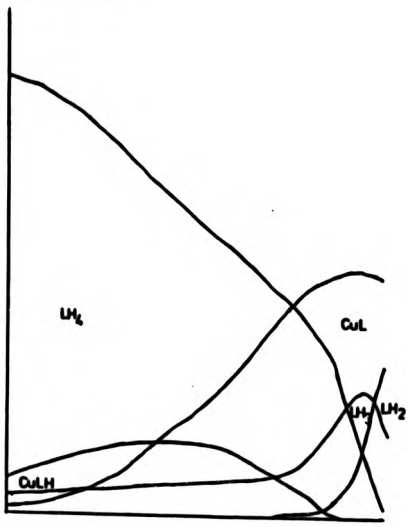

L_1-Cu(II)

Species Distribution Plots

APPENDIX 3

Vapour pressure determination

The expression used in chapter 5 to calculate the vapour pressure of a system from the rate of mass loss at a given temperature can be derived from a consideration of the kinetic theory of gases.

Consider a contained gaseous system of volume V, pressure P and temperature T. The number of collisions per unit area per unit time (z) for any surface of the container is given by the expression:

$$z = \left(\frac{KT}{2\pi M}\right)^{\frac{1}{2}} N/V \qquad \text{(i)}$$

where M is the molecular mass of the gas

N is the number of molecules of gas present in volume V,

i.e. $N = nX$ (X = Avogadro's number)

Thus:
$$\frac{N}{V} = \frac{nX}{V} = \frac{P}{KT}$$

and
$$z = \left(\frac{KT}{2\pi M}\right)^{\frac{1}{2}} \cdot \frac{P}{KT}$$

$$= \frac{P}{(2\pi MKT)^{\frac{1}{2}}} \qquad \text{(ii)}$$

If the area A of the container under consideration is assumed to be a hole or orifice in the container wall with a vaccuum on the outside, then the number of molecules emerging from the hole in unit time can be found from the expression:

$$ZA = \frac{PA}{(2\pi KT)^{\frac{1}{2}}}$$

In any time period t, the mass of the container will change by an amount ΔM, where

$$\Delta M = Z.A.t.M$$

The pressure inside the container can then be expressed as:

$$P = \left(\frac{2\pi KT}{M}\right)^{\frac{1}{2}} \frac{M}{At}$$

$$= \frac{m}{A}.\left(\frac{2\pi KT}{M}\right)^{\frac{1}{2}} \qquad \text{(iii)}$$

where $m = M/t$ is the rate of mass loss from the container.

Expression (iii) describes the vapour pressure for an ideal gas in which there is free flow through the effusion port. In most cases, collisions of the effusing species with the walls of the effusion port or with other molecules of gas give rise to a degree of viscous flow, leading to inaccuracies in the calculated vapour pressure. A consideration of the shape of the effusion port, the effects of the pressure of the effusing gas, and taking into account viscous flow aspects results in expression (iv) below.

$$P = \frac{m}{A}\left(\frac{2\pi KT}{M}\right)^{\frac{1}{2}} \frac{31 + 8r}{8r} \frac{1}{1 + 0.48r/2\lambda} \qquad \text{(iv)}$$

A more detailed discussion of these points can be found in reference (55). The derivation of equation (i) can be found in the majority of physical chemistry textbooks.

REFERENCES

1. For example, N.F.Curtis, J.Chem.Soc., 2644, (1964)

2. A thorough discussion can be found in: P.Paoletti, L. Fabbrizzi, R. Barbucci, Inorg.Chim.Acta.Rev., 7 (1973), 43

3. S.K. Cabbiness, D.W. Margerum J.AmChem.Soc., 91 (1969)

4. F.P. Hinz, D.W. Margerum Inorg.Chem., 13 (1974)2941

5. M. Kodama, E. Kimura J.Chem.Soc,Chem.Comm., 891, (1975)

6. M. Kodama, E. Kimura J.Chem.Soc,Dalton.Trans., 116, (1976)

7. A. Anichini, L. Fabbrizzi, P. Paoletti, R.M. Clay J.Chem.Soc. Chem.Comm., 244, (1977)

8. R.M. Clay, S. Corr, M. Micheloni, P. Paoletti, Inorg.Chem., 24, (1985), 330

9. R.M. Clay, H. McCormac, M. Micheloni, P. Paoletti Inorg.Chem., 21, (1982), 2494

10. R.M. Clay, S. Corr, G. Keenan, W.V. Steele J.Am.Chem.Soc., 105, (1983), 2070

11. S. Corr, PhD Thesis, University of Stirling Chemistry Department (1983)

12. J.E. Richman, T.J. Atkins J.Am.Chem.Soc., 96, (1974), 2268

13. S. Searles, S. Nukina Chem.Rev., 1077, (1959)

14. J.Van Alphen J.Recl.Trav.Chim.Pays.Bas., 55, (1936), 835

15. R.W. hay, P.R. Norman J.Chem.Soc.Dalton.Trans., 1941, (1979)

16. J. S. Pierce J.Am.Chem.Soc., 45, (1923), 785

17. R. Bembi, K.B. Virendra, R. Singh, R. Singh, K. Taneja, A. Shabana Inorg.Chem., 23, (1984), 4153

18. A.I. Vogel, "Quantitative Inorganic Analysis", 3rd Ed., Longmans Ed. 1961. "E.D.T.A. titrations with a mercury pool electrode".

19. E.Bottari et al, Annali, Di.Chim., 68(1978),813

20. G.Gran, Analyst., 77(1952),661

21. F.J.C.Rossotti, H.Rossotti, J.Chem.Ed. 42(1965),375

22. A.Sabatini, A.Vacca, P.Gans, Talanta., 21(1974),53

23. M.Micheloni, A.Sabatini, P.Paoletti, J.Chem.Soc.Perkin.Trans. (II)., 828,(1978)

24. M.Bartolini, A.Bianchi, M.Micheloni, P.Paoletti, J.Chem.Soc. Perkin,Trans.(II)., 1345,(1982)

25. E.Kimura, T.Yatsunami, Chem.Pharm.Bulletin., 28(1980),994

26. B.N.Palmer, H.K.J.Powel, J.Chem.Soc.Dalton.Trans., 2089,(1974)

27. J.Clark,D.D.Perrin, Quart,Rev., 18(1964),295

28. M.Kodama, E.Kimura, J.Chem.Soc, Chem.Comm., 326,(1975)

29. M.Kodama, E.Kimura, J.Chem.Soc,Dalton.Trans., 1720,(1976)

30. M.Micheloni, P.Paoletti, A.Poggi, L.Fabbrizzi, J.Chem.Soc. Dalton.Trans., 61,(1982)

31. M.Kodama, E.Kimura, J.Chem.Soc,Dalton.Trans., 1473,(1977)

32. M.Kodama, E.Kimura, J.Chem.Soc.Dalton.Trans., 2341,(1976)

33. A.P.Leugger, L.Hertli, T.A.Kaden, Helv.Chim.Acta., 61(1978) 2296

34. E.Gallori, E.Martini, M.Micheloni, P.Paoletti, J.Chem.Soc. Dalton.Trans., 1722,(1980)

35. P.Paoletti, M.Ciampolini, A.Vacca, J.Phys.Chem., 67(1963),1065

36. L.Sacconi, P.Paoletti, M.Ciampolini, J.Chem.Soc, 5115,(1961)

37. D.C.Weatherburn, E.J.Billo, J.P.Jones, D.W.Margerum, Inorg. Chem., 9(1970),1557

38. L.Fabbrizzi, R.Barbucci, P.Paoletti J.Chem.Soc.Dalton.Trans. 1529,(1972)

39. G.Anderegg, P.Blüenstein, Helv.Chim.Acta., 65(1982),162

40. G.Anderegg, P.Blüenstein, Helv.Chim.Acta., 65(1982),913

41. P.Paoletti, L.Fabbrizzi, R.Barbucci, Inorg.Chem., 12(1973), 1861

42. R.Barbucci, L.Fabbrizzi, P.Paoletti, A.Vacca, J.Chem.Soc. Dalton,Trans., 1763,(1973)

43. R.Barbucci, L.Fabbrizzi, P.Paoletti, J.Chem.Soc.Dalton. Trans., 745,(1972)

44. M. Micheloni, P.Paoletti, A.Vacca, J.Chem.Soc.Perkin. Trans.(II)., 945,(1978)

45. E.Gallori, E.Martini, M.Micheloni, P.Paoletti, J.Chem. Soc. Dalton,Trans., 1722,(1980)

46. L.Y.Martin, L.J.De Hayes, L.J.Zompa, D.H.Busch, J.Am.Chem. Soc., 96(1974),4046

47. Y.Komiyama, E.C.Lingafelter, Acta.Cryst., 17(1964),1145

48. A.Pajunen, Suomen.Kem., B42(1969),5

49. L.Fabbrizzi, C.Mealli, P.Paoletti, J.Chem.Res(M)., 2041, (1979)

50. R.M.Clay, J.Murray-Rust, P.Murray-Rust, J.Chem.Soc.Dalton, Trans., 1135,(1979)

51. G.Marongiu, E.C.Lingafelter, P.Paoletti, Inorg.Chem., 8(1969),2763

52. A.Anichini, L.Fabbrizzi, P.Paoletti, R.M.Clay, J.Chem.Soc, DaltonTrans., 577,(1978)

53. L.Fabbrizzi, M.Micheloni, P.Paoletti, J.Chem.Soc.Dalton Trans., 1581,(1979)

54. L.Fabbrizzi, P.Paoletti, A.B.P.Lever, Inorg.Chem., 15 (1976),1502

55. J.W.Edwards, G.L.Kington, Trans.Faraday.Soc., 58(1962),1323

56. S.W.Benson, "Thermochemical Kinetics", 2nd Edition Wiley, New York, (1976)

57. Aylward and Finley, "S.I. Chemical Data Book", 2nd Edition Wiley

58. F.P.Hinz, D.W.Margerum, J.Am.Chem.Soc., 96(1974),4993

59. Y.Hung, L.Y.Martin, S.C.Jackels, A.M.Tait, D.H.Busch, J.Am. Chem.Soc., 99(1977),4029

60. D.D.Watkins(Jnr), D.P.Riley, J.A.Stone, D.H.Busch, Inorg.Chem. 15(1976),387

61. L.Y.Martin, C.R.Sperati, D.H.Busch, J.Am.Chem.Soc., 99(1977), 2968